OXYGEN DELIVERY-UTILIZATION MATCHING IN SKELETAL MUSCLE

by

DANIEL MULLER HIRAI

B.Sc., Universidade Estadual de Londrina, 2008

AN ABSTRACT OF A DISSERTATION

submitted in partial fulfillment of the requirements for the degree

DOCTOR OF PHILOSOPHY

Department of Anatomy and Physiology
College of Veterinary Medicine

KANSAS STATE UNIVERSITY
Manhattan, Kansas

2012

Abstract

The overall aim of this dissertation is to better understand the mechanisms determining skeletal muscle oxygen delivery-utilization matching in health and disease. Emphasis is directed toward the role of nitric oxide (NO) bioavailability in modulating muscle microvascular oxygenation (PO_2mv; the sole driving force for blood-myocyte oxygen flux) during transitions in metabolic demand. The first investigation of this dissertation (Chapter 2) demonstrates that alterations in NO bioavailability have a major impact on skeletal muscle PO_2mv kinetics following both the onset and cessation of contractions. Specifically, increased NO levels (via the NO donor sodium nitroprusside; SNP) elevates whereas reduced NO levels (non-specific NOS inhibition with N^G-nitro-L-arginine methyl ester; L-NAME) diminishes muscle PO_2mv at the onset and during recovery from contractions in the spinotrapezius muscle of healthy young rats. Consistent with these results, inhibition of the neuronal NO synthase isoform (*S*-methyl-L-thiocitrulline; SMTC; Chapter 3) reveals alterations in NO-mediated regulation of skeletal muscle PO_2mv with advanced age that likely contribute to exercise intolerance in this population. In Chapter 4 we observed that pronounced oxidative stress is implicated in these pathological responses seen in aged and diseased states. Transient elevations in the oxidant hydrogen peroxide to levels seen in the early stages of senescence and cardiovascular diseases promote detrimental effects on skeletal muscle contractile function (i.e., augmented oxygen cost of force production). Chapter 5 demonstrates that endurance exercise training improves skeletal muscle microvascular oxygenation (i.e., greater PO_2mv and slower PO_2mv kinetics) across the metabolic transient partly via enhanced NO-mediated function in healthy young individuals. These data carry important clinical implications given that exercise training may ameliorate NO-mediated function, muscle microvascular oxygenation deficits and consequently exercise intolerance in aged and diseased populations. In conclusion, alterations in NO bioavailability have a major impact on the dynamic balance between skeletal muscle oxygen delivery and utilization (i.e., PO_2mv kinetics) in health and disease. While advanced age or the predations of disease impair considerably skeletal muscle microvascular oxygenation, exercise training-induced adaptations on the oxygen transport system constitute a non-pharmacological therapeutic intervention potentially capable of mitigating these microcirculatory deficits.

OXYGEN DELIVERY-UTILIZATION MATCHING IN SKELETAL MUSCLE

by

DANIEL MULLER HIRAI

B.Sc., Universidade Estadual de Londrina, 2008

A DISSERTATION

submitted in partial fulfillment of the requirements for the degree

DOCTOR OF PHILOSOPHY

Department of Anatomy and Physiology
College of Veterinary Medicine

KANSAS STATE UNIVERSITY
Manhattan, Kansas

2012

Approved by:

Major Professor
David C. Poole

Copyright

Abstract

The overall aim of this dissertation is to better understand the mechanisms determining skeletal muscle oxygen delivery-utilization matching in health and disease. Emphasis is directed toward the role of nitric oxide (NO) bioavailability in modulating muscle microvascular oxygenation (PO_2mv; the sole driving force for blood-myocyte oxygen flux) during transitions in metabolic demand. The first investigation of this dissertation (Chapter 2) demonstrates that alterations in NO bioavailability have a major impact on skeletal muscle PO_2mv kinetics following both the onset and cessation of contractions. Specifically, increased NO levels (via the NO donor sodium nitroprusside; SNP) elevates whereas reduced NO levels (non-specific NOS inhibition with N^G-nitro-L-arginine methyl ester; L-NAME) diminishes muscle PO_2mv at the onset and during recovery from contractions in the spinotrapezius muscle of healthy young rats. Consistent with these results, inhibition of the neuronal NO synthase isoform (*S*-methyl-L-thiocitrulline; SMTC; Chapter 3) reveals alterations in NO-mediated regulation of skeletal muscle PO_2mv with advanced age that likely contribute to exercise intolerance in this population. In Chapter 4 we observed that pronounced oxidative stress is implicated in these pathological responses seen in aged and diseased states. Transient elevations in the oxidant hydrogen peroxide to levels seen in the early stages of senescence and cardiovascular diseases promote detrimental effects on skeletal muscle contractile function (i.e., augmented oxygen cost of force production). Chapter 5 demonstrates that endurance exercise training improves skeletal muscle microvascular oxygenation (i.e., greater PO_2mv and slower PO_2mv kinetics) across the metabolic transient partly via enhanced NO-mediated function in healthy young individuals. These data carry important clinical implications given that exercise training may ameliorate NO-mediated function, muscle microvascular oxygenation deficits and consequently exercise intolerance in aged and diseased populations. In conclusion, alterations in NO bioavailability have a major impact on the dynamic balance between skeletal muscle oxygen delivery and utilization (i.e., PO_2mv kinetics) in health and disease. While advanced age or the predations of disease impair considerably skeletal muscle microvascular oxygenation, exercise training-induced adaptations on the oxygen transport system constitute a non-pharmacological therapeutic intervention potentially capable of mitigating these microcirculatory deficits.

Table of Contents

List of Figures

List of Tables

Acknowledgements

I wish to express my deepest appreciation to all those who have contributed to my doctoral training. It has been an honor and privilege to be surrounded by great minds during this fantastic journey.

I especially thank Dr. David C. Poole, my major Professor, whose teaching and guidance shaped me as a scientist in every aspect during these past years. I would also like to thank Dr. Timothy I. Musch for his mentoring and untiring commitment to my education. I am forever indebted to their kindness, support and friendship.

I thank Dr. Thomas J. Barstow, Dr. Brett J. Wong and Dr. Lorena Passarelli, my committee members, for their support and critical inquiry.

My sincere thanks to (current and former) members of our laboratory: Dr. Leonardo F. Ferreira, Dr. Bradley J. Behnke, K. Sue Hageman, Steven W. Copp, Robert T. Davis, Scott K. Ferguson, Clark T. Holdsworth, Gabrielle E. Sims, Dr. Tadakatsu Inagaki and Peter J. Schwagerl. I also thank Dr. Michael J. Kenney (Kansas State University), Dr. Mark D. Haub (Kansas State University) and Danielle J. McCullough (University of Florida) for their important contributions.

I am also grateful to the late Dr. Antonio F. Brunetto and Dr. Fabio Y. Nakamura from Universidade Estadual de Londrina, Brasil for their mentoring during my undergraduate and graduate (Master of Science) years, respectively. My doctoral training at K-State would not have been possible without their guidance.

In addition, I would like to express my greatest appreciation for the Poole's: David, Katherine, Shayna, Connor and Kelton. Their warm affection and continuous support made us feel welcome from day one.

I owe my deepest gratitude to my family: my mother (Irene M. M. Hirai), my father (Norio Hirai), my brother (Fabio M. Hirai), my grandparents (Jan Muller, Hermine Muller, Hiromu Hirai, Harco Hirai) and my wife (Luiza G. Castanhas).

Preface

Each investigation of this dissertation has been published previously in peer-reviewed physiology journals (citations below) and are reproduced here with permission from the publishers.

Hirai DM, Copp SW, Ferreira LF, Musch TI, and Poole DC. Nitric oxide bioavailability modulates the dynamics of microvascular oxygen exchange during recovery from contractions. *Acta Physiol (Oxf)* 200: 159-169, 2010.

Hirai DM, Copp SW, Holdsworth CT, Ferguson SK, Musch TI, and Poole DC. Effects of neuronal nitric oxide synthase inhibition on microvascular and contractile function in skeletal muscle of aged rats. *Am J Physiol Heart Circ Physiol.* 303: H1076-H1084, 2012.

Hirai DM, Copp SW, Schwagerl PJ, Musch TI, and Poole DC. Acute effects of hydrogen peroxide on skeletal muscle microvascular oxygenation from rest to contractions. *J Appl Physiol* 110: 1290-1298, 2011.

Hirai DM, Copp SW, Ferguson SK, Holdsworth CT, McCullough DJ, Behnke BJ, Musch TI, Poole DC. Exercise training and muscle microvascular oxygenation: functional role of nitric oxide. *J Appl Physiol* 113: 557-565, 2012.

Chapter 1 - Introduction

Oxygen is essential for energy metabolism of multicellular complex organisms (e.g., mammals; ref. 4). Atmospheric oxygen must be transported by means of convection and diffusion through a series of transfer steps within closely integrated systems (pulmonary, cardiovascular and muscle metabolic) to reach the mitochondria and support oxidative metabolism (30). Physical exercise represents the greatest physiological challenge to those systems. Considering the small intramuscular oxygen and high energy phosphates stores, sustained elevations in adenosine triphosphate turnover during skeletal muscle contractions require an exquisitely tight coupling between oxygen delivery and utilization.

The microcirculation within skeletal muscle constitutes the final step in the oxygen transport pathway from lungs to myocytes and provides the surface area for oxygen and substrate exchange. As described by Fick's law, oxygen diffuses from the microvascular blood to the mitochondria at a rate ($\dot{V}O_2$) determined by the oxygen partial pressure (PO_2) gradient (i.e., the PO_2 difference between the capillary (PO_2mv) and intracellular space ($PO_2intracel$)), which constitutes the sole driving force for oxygen flux into the myocyte:

$$\dot{V}O_2 = DO_2(PO_2mv - PO_2intracel)$$

where DO_2 is the muscle effective diffusing capacity. Because $PO_2intracel$ falls close to zero during muscle contractions (15), PO_2mv approximates the pressure gradient driving transcapillary oxygen flux. The temporal profile of skeletal muscle PO_2mv during transitions in metabolic demand is determined by the dynamic matching of oxygen delivery ($\dot{Q}O_2$) and $\dot{V}O_2$ (i.e., $\dot{Q}O_2/\dot{V}O_2$ ratio) (3, 19). Accordingly, alterations in skeletal muscle PO_2mv have a direct impact on oxidative metabolism and contractile performance (13, 27). Understanding muscle microcirculatory control is therefore crucial to resolve the mechanisms that determine the dynamic matching between $\dot{Q}O_2$ and $\dot{V}O_2$ in health and the dysfunction in aged and diseased states. Furthermore, as exercise training has become established as a standard non-

pharmacological treatment for many patient populations, it is important to gain insights into its role in muscle microvascular structure and function to assist in the design of therapeutic strategies for improving exercise capacity.

Nitric oxide (NO) is a ubiquitous signaling messenger synthesized primarily via the conversion of L-arginine to L-citrulline by the enzyme NO synthase (NOS). All three major NOS isoforms are expressed in mammalian skeletal muscle, namely neuronal NOS (nNOS), endothelial NOS (eNOS) and inducible NOS (iNOS) (26). NO and its derivatives modulate multiple processes within skeletal muscle including hemodynamic and metabolic control (26). Specifically, NO contributes to the increase in skeletal muscle $\dot{Q}O_2$ during contractions primarily via endothelium-dependent vasodilation (12) and to the inertia of oxidative metabolism (i.e., finite $\dot{V}O_2$ kinetics) via inhibition of mitochondrial respiration (17). Accordingly, several lines of evidence indicate that impairments in NO-mediated function in aged and/or diseased states are associated with reduced exercise capacity (21, 22), whereas enhanced NO-mediated function following exercise training underlies, at least in part, improved exercise capacity (9, 18). In this context, we developed the investigation described in Chapter 2 to examine the impact of altered NO levels on the dynamic skeletal muscle $\dot{Q}O_2/\dot{V}O_2$ matching (i.e., PO_2mv kinetics) following the onset and cessation of contractions in healthy young rats. These data provide mechanistic evidence that alterations in NO bioavailability play a key role in determining skeletal muscle microvascular oxygenation and thus the upstream pressure driving capillary-myocyte oxygen flux during transitions in metabolic demand in healthy young individuals. Moreover, based on those data we investigated how advanced age might impair NO-mediated control of skeletal muscle microvascular and contractile function (Chapter 3).

Advancing age is associated with a variety of cardiovascular perturbations that disrupt contracting skeletal muscle vascular control. Impairments in the oxygen transport pathway with aging result in temporal mismatch between muscle $\dot{Q}O_2$ and $\dot{V}O_2$ during transitions in metabolic demand (2, 11) and likely contribute to reduced exercise capacity in this population (21). These alterations in PO_2mv kinetics are considered to emanate, at least in part, from age-related disruptions in myocyte redox state. Enhanced reactive oxygen and nitrogen species accumulation during muscle contractions (6, 16) coupled with impaired antioxidant mechanisms in old individuals (31) might exacerbate the underlying oxidative stress characteristic of aging (7) and

promote NOS uncoupling and/or direct NO inactivation (10, 23, 28). In view of the typical deterioration of endothelial function in the elderly (21, 31), age-related decrements in NO-mediated function have been ascribed traditionally to eNOS dysfunction. In Chapter 3 we examined whether nNOS dysfunction is mechanistically involved in the $\dot{Q}O_2 / \dot{V}O_2$ mismatch during metabolic transitions in aged skeletal muscle. Identifying the detrimental effects of aging on distinct NOS isoforms represents the initial step toward the development of potential therapeutic strategies targeting specific enzymes.

As mentioned above, alterations in redox state modulate significantly skeletal muscle vascular and metabolic control. It is interesting to note that aged and diseased states (e.g., chronic heart failure, hypertension, diabetes) are associated with prominent oxidative stress (characterized by reactive oxygen species accumulation that overwhelms the buffering capacity of the endogenous antioxidant system) and reduced exercise capacity. Oxidants are produced at multiple sites within the skeletal muscle and vasculature at rest and during contractions (6, 16, 24). The reduction of molecular oxygen by one-, two- and three-electron transfer reactions yields the oxidizing agents superoxide anion ($O_2^{\bullet-}$), hydrogen peroxide (H_2O_2) and hydroxyl radical ($^{\bullet}OH$). H_2O_2, a small diffusible and ubiquitous molecule with a long half-life relative to other reactive oxygen species, is regarded as one of the most influential oxidants in terms of redox signaling (8). Accordingly, acute alterations in H_2O_2 bioavailability have important implications for skeletal muscle function at rest and during metabolic transients, including the modulation of arteriolar tone (5), mitochondrial respiration (29) and force production (1, 25). In Chapter 4 we examined the impact of transient elevations in H_2O_2 to levels found in the early stages of senescence and cardiovascular diseases (e.g., hypertension) on resting and contracting skeletal muscle microvascular oxygenation (PO_2mv kinetics) and force production in healthy young individuals.

Contrary to aged and diseased states, endurance exercise training induces multiple structural and functional adaptations that enhance the capacities for skeletal muscle $\dot{Q}O_2$ and $\dot{V}O_2$ (14, 20). These adaptations rely partially on improvements in NO-mediated function that occur via upregulation of NOS expression and/or activity in conjunction with augmented antioxidant capacity (9, 18). In Chapter 5 we determined the effects of endurance exercise training on skeletal muscle PO_2mv kinetics and the mechanistic role of NO to these potential adaptations in healthy young rats. These data set the stage for future investigations employing

exercise training protocols as a non-pharmacological tool to ameliorate muscle microvascular oxygenation deficits and exercise intolerance in aged and diseased populations.

Taken together, the investigations described herein were designed to further our understanding of the mechanisms determining skeletal muscle $\dot{Q}O_2 / \dot{V}O_2$ matching in health and disease. Significant focus is given to the role of NO bioavailability in modulating muscle PO_2mv kinetics during transitions in metabolic demand. Each chapter is self-contained following standard journal article format and a comprehensive conclusion is provided for this series of investigations (Chapter 6).

References

1. **Andrade FH, Reid MB, Allen DG, and Westerblad H**. Effect of hydrogen peroxide and dithiothreitol on contractile function of single skeletal muscle fibres from the mouse. *J Physiol* 509 (Pt 2): 565-575, 1998.

2. **Behnke BJ, Delp MD, Dougherty PJ, Musch TI, and Poole DC**. Effects of aging on microvascular oxygen pressures in rat skeletal muscle. *Respir Physiol Neurobiol* 146: 259-268, 2005.

3. **Behnke BJ, Kindig CA, Musch TI, Koga S, and Poole DC**. Dynamics of microvascular oxygen pressure across the rest-exercise transition in rat skeletal muscle. *Respir Physiol* 126: 53-63, 2001.

4. **Catling DC, Glein CR, Zahnle KJ, and McKay CP**. Why O_2 is required by complex life on habitable planets and the concept of planetary "oxygenation time". *Astrobiology* 5: 415-438, 2005.

5. **Csekő C, Bagi Z, and Koller A**. Biphasic effect of hydrogen peroxide on skeletal muscle arteriolar tone via activation of endothelial and smooth muscle signaling pathways. *J Appl Physiol* 97: 1130-1137, 2004.

6. **Ferreira LF, and Reid MB**. Muscle-derived ROS and thiol regulation in muscle fatigue. *J Appl Physiol* 104: 853-860, 2008.

7. **Finkel T, and Holbrook NJ**. Oxidants, oxidative stress and the biology of ageing. *Nature* 408: 239-247, 2000.

8. **Forman HJ, Maiorino M, and Ursini F**. Signaling functions of reactive oxygen species. *Biochemistry* 49: 835-842, 2010.

9. **Green DJ, Maiorana A, O'Driscoll G, and Taylor R**. Effect of exercise training on endothelium-derived nitric oxide function in humans. *J Physiol* 561: 1-25, 2004.

10. **Gryglewski RJ, Palmer RM, and Moncada S**. Superoxide anion is involved in the breakdown of endothelium-derived vascular relaxing factor. *Nature* 320: 454-456, 1986.

11. **Hirai DM, Copp SW, Herspring KF, Ferreira LF, Poole DC, and Musch TI**. Aging impacts microvascular oxygen pressures during recovery from contractions in rat skeletal muscle. *Respir Physiol Neurobiol* 169: 315-322, 2009.

12. **Hirai T, Visneski MD, Kearns KJ, Zelis R, and Musch TI**. Effects of NO synthase inhibition on the muscular blood flow response to treadmill exercise in rats. *J Appl Physiol* 77: 1288-1293, 1994.

13. **Hogan MC, Arthur PG, Bebout DE, Hochachka PW, and Wagner PD**. Role of O_2 in regulating tissue respiration in dog muscle working in situ. *J Appl Physiol* 73: 728-736, 1992.

14. **Holloszy JO, and Coyle EF**. Adaptations of skeletal muscle to endurance exercise and their metabolic consequences. *J Appl Physiol* 56: 831-838, 1984.

15. **Honig CR, Gayeski TEJ, and Groebe K**. Myoglobin and oxygen gradients. In: *The Lung: Scientific Foundations*, edited by Crystal RG, West JB, Weibel ER, and Barnes P. Philadelphia: Lippincott-Raven Publishers, 1997, p. 1925-1933.

16. **Jackson MJ, Pye D, and Palomero J**. The production of reactive oxygen and nitrogen species by skeletal muscle. *J Appl Physiol* 102: 1664-1670, 2007.

17. **Kindig CA, McDonough P, Erickson HH, and Poole DC**. Nitric oxide synthase inhibition speeds oxygen uptake kinetics in horses during moderate domain running. *Respir Physiol Neurobiol* 132: 169-178, 2002.

18. **McAllister RM, Newcomer SC, and Laughlin MH**. Vascular nitric oxide: effects of exercise training in animals. *Appl Physiol Nutr Metab* 33: 173-178, 2008.

19. **McDonough P, Behnke BJ, Kindig CA, and Poole DC**. Rat muscle microvascular PO_2 kinetics during the exercise off-transient. *Exp Physiol* 86: 349-356, 2001.

20. **Poole DC**. Influence of exercise training on skeletal muscle oxygen delivery and utilization. In: *The Lung: Scientific Foundations*, edited by Crystal RG, West JB, Weibel ER, and Barnes PJ. New York: Raven Press, 1997, p. 1957-1967.

21. **Poole DC, and Ferreira LF**. Oxygen exchange in muscle of young and old rats: muscle-vascular-pulmonary coupling. *Exp Physiol* 92: 341-346, 2007.

22. **Poole DC, Hirai DM, Copp SW, and Musch TI**. Muscle oxygen transport and utilization in heart failure: implications for exercise (in)tolerance. *Am J Physiol Heart Circ Physiol* 302: H1050-1063, 2012.

23. **Pou S, Pou WS, Bredt DS, Snyder SH, and Rosen GM**. Generation of superoxide by purified brain nitric oxide synthase. *J Biol Chem* 267: 24173-24176, 1992.

24. **Powers SK, and Jackson MJ**. Exercise-induced oxidative stress: cellular mechanisms and impact on muscle force production. *Physiol Rev* 88: 1243-1276, 2008.

25. **Reid MB, Khawli FA, and Moody MR**. Reactive oxygen in skeletal muscle. III. Contractility of unfatigued muscle. *J Appl Physiol* 75: 1081-1087, 1993.

26. **Stamler JS, and Meissner G**. Physiology of nitric oxide in skeletal muscle. *Physiol Rev* 81: 209-237, 2001.

27. **Stary CM, and Hogan MC**. Effect of varied extracellular PO_2 on muscle performance in Xenopus single skeletal muscle fibers. *J Appl Physiol* 86: 1812-1816, 1999.

28. **Sun J, Druhan LJ, and Zweier JL**. Dose dependent effects of reactive oxygen and nitrogen species on the function of neuronal nitric oxide synthase. *Arch Biochem Biophys* 471: 126-133, 2008.

29. **Tonkonogi M, Walsh B, Svensson M, and Sahlin K**. Mitochondrial function and antioxidative defence in human muscle: effects of endurance training and oxidative stress. *J Physiol* 528 Pt 2: 379-388, 2000.

30. **Weibel ER**. *The pathway for oxygen: structure and function in the mammalian respiratory system*. London: Harvard University press, 1984.

31. **Woodman CR, Price EM, and Laughlin MH**. Aging induces muscle-specific impairment of endothelium-dependent dilation in skeletal muscle feed arteries. *J Appl Physiol* 93: 1685-1690, 2002.

Chapter 2 - Nitric oxide bioavailability modulates the dynamics of microvascular oxygen exchange during recovery from contractions

Summary

Lowered microvascular PO_2 (PO_2mv) during the exercise off-transient likely impairs muscle metabolic recovery and limits the capacity to perform repetitive tasks. The current investigation explored the impact of altered nitric oxide (NO) bioavailability on PO_2mv during recovery from contractions in healthy skeletal muscle. We hypothesized that increased NO bioavailability (sodium nitroprusside; SNP) would enhance PO_2mv and speed its recovery kinetics while decreased NO bioavailability (L-nitro arginine methyl ester; L-NAME) would reduce PO_2mv and slow its recovery kinetics. PO_2mv was measured by phosphorescence quenching during transitions (rest - 1 Hz twitch-contractions for 3 min - recovery) in the spinotrapezius muscle of Sprague-Dawley rats under SNP (300 μM), Krebs-Henseleit (Control) and L-NAME (1.5 mM) superfusion conditions. Relative to recovery in Control, SNP resulted in greater overall microvascular oxygenation as assessed by the area under the PO_2mv curve (PO_{2AREA}; Control: 3471 ± 292 mmHg·s; SNP: 4307 ± 282 mmHg·s; $P<0.05$) and faster off-kinetics as evidenced by the mean response time (MRT*off*; Control: 60.2 ± 6.9 s; SNP: 34.8 ± 5.7 s; $P<0.05$), whereas L-NAME produced lower PO_{2AREA} (2339 ± 444 mmHg·s; $P<0.05$) and slower MRT*off* (86.6 ± 14.5 s; $P<0.05$). In conclusion, NO bioavailability plays a key role in determining the matching of O_2 delivery-to-O_2 uptake and thus the upstream O_2 pressure driving capillary-myocyte O_2 flux (i.e., PO_2mv) following cessation of contractions in healthy skeletal muscle. Additionally, these data support a mechanistic link between reduced NO bioavailability and prolonged muscle metabolic recovery commonly observed in aging and diseased populations.

Introduction

Daily life is rarely accompanied by constant energetic demands (i.e., steady-state oxygen utilization ($\dot{V}o_2$)) and consequently prolonged muscle metabolic recovery will impair the ability to perform repetitive activities. Reduced O_2 availability following the cessation of submaximal contractions will decrease the O_2 pressure within the microvasculature (PO_2mv) and, in so doing, slows the rate of skeletal muscle metabolic recovery (28, 33). As described by Fick's law, O_2 diffuses from the microvascular blood to the mitochondria at a rate ($\dot{V}o_2$) determined by the oxygen pressure (PO_2) gradient (i.e., the PO_2 difference between PO_2mv and the intracellular space (PO_2intra)), which constitutes the sole driving force for O_2 flux into the myocyte:

$$\dot{V}o_2 = Do_2m(Po_2mv - Po_2intra)$$

where DO_2m is the muscle effective diffusing capacity. Because PO_2intra falls close to zero during contractions (32), PO_2mv approximates the PO_2 gradient driving transcapillary O_2 flux. The temporal profile of skeletal muscle PO_2mv during transitions in metabolic demand is determined by the dynamic matching of oxygen delivery ($\dot{Q}o_2$) and $\dot{V}o_2$ (i.e., $\dot{Q}o_2/\dot{V}o_2$ ratio) (5, 48). In this context, evaluation of PO_2mv off-kinetics is of crucial importance since a lowered $\dot{Q}o_2/\dot{V}o_2$ ratio will, via decreased PO_2mv and blood-myocyte O_2 flux, retard the rate of oxidative phosphorylation during recovery thereby impairing subsequent contractile performance (42).

Conditions associated with reduced nitric oxide (NO) bioavailability and/or downregulation of endothelial function such as aging (51, 64) and chronic heart failure (CHF; 17, 19) are characterized by decreased exercise tolerance (11, 34). Therefore, it is conceivable that reduced NO bioavailability is linked mechanistically to compromised muscle function through impaired $\dot{Q}o_2/\dot{V}o_2$ matching and lowered PO_2mv. NO and its derivatives mediate multiple biological responses, including the modulation of vascular smooth muscle tone and skeletal muscle oxidative metabolism (rev. 9, 71). Specifically, considerable evidence indicates that NO contributes to the sustained vasodilation (and thus $\dot{Q}o_2$) during recovery from contractions (25, 59, 67). Moreover, NO synthase (NOS) inhibition (i) accelerates $\dot{V}o_2$ kinetics

at the onset of contractions in humans (35, 36, 73) and horses (38, 39) but not in the isolated canine muscle preparation (26); and (ii) increases skeletal muscle $\dot{V}o_2$ at rest and during submaximal exercise in dogs (65).

The purpose of the present investigation was to determine the effects of altered NO bioavailability on PO_2mv kinetics during recovery from contractions in healthy rat skeletal muscle. Considering that NO bioavailability modulates $\dot{Q}o_2/\dot{V}o_2$ matching following the onset of contractions in health (23) and is implicated in the $\dot{Q}o_2/\dot{V}o_2$ dysregulation characteristic of aging and diseased populations (20), the following hypotheses were tested: (i) increased NO bioavailability (via the NO donor sodium nitroprusside; SNP) would elevate PO_2mv throughout recovery from contractions and accelerate PO_2mv off-kinetics; while (ii) reduced NO bioavailability (NOS blockade via L-nitro arginine methyl ester; L-NAME) would lower PO_2mv throughout recovery from contractions and slow PO_2mv off-kinetics relative to the control condition.

Methods

Animals

Seven female Sprague-Dawley rats (body mass = 298 ± 10 g) were used in the present study. The on-transient PO_2mv response from these animals has been the focus of a previous study (23). Results from the present investigation focus on the off-transient PO_2mv response. Due to animal preparation instability (e.g., movement of the PO_2mv measurement plane during electrically-induced muscle contractions), off-transient PO_2mv profile analysis could not be obtained from one rat in the Control, two rats in the SNP, and three rats in the L-NAME groups. Therefore, results from the current investigation are presented from animals under the following conditions, Control: $n = 6$; SNP: $n = 5$; L-NAME: $n = 4$. Animals were maintained on a 12:12 hour light-dark cycle and received water and food *ad libitum*. Upon completion of the study, rats were euthanized with an overdose of pentobarbital sodium (>100 $mg.kg^{-1}$, i.a.). All protocols described herein were approved by the Kansas State University Institutional Animal Care and Use Committee (IACUC).

Surgical preparation and experimental protocol

All rats were anesthetized initially with pentobarbital sodium (~35-50 $mg{\cdot}kg^{-1}$, i.p.) administered to effect and maintained at a constant core temperature at ~37-38°C with a heating pad. The level of anesthesia was monitored frequently throughout the experimental protocol via the toe-pinch reflex and supplemented as necessary. The left carotid artery was surgically isolated and cannulated (PE-50; Intra-Medic Tubing, Clay Adams Brand, Sparks, MD, USA) for continuous monitoring of mean arterial blood pressure (MAP; Digi-Med BPA model 200, Louisville, KY, USA), infusion of the phosphorescent probe palladium *meso*-tetra (4-carboxyphenyl) porphyrin dendrimer (R2; 15 $mg{\cdot}kg^{-1}$ i.a.) and blood sampling. Blood was sampled at the end of each experimental protocol for the determination of arterial blood gases and pH (Nova Stat Profile M, Waltham, MA, USA).

The surgical preparation consisted of opening the skin and fascia from the mid-dorsal region of the rat to expose the right spinotrapezius muscle. The spinotrapezius muscle exhibits a mixed fiber type composition and citrate synthase activity that resembles the human quadriceps

(16, 45), thus representing a useful analog of human locomotor muscle. The spinotrapezius muscle was moistened constantly throughout the surgical preparation via superfusion of Krebs-Henseleit (K-H) bicarbonate-buffered solution (4.7 mM KCl, 2.0 mM $CaCl_2$, 2.4 mM $MgSO_4$, 131 mM NaCl and 22 mM $NaHCO_3$) equilibrated with 5% CO_2–95% N_2 at ~38°C. Stainless steel electrodes were sutured to the rostral (cathode) and caudal (anode) regions of the spinotrapezius muscle using 6-0 sutures to ensure unchanged electrode position throughout the procedures.

Three separate contraction bouts were performed under distinct superfusion conditions. The order of superfusion was SNP (300 μM in K-H), K-H (Control) and L-NAME (1.5 mM in K-H). These concentrations were selected based on preliminary studies in our laboratory (23). L-NAME was in all instances the last treatment because of its relatively long half-life. The muscle was superfused with each solution (average flow rate of 1-2 $mL.min^{-1}$, warmed to ~38°C) for a total time of 15-20 min prior to electrically-induced muscle contractions. Electrical stimulation (1 Hz, 4-6 V, 2 ms pulse duration) of the muscle was evoked via a Grass Stimulator (model S48, Quincy, MA, USA) for 3 min. The muscle was then allowed to recover for 3 min before the start of a ~10 min period of constant flushing to wash out the respective solution. Subsequent to the recovery and wash out periods the next condition was initiated (stimulation parameters held constant).

The spinotrapezius preparation exhibits reproducible PO_2mv parameters during transitions in metabolic demand when a minimum of 20 min of recovery is allowed between contraction bouts (14, 29). Importantly, 25-30 min of recovery (10 min wash out and 15-20 min of condition-specific superfusion) was undertaken herein to avoid any priming (6) and drug ordering (23) effects that might confound the experimental interpretation of the PO_2mv responses to muscle contractions.

Measurement of PO_2mv

PO_2mv was measured by phosphorescence quenching using a Frequency Domain Phosphorometer (PMOD 1000, Oxygen Enterprises, Philadelphia, PA, USA). As described previously (5, 48), the phosphorescence quenching technique applies the Stern-Volmer relationship (63) for determination of PO_2mv based on the time constant of phosphorescence decay at the muscle:

$$Po_2mv = [(\tau^\circ / \tau) - 1]/(k_Q \times \tau^\circ)$$

where k_Q is the quenching constant and τ° is the phosphorescence lifetime in an O_2-free environment. The τ of phosphorescence decay was determined using 10 scans (100 ms) in the single frequency mode (63, 72). The phosphor R2 (τ° = 601 μs and k_Q = 409 mmHg·s^{-1} at pH = 7.4 and temperature ~38°C) was infused ~15 min prior to initiation of spinotrapezius contractions. The R2 probe is bound to albumin and is restricted to the intravascular space within the muscle (57), providing a signal that corresponds to the weighted average of muscle microvascular volume sampled (i.e., mostly capillaries; 58). Therefore, *PO_2mv* describes the O_2 pressure head for diffusive blood-myocyte O_2 transfer. The common end of the bifurcated light guide was placed 2-4 mm superficial to the dorsal surface of the exposed muscle. The phosphorometer modulates sinusoidal excitation frequencies between 100 Hz and 20 kHz, which allows phosphorescence lifetime measurements from 10 μs to ~2.5 ms. The excitation light (524 nm) focuses on a circle of ~2 mm diameter of exposed muscle with a resulting penetration depth of ~500 μm. *PO_2mv* measurements were recorded at 2 s intervals during rest and throughout the duration of the contraction (3 min) and recovery (3 min) periods.

Analysis of PO_2mv kinetics

The kinetics of *PO_2mv* were described by nonlinear regression analysis using the Marquardt-Levenberg algorithm (SigmaPlot 9.01; Systat Software, San Jose, CA, USA) for the recovery period. Transient *PO_2mv* responses were fit with either a one- or two-component model (48):

One-component:

$$Po_2mv_{(t)} = Po_2mv_{(\text{end}-\text{con})} + \Delta Po_2mv(1 - e^{-(t-TD)/\tau})$$

Two-component:

$$Po_2mv_{(t)} = Po_2mv_{(\text{end}-\text{con})} + \Delta_1 Po_2mv(1 - e^{-(t-TD_1)/\tau_1}) + \Delta_2 Po_2mv(1 - e^{-(t-TD_2)/\tau_2})$$

where $PO_2mv_{(t)}$ is the Po_2mv at a given time *t*, $PO_2mv_{(\text{end-con})}$ is the end-contraction PO_2mv, Δ_1 and Δ_2 are the amplitudes for the first and second components, respectively, TD_1 and TD_2 are the independent time delays for each component, and τ_1 and τ_2 are the time constants (i.e., time taken to reach 63% of the response) for each component. Goodness of fit was determined using three criteria: (i) the coefficient of determination (r^2); (ii) the sum of the squared residuals (χ^2); and (iii) visual inspection.

The mean response time for the off-transient (MRT*off*; as calculated by 47) was used to describe the overall dynamics of the PO_2mv response:

One-component:

$$MRT = TD + \tau$$

Two-component:

$$MRT = (\Delta_1 / \Delta_{tot})(TD_1 + \tau_1) + (\Delta_2 / \Delta_{tot})(TD_2 + \tau_2)$$

where Δ_1 and Δ_2, TD_1 and TD_2, and τ_1 and τ_2 are defined above and Δ_{tot} corresponds to the total change in PO_2mv (i.e., $\Delta_1 + \Delta_2$) when using the two-component model. Furthermore, the overall time necessary to reach 63% of the final amplitude of the response during recovery was determined independent of modeling procedures (T_{63}; 38) as an additional means of checking the model fits to the data.

The area under the PO_2mv curve plotted as function of time (PO_{2AREA}) was calculated during 3 min following cessation of contractions to provide an index of overall muscle microvascular oxygenation throughout the exercise transient for each condition (i.e., incorporating end-contraction and end-recovery PO_2mv values, amplitudes, time delays and time constants of the response to yield a value expressed in mmHg·s).

Statistical analysis

The MRT, T_{63}, pre-contracting PO_2mv ($PO_2mv_{(\text{Baseline})}$) and $PO_2mv_{(\text{end-rec})}$ were compared among (Control vs. SNP vs. L-NAME) and within (MRT*on* vs. MRT*off*; MRT*off* vs. T_{63}; $PO_2mv_{(\text{Baseline})}$ vs. $PO_2mv_{(\text{end-rec})}$) groups with two-way ANOVAs. All other comparisons among

groups were conducted with one-way ANOVAs. *Post hoc* analyses were performed with the Student-Newman-Keuls test when a significant *F*-ratio was detected. The level of significance was set at $P<0.05$. Unidirectional probabilities were considered when examining the effects of SNP and L-NAME superfusion on PO_2mv kinetics based on initial directional hypotheses (20, 23). Pearson's product-moment correlations were conducted to determine association between variables using individual animal data. Results are reported as mean ± standard error of the mean (SE).

Results

Arterial PO_2 was 99 ± 3 mmHg, O_2 saturation 93 ± 1 % and blood pH 7.45 ± 0.01. SNP superfusion promoted a systemic vasodilation which decreased MAP when compared to Control and L-NAME conditions (SNP: 99 ± 5; Control: 126 ± 3; L-NAME: 126 ± 4 mmHg; $P<0.05$).

Effects of altered NO bioavailability on PO_2mv kinetics during the off-transient

The time course of PO_2mv following the cessation of contractions during SNP and L-NAME treatments presented significant qualitative and quantitative differences relative to the Control condition (Fig. 2.1 and Table 2.1). Specifically, $PO_2mv_{(end\text{-}con)}$ was higher for SNP and lower for L-NAME when compared to Control ($P<0.05$). The one-component exponential model provided an excellent fit to the PO_2mv data for Control and SNP. Conversely, a more complex two-component exponential model was required to fit the L-NAME response. Within the three different experimental conditions (Control, SNP and L-NAME), MRT (model dependent) and T_{63} (model independent) were not different from one another during the recovery protocol ($P>0.05$).

In accordance with our hypotheses, SNP treatment accelerated PO_2mv off-kinetics (MRT*off*, T_{63}; $P<0.05$) while L-NAME slowed the response (MRT*off*, T_{63}; $P<0.05$). It is noteworthy that the $PO_2mv_{(end\text{-}rec)}$ reached during the recovery protocol was not different from the corresponding pre-contracting PO_2mv value under each condition ($PO_2mv_{(Baseline)}$; Control: 24.0 ± 1.0; SNP: 25.9 ± 1.4; L-NAME: 16.9 ± 1.8 mmHg; $P>0.05$). The effects of altered NO bioavailability on PO_2mv off-kinetics were reflected in the overall muscle microvascular oxygenation (PO_{2AREA}) throughout the recovery period, as SNP was associated with greater PO_{2AREA} whereas L-NAME induced smaller PO_{2AREA} when compared to Control (Fig. 2.2). As illustrated in Fig. 2.3, $PO_2mv_{(end\text{-}con)}$ was inversely correlated with MRT*off* across conditions ($r = -0.64$; $P<0.01$).

Discussion

The principal original finding of this investigation is that NO bioavailability exerts a key role on the mechanisms determining the dynamic matching between $\dot{Q}o_2$ and $\dot{V}o_2$ following the cessation of contractions in healthy skeletal muscle. Consistent with our hypothesis, increased NO bioavailability (SNP) elevated *PO₂mv* during the recovery phase and speeded its kinetics. Conversely, reduced NO bioavailability (L-NAME) decreased *PO₂mv* during the recovery phase and slowed its kinetics. The effects of altered NO bioavailability on *PO₂mv* off-kinetics can be summarized by analysis of the overall muscle microvascular oxygenation (*PO₂AREA*), which was increased with SNP and decreased with L-NAME compared to Control.

Effects of altered NO bioavailability on PO₂mv off-kinetics

Altering NO bioavailability in recovery is expected to impact (i) muscle $\dot{Q}o_2$ through modulation of smooth muscle relaxation and thus vascular conductance (71) and (ii) muscle $\dot{V}o_2$ via regulation of oxidative metabolism (e.g., inhibition of cellular respiration by NO and its derivatives; 9). Considering that *PO₂mv* represents the conflation of muscle $\dot{Q}o_2$ and $\dot{V}o_2$ at any given time (5, 48), relative to Control increased NO bioavailability (SNP) should act to increase $\dot{Q}o_2$ and decrease $\dot{V}o_2$ while reduced NO bioavailability (L-NAME) is expected to decrease $\dot{Q}o_2$ and increase $\dot{V}o_2$ throughout recovery from contractions, thereby impacting *PO₂mv* off-kinetics. Since *PO₂mv* denotes the sole driving force for blood-myocyte O_2 flux, alterations in its off-kinetics influence the rate of oxidative phosphorylation during recovery and consequently the capacity to perform repetitive tasks (42).

SNP increased whereas L-NAME decreased $PO_2mv_{(end\text{-}con)}$ relative to Control (Table 2.1 and Fig. 2.1). Despite substantial within-group variability, we found a negative correlation between $PO_2mv_{(end\text{-}con)}$ and MRT*off* across conditions (Fig. 2.3), suggesting that NO-mediated events that compromise microvascular oxygenation during steady-state contractions result in sluggish *PO₂mv* recovery, at least in these young healthy muscles. Similar to the Control condition, SNP and L-NAME evidenced an initial time delay before any *PO₂mv* increase during recovery which must result from a similar rate of change (or lack thereof) in $\dot{Q}o_2$ and $\dot{V}o_2$

during the initial period following cessation of muscle contractions. The fact that PO_2mv in recovery does not fall below $PO_2mv_{(end\text{-}con)}$ denotes that $\dot{Q}o_2/\dot{V}o_2$ ratio and thus the driving force for capillary-myocyte O_2 diffusion does not decrease further even under the L-NAME condition. It is noteworthy that the PO_2mv profile in recovery during L-NAME was qualitatively similar (i.e., markedly slower than healthy control) to that found in conditions associated with reduced NO bioavailability such as aging (30) and CHF (3, 49).

Our results are consistent with previous theoretical studies (3, 24, 30) indicating that the altered magnitude and kinetics of $\dot{Q}o_2$ and $\dot{V}o_2$ impact the PO_2mv profile during exercise transitions. Specifically, (i) a relatively lower end-contraction $\dot{Q}o_2$ amplitude and faster $\dot{Q}o_2$ off-kinetics and/or (ii) a relatively higher end-contraction $\dot{V}o_2$ amplitude and slower $\dot{V}o_2$ off-kinetics act to reduce PO_2mv and slow its kinetics during recovery (i.e., $\dot{Q}o_2/\dot{V}o_2$ mismatch), consequently impairing muscle microvascular oxygenation. Taken together, these observations are consonant with decreased muscle $\dot{Q}o_2$ during exercise transitions in aging (1, 15, 27) and CHF (61) that result, at least in part, from blunted vasodilation secondary to decrements in endothelial function (17, 19, 51, 64).

Effects of altered NO bioavailability on PO_2mv on-off asymmetry

Comparison between the overall PO_2mv kinetic profiles (assessed via MRT) during exercise on- and off-transients in healthy skeletal muscle has revealed an asymmetry (i.e., faster on- and slower off-kinetics; 50). These findings are consistent with reports of symmetrical on-off muscle $\dot{V}o_2$ (3, 43, cf. 62) combined with asymmetric $\dot{Q}o_2$ (fast on- and relatively slower off-kinetics; 22, 40) profiles. In healthy muscle, faster on- and slower off-kinetics of capillary red blood cell flux (f_{RBC}, an index of convective $\dot{Q}o_2$) relative to muscle $\dot{V}o_2$ kinetics act to elevate Po_2mv and thereby O_2 availability in skeletal muscle across exercise transitions (22, 40). Conceptually, the on-off asymmetry in the microvascular $\dot{Q}o_2$ profile suggests the participation of different mechanisms in the control of the blood flow response during the onset and recovery from contractions. Although the precise mechanisms underlying the time course of muscle blood flow throughout exercise transitions have not yet been elucidated (e.g., 12), asymmetric capillary

hemodynamics may result from the contribution of the muscle pump to exercise hyperemia during the onset but not offset of contractions in the healthy rat spinotrapezius muscle (22).

On the other hand, conditions that impair muscle microvascular control such as CHF (61), aging (1, 15, 27) and diabetes (41, 54) are characterized by a lower $\dot{Q}o_2/\dot{V}o_2$ ratio during metabolic transients induced by muscle contractions (2, 4, 18, 55) and a greater degree of PO_2mv on-off asymmetry (30, 49). Notwithstanding appreciable within-group variability, the negative correlation found between MRT*on* and MRT*off* (r = -0.64; $P<0.02$; Fig. 2.4) under Control, SNP and L-NAME treatments suggests a significant influence of altered NO bioavailability on PO_2mv kinetics during both on- and off-transitions. This finding is in agreement with the role of NO (i) as an important component of the hyperemic response following the onset (31, 53, 65, 66) and cessation (25, 59, 67) of contractions; and (ii) as a modulator of the rate of oxidative phosphorylation at rest and during exercise transitions (9, 65). Where disease or advanced aging mandate an O_2 supply dependency of $\dot{V}o_2$ kinetics (56), diminished NO bioavailability and/or downregulation of endothelial function will ultimately limit capillary-myocyte O_2 flux thereby compromising pulmonary $\dot{V}o_2$ (10, 60, 68) during transitions in metabolic demand.

Considering the heterogeneous control of blood flow to skeletal muscle composed of distinct fiber types (rev. 44), slow-twitch fibers place a relatively greater reliance on increased convective $\dot{Q}o_2$ (and thus endothelium-dependent vasodilation; 31) while fast-twitch fibers mandate a greater O_2 extraction in response to a given metabolic demand (7, 21, 50). In this context, the present results support that the progressively greater degree of PO_2mv on-off asymmetry with increasing severity of CHF observed in slow- but not in fast-twitch fibers (49) can be attributed, at least in part, to reduced NO-induced vasodilation in CHF (17, 19). Similarly, aging induces muscle-specific dysfunction of endothelium-dependent vasodilation (primarily through diminished NO bioavailability; 51, 70) that is likely to increase the degree of PO_2mv on-off asymmetry only in slow-twitch fibers.

The effects of altered NO bioavailability on microvascular oxygenation of the healthy spinotrapezius muscle during exercise transitions were such that the degree of PO_2mv on-off asymmetry was abolished with SNP (i.e., MRT*on* and MRT*off* not significantly different) and markedly increased with L-NAME (faster MRT*on* and slower MRT*off*) relative to Control (Fig. 2.5). Collectively, these findings provide a mechanistic basis for the greater degree of PO_2mv on-

off asymmetry (faster on- and slower off-kinetics) observed in conditions accompanied by reduced NO bioavailability and/or impaired endothelium-dependent vasodilation, for instance aging (30) and CHF (49). This behavior is likely involved in the reduced exercise tolerance during muscle contractions along with extended metabolic recovery that impairs the ability to perform repetitive tasks.

Clinical implications

As noted above, limited O_2 transport at the capillary-myocyte level is implicated in sluggish pulmonary $\dot{V}o_2$ kinetics (10, 68) and muscle metabolic (13, 37) recovery responses that may constrain the ability to perform repetitive daily activities (42) in aging and diseased (e.g., CHF) populations. Recently, Ferreira et al. (20) demonstrated that L-NAME superfusion had virtually no effects on PO_2mv kinetics of rats with severe CHF, while SNP practically restored their PO_2mv profile towards that seen in healthy animals during the onset of contractions. In addition, preliminary results from our laboratory suggest that the PO_2mv time course during contractions in aged muscle responds in a similar fashion to that described previously in severe CHF under SNP and L-NAME treatments (SW Copp, KF Herspring, TI Musch, DC Poole; unpublished observations). Combined with the present results, these findings suggest that therapeutic interventions aimed at improving endothelial function (i.e., enhanced NO bioavailability) such as endurance exercise training (46, 70) or possibly augmented tetrahydrobiopterin levels (BH_4; 69) could potentially ameliorate muscle microvascular oxygenation deficits (thereby reducing the pronounced degree of PO_2mv on-off asymmetry) and increase exercise tolerance in the elderly and patients with CHF.

Experimental considerations

A lower perfusion pressure (MAP) for SNP compared to Control and L-NAME conditions could potentially constrain blood flow dynamics and thus influence PO_2mv kinetics during exercise transients. However, recent evidence in healthy animals demonstrates that this effect is negligible when MAP is above ~70 mmHg (8) as herein. On the other hand, local L-NAME superfusion of the spinotrapezius muscle prevented the potential confound of the marked MAP elevation that is usually seen following systemic NOS blockade which, if present, could

have triggered a partial baroreflex-mediated sympathetic withdrawal to compensate for the removal of NO vasodilation (66, cf. 59).

Given the potential of altered NO bioavailability to impact intracellular redox state (52) and contractile function, it is important to consider that SNP and L-NAME treatments could influence the regulation of muscle microvascular oxygenation and muscle performance through mechanisms that do not directly involve NO.

Conclusions

In skeletal muscle, altered NO bioavailability impacts profoundly the dynamic matching between $\dot{Q}o_2$ and $\dot{V}o_2$ during recovery from contractions. Increased NO bioavailability (SNP) enhanced muscle microvascular oxygenation (elevated PO_2mv throughout recovery and faster off-kinetics) while reduced NO bioavailability (L-NAME) impaired muscle microvascular oxygenation (decreased PO_2mv throughout recovery and slower off-kinetics) relative to Control. The importance of a lowered PO_2mv is that it reduces the blood-myocyte O_2 flux and could potentially constrain oxidative phosphorylation during transitions in metabolic demand. Such behavior may contribute to the reduced exercise tolerance found in aged individuals and CHF patients in whom NO bioavailability may be compromised (17, 19, 51, 64). Enhanced endothelial function (through increased NO bioavailability) produced by endurance exercise training in these populations (46, 69, 70) could serve to elevate PO_2mv and thus benefit muscle metabolic control and increase exercise tolerance. The present investigation also supports that reduced NO bioavailability is implicated in the greater degree of PO_2mv on-off asymmetry (faster on- and slower off-kinetics) that is commonly observed in aging (30) and CHF (49).

Table 2.1 Muscle PO_2mv kinetics during recovery from contractions under Control, SNP and L-NAME

	Control	SNP	L-NAME
$PO_2mv_{(end\text{-}con)}$, mmHg	14.4 ± 1.3	18.3 ± 1.5*	8.2 ± 1.7*†
Δ_1PO_2mv, mmHg	7.7 ± 1.2	7.3 ± 1.2	5.6 ± 1.2
Δ_2PO_2mv, mmHg	-	-	5.7 ± 0.5
$PO_2mv_{(end\text{-}rec)}$, mmHg	22.1 ± 1.8	25.6 ± 1.8	16.6 ± 2.8*†
TD_1, s	3.3 ± 1.3	5.4 ± 2.3	3.6 ± 1.4
TD_2, s	-	-	81.5 ± 1.9
τ_1, s	56.9 ± 6.5	29.4 ± 5.3	52.4 ± 14.9
τ_2, s	-	-	64.9 ± 21.2
MRT*off*, s	60.2 ± 6.9	34.8 ± 5.7*	88.6 ± 14.5*†
T_{63}, s	59.8 ± 7.2	36.0 ± 5.5*	98.0 ± 17.2*†

$PO_2mv_{(end\text{-}con)}$, end-contraction PO_2mv; Δ_1PO_2mv, amplitude of the first component; Δ_2PO_2mv, amplitude of the second component; $PO_2mv_{(end\text{-}rec)}$, end-recovery PO_2mv; TD_1, time delay for the first component; TD_2, time delay for the second component; τ_1, time constant for the first component; τ_2, time constant for the second component; MRT*off*, mean response time for the off-transient; T_{63}, time to reach 63% of the overall amplitude as determined independent of modeling procedures. * Significantly different from Control. † Significantly different from SNP.

Figure 2.1 Muscle *PO_2mv* profiles during recovery from contractions under Control, SNP and L-NAME

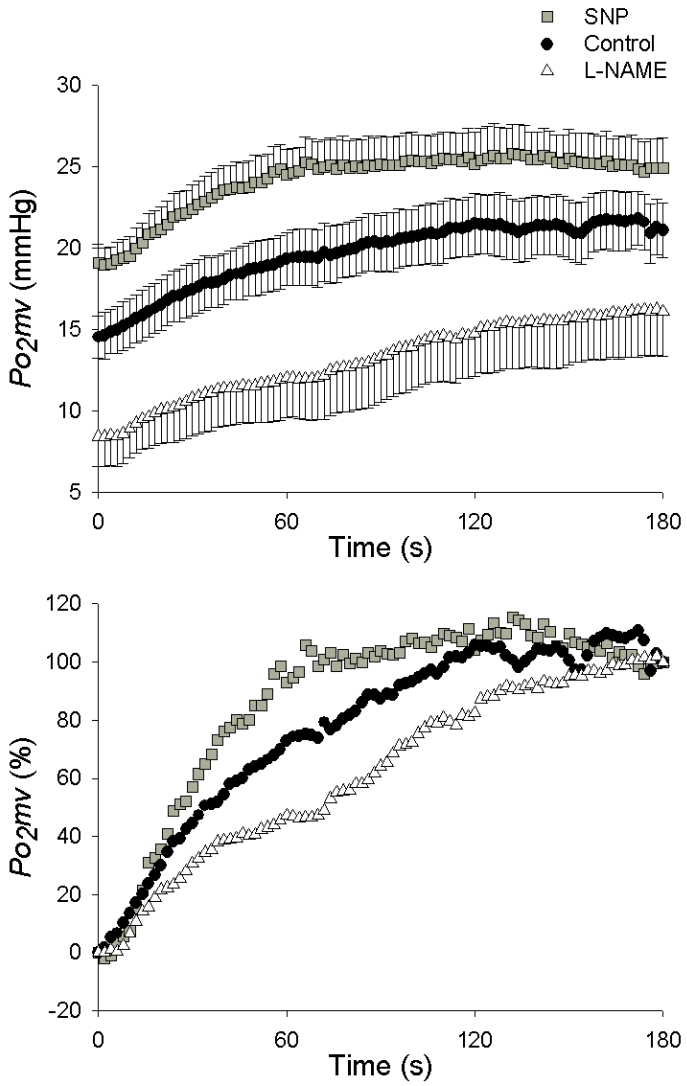

Figure 2.1 Mean muscle microvascular PO_2 (*PO_2mv*) during recovery from contractions under Control, sodium nitroprusside (SNP; increased nitric oxide) and L-nitro arginine methyl ester (L-NAME; decreased nitric oxide) superfusion. *Top* and *bottom panels* exhibit absolute and relative *PO_2mv*, respectively. SE bars omitted from *bottom panel* for clarity. Time zero depicts the onset of the recovery phase. Note that altered nitric oxide bioavailability markedly affected *PO_2mv* kinetics during the off-transition in the healthy rat spinotrapezius muscle.

Figure 2.2 Overall muscle microvascular oxygenation during recovery from contractions under Control, SNP and L-NAME

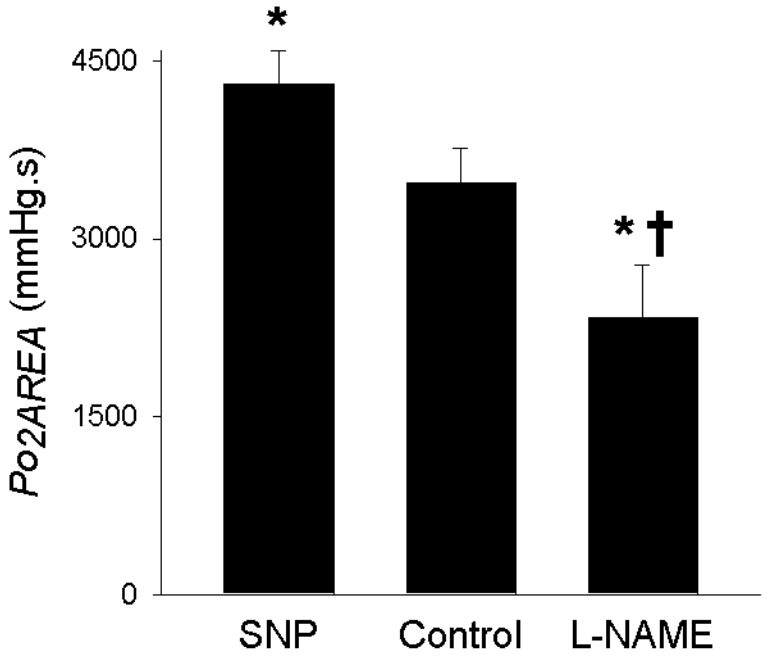

Figure 2.2 Mean values for the area under the muscle microvascular PO_2 curve (PO_{2AREA}) during recovery from contractions under Control, sodium nitroprusside (SNP) and L-nitro arginine methyl ester (L-NAME) superfusion. PO_{2AREA} was obtained through integration of the area under the PO_2mv curve over the 3 min of recovery from contractions for each condition. * Significantly different from Control. † Significantly different from SNP.

Figure 2.3 Correlation between $PO_2mv_{(end-con)}$ and MRT*off* for each animal

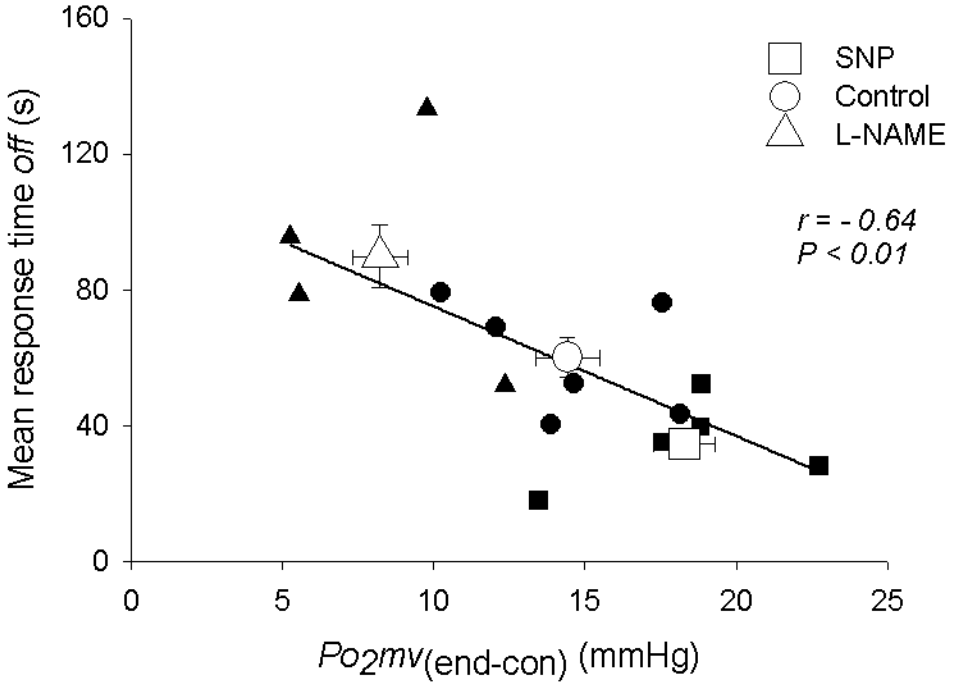

Figure 2.3 Correlation between $PO_2mv_{(end-con)}$ and MRT*off* for each animal. Control (n = 6); sodium nitroprusside (SNP; n = 5); L-nitro arginine methyl ester (L-NAME; n = 4). $PO_2mv_{(end-con)}$, end-contraction PO_2mv; MRT*off*, mean response time for the off-transient. Individual (*filled symbols*) and mean (*open symbols*) values are shown.

Figure 2.4 Correlation between MRT*on* and MRT*off* for each animal

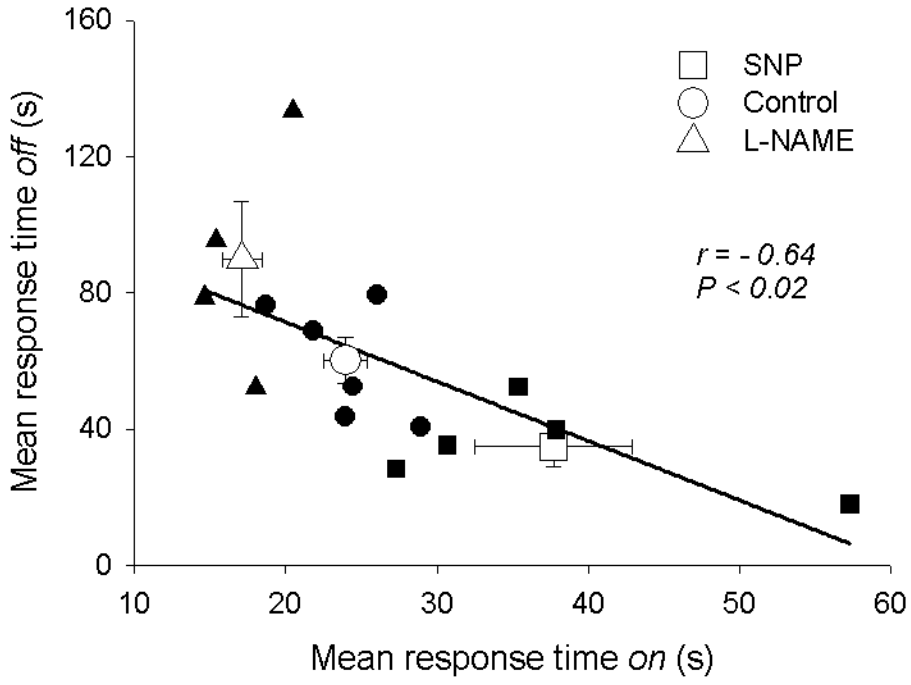

Figure 2.4 Correlation between MRT*on* and MRT*off* for each animal. On-transient data from Ferreira et al. (23). Control (n = 6); sodium nitroprusside (SNP; n = 5); L-nitro arginine methyl ester (L-NAME; n = 4). MRT*on*, mean response time for the on-transient; MRT*off*, mean response time for the off-transient. Individual (*filled symbols*) and mean (*open symbols*) values are shown.

Figure 2.5 Effects of altered nitric oxide bioavailability on muscle PO_2mv on-off kinetics

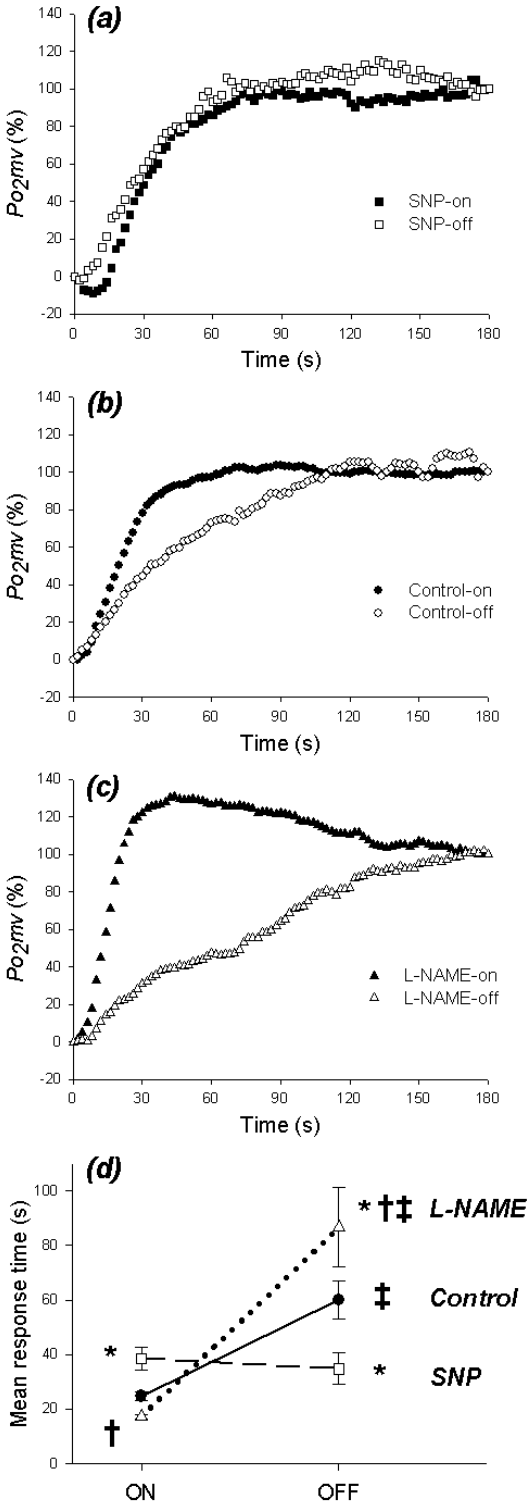

Figure 2.5 Effects of altered nitric oxide bioavailability on the muscle microvascular PO_2 (PO_2mv) on-off responses. *Panels (a-c)* depict the normalized change in mean PO_2mv kinetics following the onset and cessation of contractions under sodium nitroprusside (SNP), Control and L-nitro arginine methyl ester (L-NAME) treatments, respectively. *Filled symbols* in *panels (a-c)* illustrate the 'mirror image' of data from Ferreira et al. (23) for PO_2mv on-kinetics. SE bars omitted for clarity. *Panel (d)* shows the mean response time for the exercise on- (MRT*on*) and off- (MRT*off*) transients under Control, SNP and L-NAME. Note the symmetry between PO_2mv on-off responses for SNP and the pronounced asymmetry for Control and L-NAME. * Significantly different from Control. † Significantly different from SNP. ‡ Significantly different from the on-transient within condition. See text for further details.

References

1. **Bearden SE**. Advancing age produces sex differences in vasomotor kinetics during and after skeletal muscle contraction. *Am J Physiol Regul Integr Comp Physiol* 293: R1274-1279, 2007.

2. **Behnke BJ, Delp MD, Dougherty PJ, Musch TI, and Poole DC**. Effects of aging on microvascular oxygen pressures in rat skeletal muscle. *Respir Physiol Neurobiol* 146: 259-268, 2005.

3. **Behnke BJ, Ferreira LF, McDonough PJ, Musch TI, and Poole DC**. Recovery Dynamics of Skeletal Muscle Oxygen Uptake during the Exercise Off-Transient. *Respir Physiol Neurobiol* 2009.

4. **Behnke BJ, Kindig CA, McDonough P, Poole DC, and Sexton WL**. Dynamics of microvascular oxygen pressure during rest-contraction transition in skeletal muscle of diabetic rats. *Am J Physiol Heart Circ Physiol* 283: H926-932, 2002.

5. **Behnke BJ, Kindig CA, Musch TI, Koga S, and Poole DC**. Dynamics of microvascular oxygen pressure across the rest-exercise transition in rat skeletal muscle. *Respir Physiol* 126: 53-63, 2001.

6. **Behnke BJ, Kindig CA, Musch TI, Sexton WL, and Poole DC**. Effects of prior contractions on muscle microvascular oxygen pressure at onset of subsequent contractions. *J Physiol* 539: 927-934, 2002.

7. **Behnke BJ, McDonough P, Padilla DJ, Musch TI, and Poole DC**. Oxygen exchange profile in rat muscles of contrasting fibre types. *J Physiol* 549: 597-605, 2003.

8. **Behnke BJ, Padilla DJ, Ferreira LF, Delp MD, Musch TI, and Poole DC**. Effects of arterial hypotension on microvascular oxygen exchange in contracting skeletal muscle. *J Appl Physiol* 100: 1019-1026, 2006.

9. **Brown GC**. Nitric oxide and mitochondrial respiration. *Biochim Biophys Acta* 1411: 351-369, 1999.

10. **Chilibeck PD, Paterson DH, Smith WD, and Cunningham DA**. Cardiorespiratory kinetics during exercise of different muscle groups and mass in old and young. *J Appl Physiol* 81: 1388-1394, 1996.

11. **Clark AL, Poole-Wilson PA, and Coats AJ**. Exercise limitation in chronic heart failure: central role of the periphery. *J Am Coll Cardiol* 28: 1092-1102, 1996.

12. **Clifford PS, and Hellsten Y**. Vasodilatory mechanisms in contracting skeletal muscle. *J Appl Physiol* 97: 393-403, 2004.

13. **Conley KE, Jubrias SA, and Esselman PC**. Oxidative capacity and ageing in human muscle. *J Physiol* 526 Pt 1: 203-210, 2000.

14. **Copp SW, Ferreira LF, Herspring KF, Hirai DM, Snyder BS, Poole DC, and Musch TI**. The effects of antioxidants on microvascular oxygenation and blood flow in skeletal muscle of young rats. *Exp Physiol* 94: 961-971, 2009.

15. **Copp SW, Ferreira LF, Herspring KF, Musch TI, and Poole DC**. The effects of aging on capillary hemodynamics in contracting rat spinotrapezius muscle. *Microvascular Research* 77: 113-119, 2009.

16. **Delp MD, and Duan C**. Composition and size of type I, IIA, IID/X, and IIB fibers and citrate synthase activity of rat muscle. *J Appl Physiol* 80: 261-270, 1996.

17. **Didion SP, and Mayhan WG**. Effect of chronic myocardial infarction on in vivo reactivity of skeletal muscle arterioles. *Am J Physiol* 272: H2403-2408, 1997.

18. **Diederich ER, Behnke BJ, McDonough P, Kindig CA, Barstow TJ, Poole DC, and Musch TI**. Dynamics of microvascular oxygen partial pressure in contracting skeletal muscle of rats with chronic heart failure. *Cardiovasc Res* 56: 479-486, 2002.

19. **Drexler H, Hayoz D, Munzel T, Hornig B, Just H, Brunner HR, and Zelis R**. Endothelial function in chronic congestive heart failure. *Am J Cardiol* 69: 1596-1601, 1992.

20. **Ferreira LF, Hageman KS, Hahn SA, Williams J, Padilla DJ, Poole DC, and Musch TI**. Muscle microvascular oxygenation in chronic heart failure: role of nitric oxide availability. *Acta Physiol (Oxf)* 188: 3-13, 2006.

21. **Ferreira LF, McDonough P, Behnke BJ, Musch TI, and Poole DC**. Blood flow and O_2 extraction as a function of O_2 uptake in muscles composed of different fiber types. *Respir Physiol Neurobiol* 153: 237-249, 2006.

22. **Ferreira LF, Padilla DJ, Musch TI, and Poole DC**. Temporal profile of rat skeletal muscle capillary haemodynamics during recovery from contractions. *J Physiol* 573: 787-797, 2006.

23. **Ferreira LF, Padilla DJ, Williams J, Hageman KS, Musch TI, and Poole DC**. Effects of altered nitric oxide availability on rat muscle microvascular oxygenation during contractions. *Acta Physiol (Oxf)* 186: 223-232, 2006.

24. **Ferreira LF, Poole DC, and Barstow TJ**. Muscle blood flow-O_2 uptake interaction and their relation to on-exercise dynamics of O_2 exchange. *Respir Physiol Neurobiol* 147: 91-103, 2005.

25. **Frandsenn U, Bangsbo J, Sander M, Hoffner L, Betak A, Saltin B, and Hellsten Y**. Exercise-induced hyperaemia and leg oxygen uptake are not altered during effective inhibition of nitric oxide synthase with N(G)-nitro-L-arginine methyl ester in humans. *J Physiol* 531: 257-264, 2001.

26. **Grassi B, Hogan MC, Kelley KM, Howlett RA, and Gladden LB**. Effects of nitric oxide synthase inhibition by L-NAME on oxygen uptake kinetics in isolated canine muscle in situ. *J Physiol* 568: 1021-1033, 2005.

27. **Hammer LW, and Boegehold MA**. Functional hyperemia is reduced in skeletal muscle of aged rats. *Microcirculation* 12: 517-526, 2005.

28. **Haseler LJ, Hogan MC, and Richardson RS**. Skeletal muscle phosphocreatine recovery in exercise-trained humans is dependent on O_2 availability. *J Appl Physiol* 86: 2013-2018, 1999.

29. **Herspring KF, Ferreira LF, Copp SW, Snyder BS, Poole DC, and Musch TI**. Effects of antioxidants on contracting spinotrapezius muscle microvascular oxygenation and blood flow in aged rats. *J Appl Physiol* 105: 1889-1896, 2008.

30. **Hirai DM, Copp SW, Herspring KF, Ferreira LF, Poole DC, and Musch TI**. Aging impacts microvascular oxygen pressures during recovery from contractions in rat skeletal muscle. *Respir Physiol Neurobiol* 2009.

31. **Hirai T, Visneski MD, Kearns KJ, Zelis R, and Musch TI**. Effects of NO synthase inhibition on the muscular blood flow response to treadmill exercise in rats. *J Appl Physiol* 77: 1288-1293, 1994.

32. **Honig CR, Gayeski TEJ, and Groebe K**. Myoglobin and oxygen gradients. In: *The Lung: Scientific Foundations*, edited by Crystal RG, West JB, Weibel ER, and Barnes P. Philadelphia: Lippincott-Raven Publishers, 1997, p. 1925-1933.

33. **Idstrom JP, Subramanian VH, Chance B, Schersten T, and Bylund-Fellenius AC**. Oxygen dependence of energy metabolism in contracting and recovering rat skeletal muscle. *Am J Physiol* 248: H40-48, 1985.

34. **Inbar O, Oren A, Scheinowitz M, Rotstein A, Dlin R, and Casaburi R**. Normal cardiopulmonary responses during incremental exercise in 20- to 70-yr-old men. *Med Sci Sports Exerc* 26: 538-546, 1994.

35. **Jones AM, Wilkerson DP, Koppo K, Wilmshurst S, and Campbell IT**. Inhibition of nitric oxide synthase by L-NAME speeds phase II pulmonary VO_2 kinetics in the transition to moderate-intensity exercise in man. *J Physiol* 552: 265-272, 2003.

36. **Jones AM, Wilkerson DP, Wilmshurst S, and Campbell IT**. Influence of L-NAME on pulmonary O_2 uptake kinetics during heavy-intensity cycle exercise. *J Appl Physiol* 96: 1033-1038, 2004.

37. **Kemps HM, Prompers JJ, Wessels B, de Vries WR, Zonderland ML, Thijssen EJ, Nicolay K, Schep G, and Doevendans PA**. Skeletal muscle metabolic recovery following submaximal exercise in chronic heart failure is limited more by O_2 delivery than O_2 utilization. *Clin Sci (Lond)* 2009.

38. **Kindig CA, McDonough P, Erickson HH, and Poole DC**. Effect of L-NAME on oxygen uptake kinetics during heavy-intensity exercise in the horse. *J Appl Physiol* 91: 891-896, 2001.

39. **Kindig CA, McDonough P, Erickson HH, and Poole DC**. Nitric oxide synthase inhibition speeds oxygen uptake kinetics in horses during moderate domain running. *Respir Physiol Neurobiol* 132: 169-178, 2002.

40. **Kindig CA, Richardson TE, and Poole DC**. Skeletal muscle capillary hemodynamics from rest to contractions: implications for oxygen transfer. *J Appl Physiol* 92: 2513-2520, 2002.

41. **Kindig CA, Sexton WL, Fedde MR, and Poole DC**. Skeletal muscle microcirculatory structure and hemodynamics in diabetes. *Respir Physiol* 111: 163-175, 1998.

42. **Kindig CA, Walsh B, Howlett RA, Stary CM, and Hogan MC**. Relationship between intracellular PO_2 recovery kinetics and fatigability in isolated single frog myocytes. *J Appl Physiol* 98: 2316-2319, 2005.

43. **Krustrup P, Jones AM, Wilkerson DP, Calbet JA, and Bangsbo J**. Muscular and pulmonary O_2 uptake kinetics during moderate- and high-intensity sub-maximal knee-extensor exercise in humans. *J Physiol* 587: 1843-1856, 2009.

44. **Laughlin MH, McAllister RM, and Delp MD**. Heterogeneity of blood flow in striated muscle. In: *The Lung: Scientific Foundations*, edited by Crystal RG, West JB, Weibel ER, and Barnes P. Philadelphia: Lippincott-Raven Publishers, 1997, p. 1945-1955.

45. **Leek BT, Mudaliar SR, Henry R, Mathieu-Costello O, and Richardson RS**. Effect of acute exercise on citrate synthase activity in untrained and trained human skeletal muscle. *Am J Physiol Regul Integr Comp Physiol* 280: R441-447, 2001.

46. **Linke A, Schoene N, Gielen S, Hofer J, Erbs S, Schuler G, and Hambrecht R**. Endothelial dysfunction in patients with chronic heart failure: systemic effects of lower-limb exercise training. *J Am Coll Cardiol* 37: 392-397, 2001.

47. **Macdonald M, Pedersen PK, and Hughson RL**. Acceleration of VO_2 kinetics in heavy submaximal exercise by hyperoxia and prior high-intensity exercise. *J Appl Physiol* 83: 1318-1325, 1997.

48. **McDonough P, Behnke BJ, Kindig CA, and Poole DC**. Rat muscle microvascular PO_2 kinetics during the exercise off-transient. *Exp Physiol* 86: 349-356, 2001.

49. **McDonough P, Behnke BJ, Musch TI, and Poole DC**. Effects of chronic heart failure in rats on the recovery of microvascular PO_2 after contractions in muscles of opposing fibre type. *Exp Physiol* 89: 473-485, 2004.

50. **McDonough P, Behnke BJ, Musch TI, and Poole DC**. Recovery of microvascular PO_2 during the exercise off-transient in muscles of different fiber type. *J Appl Physiol* 96: 1039-1044, 2004.

51. **Muller-Delp JM, Spier SA, Ramsey MW, and Delp MD**. Aging impairs endothelium-dependent vasodilation in rat skeletal muscle arterioles. *Am J Physiol Heart Circ Physiol* 283: H1662-1672, 2002.

52. **Murrant CL, Andrade FH, and Reid MB**. Exogenous reactive oxygen and nitric oxide alter intracellular oxidant status of skeletal muscle fibres. *Acta Physiol Scand* 166: 111-121, 1999.

53. **Musch TI, McAllister RM, Symons JD, Stebbins CL, Hirai T, Hageman KS, and Poole DC**. Effects of nitric oxide synthase inhibition on vascular conductance during high speed treadmill exercise in rats. *Exp Physiol* 86: 749-757, 2001.

54. **Padilla DJ, McDonough P, Behnke BJ, Kano Y, Hageman KS, Musch TI, and Poole DC**. Effects of Type II diabetes on capillary hemodynamics in skeletal muscle. *Am J Physiol Heart Circ Physiol* 291: H2439-2444, 2006.

55. **Padilla DJ, McDonough P, Behnke BJ, Kano Y, Hageman KS, Musch TI, and Poole DC**. Effects of Type II diabetes on muscle microvascular oxygen pressures. *Respir Physiol Neurobiol* 156: 187-195, 2007.

56. **Poole DC, Barstow TJ, McDonough P, and Jones AM**. Control of oxygen uptake during exercise. *Med Sci Sports Exerc* 40: 462-474, 2008.

57. **Poole DC, Behnke BJ, McDonough P, McAllister RM, and Wilson DF**. Measurement of muscle microvascular oxygen pressures: compartmentalization of phosphorescent probe. *Microcirculation* 11: 317-326, 2004.

58. **Poole DC, Wagner PD, and Wilson DF**. Diaphragm microvascular plasma PO_2 measured in vivo. *J Appl Physiol* 79: 2050-2057, 1995.

59. **Radegran G, and Saltin B**. Nitric oxide in the regulation of vasomotor tone in human skeletal muscle. *Am J Physiol* 276: H1951-1960, 1999.

60. **Regensteiner JG, Bauer TA, Reusch JE, Brandenburg SL, Sippel JM, Vogelsong AM, Smith S, Wolfel EE, Eckel RH, and Hiatt WR**. Abnormal oxygen uptake kinetic responses in women with type II diabetes mellitus. *J Appl Physiol* 85: 310-317, 1998.

61. **Richardson TE, Kindig CA, Musch TI, and Poole DC**. Effects of chronic heart failure on skeletal muscle capillary hemodynamics at rest and during contractions. *J Appl Physiol* 95: 1055-1062, 2003.

62. **Rossiter HB, Ward SA, Kowalchuk JM, Howe FA, Griffiths JR, and Whipp BJ**. Dynamic asymmetry of phosphocreatine concentration and O_2 uptake between the on- and off-transients of moderate- and high-intensity exercise in humans. *J Physiol* 541: 991-1002, 2002.

63. **Rumsey WL, Vanderkooi JM, and Wilson DF**. Imaging of phosphorescence: a novel method for measuring oxygen distribution in perfused tissue. *Science* 241: 1649-1651, 1988.

64. **Schrage WG, Eisenach JH, and Joyner MJ**. Ageing reduces nitric-oxide- and prostaglandin-mediated vasodilatation in exercising humans. *J Physiol* 579: 227-236, 2007.

65. **Shen W, Xu X, Ochoa M, Zhao G, Bernstein RD, Forfia P, and Hintze TH**. Endogenous nitric oxide in the control of skeletal muscle oxygen extraction during exercise. *Acta Physiol Scand* 168: 675-686, 2000.

66. **Sheriff DD, Nelson CD, and Sundermann RK**. Does autonomic blockade reveal a potent contribution of nitric oxide to locomotion-induced vasodilation? *Am J Physiol Heart Circ Physiol* 279: H726-732, 2000.

67. **Shoemaker JK, Halliwill JR, Hughson RL, and Joyner MJ**. Contributions of acetylcholine and nitric oxide to forearm blood flow at exercise onset and recovery. *Am J Physiol* 273: H2388-2395, 1997.

68. **Sietsema KE, Ben-Dov I, Zhang YY, Sullivan C, and Wasserman K**. Dynamics of oxygen uptake for submaximal exercise and recovery in patients with chronic heart failure. *Chest* 105: 1693-1700, 1994.

69. **Sindler AL, Delp MD, Reyes R, Wu G, and Muller-Delp JM**. Effects of ageing and exercise training on eNOS uncoupling in skeletal muscle resistance arterioles. *J Physiol* 587: 3885-3897, 2009.

70. **Spier SA, Delp MD, Meininger CJ, Donato AJ, Ramsey MW, and Muller-Delp JM**. Effects of ageing and exercise training on endothelium-dependent vasodilatation and structure of rat skeletal muscle arterioles. *J Physiol* 556: 947-958, 2004.

71. **Stamler JS, and Meissner G**. Physiology of nitric oxide in skeletal muscle. *Physiol Rev* 81: 209-237, 2001.

72. **Vinogradov SA, Fernandez-Searra MA, Dugan BW, and Wilson DF**. Frequency domain instrument for measuring phosphorescence lifetime distributions in heterogeneous samples. *Rev Sci Instrum* 72: 3396-3406, 2001.

73. **Wilkerson DP, Campbell IT, and Jones AM**. Influence of nitric oxide synthase inhibition on pulmonary O_2 uptake kinetics during supra-maximal exercise in humans. *J Physiol* 561: 623-635, 2004.

Chapter 3 - Effects of neuronal nitric oxide synthase inhibition on microvascular and contractile function in skeletal muscle of aged rats

Summary

Advanced age is associated with derangements in skeletal muscle microvascular function during the transition from rest to contractions. We tested the hypothesis that, contrary to what was reported previously in young rats, selective neuronal nitric oxide synthase (nNOS)-inhibition would result in attenuated or absent alterations in skeletal muscle microvascular oxygenation (PO_2mv; which reflects the matching between muscle O_2 delivery and utilization) following the onset of contractions in old rats. Spinotrapezius muscle blood flow (radiolabeled microspheres), PO_2mv (phosphorescence quenching), O_2 utilization ($\dot{V}O_2$; Fick calculation) and submaximal force production were measured at rest and following the onset of contractions in anesthetized old male Fisher 344 x Brown Norway rats (27-28 mo) pre- and post-selective nNOS inhibition (2.1 µmol/kg S-methyl-L-thiocitrulline; SMTC). At rest, SMTC had no effects on muscle blood flow ($p>0.05$) but reduced $\dot{V}O_2$ by ~23% ($p<0.05$), which elevated basal PO_2mv by ~18% ($p<0.05$). During contractions, steady-state muscle blood flow, $\dot{V}O_2$, PO_2mv and force production were not altered after SMTC ($p>0.05$ for all). The overall PO_2mv dynamics at contractions onset was also unaffected by SMTC (mean response time; pre: 19.7 ± 1.5; post: 20.0 ± 2.0 s; $p>0.05$). These results indicate that the locus of nNOS-derived NO control in skeletal muscle depends on age and metabolic rate (i.e., rest vs. contractions). Alterations in nNOS-mediated regulation of contracting skeletal muscle microvascular function with aging may contribute to poor exercise capacity in this population.

Introduction

Nitric oxide (NO) is a ubiquitous signaling messenger synthesized primarily through the conversion of L-arginine to L-citrulline by the enzyme nitric oxide synthase (NOS). Within skeletal muscle, NO plays a critical role in the modulation of several physiological processes including vascular relaxation, oxidative metabolism and excitation-contraction coupling (56). All three major NOS isoforms are expressed in mammalian skeletal muscle, namely neuronal NOS (nNOS), endothelial NOS (eNOS) and inducible NOS (iNOS) (56). Several lines of evidence indicate that NO derived from nNOS participates significantly in the matching of muscle O_2 delivery and utilization ($\dot{Q}O_2/\dot{V}O_2$) at rest and during contractions as well as submaximal force production in healthy young individuals (12, see also refs. 13, 15, 19, 28, 33, 36, 39, 45, 52, 53, 60).

Advancing age is associated with impairments in the O_2 transport pathway and exercise capacity (47). Derangements in NO-mediated function likely represent one of the main mechanisms underlying temporal $\dot{Q}O_2/\dot{V}O_2$ mismatch during transitions in metabolic demand in aged skeletal muscle (5, 16, 23, 25). Impairments in the ability to regulate $\dot{Q}O_2$ relative to $\dot{V}O_2$ diminish muscle microvascular O_2 pressures (PO_2mv) and thus the driving force for blood-myocyte O_2 flux as dictated by Fick's law of diffusion. These alterations are of functional significance given that reductions in PO_2mv impact negatively on mitochondrial control and could explain, at least in part, poor exercise capacity with aging (29, 57). In view of the typical deterioration of endothelial function in the elderly (54, 65), age-related decrements in NO bioavailability have been ascribed traditionally to eNOS dysfunction. Whether nNOS dysfunction is potentially involved in impaired muscle $\dot{Q}O_2/\dot{V}O_2$ control with aging remains unexplored.

Given that advanced aging might impact both nNOS and eNOS function possibly due to prominent oxidative stress that promotes NOS uncoupling and/or direct NO inactivation (21, 49, 54, 58), we examined whether nNOS-derived control of skeletal muscle microvascular and contractile function is altered in old rats. The hypothesis was tested that, contrary to what was observed previously in young rats (12), selective nNOS inhibition in old rats would result in

attenuated or absent alterations in resting and contracting muscle blood flow, $\dot{V}O_2$, PO_2mv and submaximal force production, thus indicating impaired nNOS-mediated microvascular and contractile control with aging.

Methods

A total of 21 old (27-28 mo; body mass 614 ± 11 g) male Fisher 344 x Brown Norway (F344xBN) rats were used in the present study for measurements of PO_2mv and muscle blood flow (phosphorescence quenching and radiolabeled microspheres, respectively; n = 11), force production (n = 6) and time-control experiments (n = 4). Rats were obtained from Charles Rivers Laboratories and maintained on a 12:12-h light-dark cycle with food and water provided *ad libitum*. The selected age represents senescent rats according to the life-span of the F344xBN rodent strain (38). The F344xBN rat has the distinct advantage of not acquiring many of the age-related pathologies that proliferate in their highly inbred counterparts (40). Upon completion of the study, rats were euthanized with intra-arterial pentobarbital overdose (~50 mg/kg). All procedures described herein were conducted under the guidelines established by the National Institutes of Health and approved by the Institutional Animal Care and Use Committee of Kansas State University.

Experimental design consideration

Comparison with young rats is facilitated using data from ref. 12. The rationale for this procedure is based on the IACUC stipulation that additional animals not be sacrificed for replication of data. In addition, direct comparison between old and young (12) animals is facilitated by the fact that both experimental groups underwent the exact same protocols and old and young animal experiments were temporally interdigitated.

Surgical preparation

Rats were anesthetized initially with 5% isoflurane-O_2 mixture and maintained on 2-3% isoflurane-O_2. The caudal (tail) artery was isolated surgically and cannulated (PE-50; Intra-Medic Tubing, Clay Adams Brand) for continuous monitoring of heart rate and mean arterial pressure (HR and MAP, respectively; Digi-Med BPA model 200) and infusion of the phosphorescent probe palladium *meso*-tetra (4-carboxyphenyl) porphyrin dendrimer (R2; 15 mg/kg; Oxygen Enterprises). Blood from the tail artery catheter was sampled at the end of each experimental condition (control and selective nNOS inhibition with S-methyl-L-thiocitrulline;

SMTC) for the determination of arterial blood gases, pH, systemic hematocrit and plasma lactate (n = 11). For blood flow measurements, an additional catheter (PE-10 connected to PE-50) was placed in the ascending aorta via the right carotid artery to allow injection of differently radiolabeled microspheres into the aortic arch. Anesthetized rats were maintained on a heating pad to maintain core temperature at ~37-38°C as measured via rectal probe.

Isoflurane-O_2 mixture inhalation was progressively discontinued after catheter placement procedures and rats were then kept under anesthesia with pentobarbital sodium (administered i.a. to effect). The level of anesthesia was monitored frequently via the toe-pinch and blink reflexes and supplemented as necessary. Overlying skin and fascia from the middorsal region of the rat were reflected surgically to expose the right spinotrapezius muscle. The muscle was moistened constantly throughout the surgery and experimental protocol via superfusion of Krebs-Henseleit bicarbonate-buffered solution (4.7 mM KCl, 2.0 mM $CaCl_2$, 2.4 mM $MgSO_4$, 131 mM NaCl and 22 mM $NaHCO_3$; equilibrated with 5% CO_2 and 95% N_2; pH 7.4; warmed to 37-38°C) and surrounding tissue was covered with Saran wrap (Dow Brands). Stainless steel electrodes were sutured to the rostral (cathode) and caudal (anode) regions of the spinotrapezius muscle for electrically induced contractions. Our laboratory has demonstrated previously that these surgical procedures do not alter the microvascular integrity and responsiveness of the spinotrapezius muscle (3).

Experimental protocol

Two separate contraction bouts were performed under control (1.2 ml heparinized saline) and selective nNOS inhibition (2.1 μmol/kg SMTC dissolved in 1.2 ml heparinized saline) conditions. This dose of SMTC was selected based on previous studies designed to inhibit selectively nNOS in both humans and rodents (18, 30, 53, 64) and our analysis of the highest possible SMTC dose that could be administered without affecting the hypotensive response to acetylcholine (indicative of non-specific eNOS inhibition; refs. 12, 13). Each solution was infused at a rate of 0.2 ml/min into the tail artery catheter for a total time of 6 min, after which a ~2 min period was allowed for resting muscle PO_2mv to stabilize. Subsequently, 1 Hz twitch contractions (~7 V, 2 ms pulse duration) were evoked via a stimulator (model s48; Grass Technologies) for 3 min. The muscle was then allowed to recover for a minimum of 25 min before the next condition was initiated (stimulation parameters held constant). Due to its

relatively long half-life (~40 min; refs. 18, 64), SMTC was always the last condition in order to prevent residual effects on vascular and skeletal muscle function. Importantly, there is no ordering (priming) effect on the PO_2mv response to muscle contractions when a minimum of 20 min of recovery is allowed between stimulations (7, 16).

Effects of SMTC and L-NAME on the hypotensive responses to acetylcholine

In a subset of animals (n = 8 of 21 total rats), rapid acetylcholine infusions (5 μg/kg in 0.2 ml of heparinized saline) were performed under control and SMTC conditions as well as after non-selective NOS inhibition with N^G-nitro-L-arginine-methyl-ester (L-NAME; 10 mg/kg) administered into the caudal artery. The hypotensive responses to these infusions were recorded via the carotid artery catheter to confirm the efficacy of selective nNOS inhibition with SMTC (12, 13).

Measurement of PO_2mv

PO_2mv was measured by phosphorescence quenching using a Frequency Domain Phosphorometer (PMOD 5000; Oxygen Enterprises). As described in detail previously (6), this method applies the Stern-Volmer relationship (51) which describes quantitatively the O_2 dependence of the phosphorescent probe (i.e., R2) via the following equation:

$$Po_2mv = [(\tau^\circ / \tau) - 1]/(k_Q \times \tau^\circ)$$

where k_Q is the quenching constant and τ and τ° are the phosphorescence lifetimes in the absence of O_2 and at the ambient O_2 pressure, respectively. The τ of phosphorescence decay was determined using 10 scans (100 ms) in the single-frequency mode. The phosphorescent probe R2 (τ° = 601 μs and k_Q = 409 $mmHg^{-1}{\cdot}s^{-1}$ at pH = 7.4 and temperature 38°C) (51, 63) was infused approximately 15 min before initiation of muscle contractions. R2 is bound to albumin and is distributed uniformly in the plasma, thus providing a signal corresponding to the volume-weighted O_2 pressure within the microvascular compartment (i.e., mainly the PO_2 within the capillaries, which volumetrically constitutes the major intramuscular space) (48). The negative charge of the R2 probe also facilitates its restriction to the intravascular space (46).

The common end of the light guide was placed ~2-4 mm superficial to the dorsal surface of the exposed right spinotrapezius muscle. The phosphorometer modulates sinusoidal excitation frequencies between 100 Hz and 20 kHz and allows phosphorescence lifetime measurements from 10 μs to ~ 2.5 ms. The excitation light (524 nm) was focused on a randomly-selected area of ~2 mm diameter within the central region of the exposed muscle and has a penetration depth of ~500 μm. PO_2mv was measured continuously and recorded at 2 s intervals throughout the duration of the experimental protocols.

Analysis of PO_2mv kinetics

The kinetics of PO_2mv were described by nonlinear regression analysis using the Marquardt-Levenberg algorithm (SigmaPlot 11.2; Systat software) for the onset of contractions. Transient PO_2mv responses were fit with either a one- or two-component model:

One component:

$$PO_2mv_{(t)} = PO_2mv_{(BL)} - \Delta PO_2mv(1 - e^{-(t-TD)/\tau})$$

Two-component:

$$PO_2mv_{(t)} = PO_2mv_{(BL)} - \Delta_1 PO_2mv(1 - e^{-(t-TD_1)/\tau_1}) + \Delta_2 PO_2mv(1 - e^{-(t-TD_2)/\tau_2})$$

where $PO_2mv_{(t)}$ is the PO_2mv at a given time *t*, $PO_2mv_{(BL)}$ corresponds to the pre-contracting resting PO_2mv, Δ_1 and Δ_2 are the amplitudes for the first and second components, respectively, TD_1 and TD_2 are the independent time delays for each component, and τ_1 and τ_2 are the time constants (i.e., time to reach 63% of the response) for each component. Goodness of fit was determined using three criteria: 1) the coefficient of determination; 2) the sum of squared residuals; and 3) visual inspection.

The amplitude of the first component was normalized to its time constant ($\Delta_1 PO_2mv/\tau_1$) in order to provide an index of the relative rate of PO_2mv fall. The overall time necessary to attain 63% of the final amplitude of the PO_2mv response following contractions onset was determined independent of modeling procedures (T_{63}; ref. 34) to ensure appropriateness of the model fits.

The mean response time (MRT; ref. 43) was employed to describe the overall dynamics of the PO_2mv response:

$$MRT = TD_1 + \tau_1$$

where TD_1 and τ_1 are defined above. The MRT analysis was constrained to the first phase of the PO_2mv response since inclusion of the emergent second phase underestimates the actual rate of PO_2mv fall following initiation of contractions (25).

The area under the PO_2mv curve plotted as function of time (PO_{2AREA}; ref. 23) was calculated during the 3 min contraction protocol to provide an index of the overall muscle microvascular oxygenation (i.e., incorporating resting and contracting steady-state PO_2mv, time delays, amplitudes and time constants of the response to yield a value expressed in mmHg·s).

Measurement of blood flow

Spinotrapezius muscle blood flow was measured using the radiolabeled microsphere technique, as described in detail previously (44). In each condition (control and SMTC), the stimulated right and non-stimulated left spinotrapezius muscles represented the contracting and resting blood flow measurements, respectively. Briefly, the tail artery catheter was connected to a 1 ml syringe, and blood withdrawal at a constant rate of 0.25 ml/min was performed via a Harvard pump (model 907). Differently radiolabeled microspheres (^{46}Sc or ^{85}Sr; 15 µm diameter; Perkin Elmer Life and Analytical Sciences) were injected in random order into the aortic arch via the carotid artery catheter during the contracting steady-state (i.e., ~3 min after onset of stimulation). Upon completion of the experiment, the right and left spinotrapezius muscles, right and left kidneys and organs of the splanchnic region (stomach, adrenals, spleen, pancreas, small intestine, large intestine and liver) were carefully dissected, removed and weighed immediately after euthanasia. The thorax was opened and placement of the carotid artery catheter into the aortic arch was confirmed by anatomic dissection. Tissue radioactivity was determined on a gamma scintillation counter (Auto Gamma Spectrometer, Cobra model 5003; Hewlett-Packard), and blood flow was determined by the reference sample method (31) and expressed as ml/min/100 g of tissue. Adequate mixing of the microspheres was verified for each injection by demonstrating a <15% difference in blood flow between the right and left kidneys. Blood flow

data were also normalized to MAP and expressed as vascular conductance (VC; ml/min/100g/mmHg).

Calculation of muscle $\dot{V}O_2$

Muscle $\dot{V}O_2$ was calculated from PO_2mv and blood flow measurements as described previously (12, 27). Briefly, arterial O_2 concentration (CaO_2) was calculated directly from arterial blood samples, whereas venous O_2 concentration (CvO_2) was estimated from either the baseline (rest) or the contracting steady-state (contractions) PO_2mv using the rat O_2 dissociation curve (Hill coefficient of 2.6), the measured Hb concentration, a P_{50} of 38 mmHg and an O_2 carrying capacity of 1.34 ml O_2/g Hb (1). The measures of the resting and contracting spinotrapezius blood flow ($\dot{Q}m$) were then used to determine $\dot{V}O_2$ via the Fick equation [i.e., $\dot{V}O_2 = \dot{Q}m(CaO_2 - CvO_2)$].

Measurement of submaximal muscle force production

The caudal end of the spinotrapezius muscle was exteriorized and sutured to a swivel apparatus and a non-distensible light-weight (0.4 g) cable, which linked the muscle to a force transducer (model FTO3; Grass Technologies). The preload tension was set at ~0.04 N to elicit the optimal length of the muscle for twitch force production (12, 27). Muscle force production was measured throughout control and SMTC contraction bouts which were identical to the contraction protocols described above for the measurement of PO_2mv and blood flow. Force production was expressed as N/g muscle.

Time-control experiments

The stability and reproducibility of the spinotrapezius muscle preparation has been addressed previously (12, 27) and was reconfirmed in the current study via time-control experiments (i.e., 2 control contraction bouts performed as described above). The average coefficient of variation for PO_2mv kinetics and muscle force production was 9 ± 5% with no ordering effects (p>0.05). These data provide confidence that the significant effects (or lack thereof) detected herein were the direct result of selective nNOS inhibition with SMTC.

Statistical analyses

Data comparison was performed using paired Student's *t*-tests, one-way repeated measures analysis of variance (ANOVA) or two-way repeated measures ANOVA where appropriate. *Post hoc* analyses were performed with the Student-Newman-Keuls test when a significant *F* ratio was detected. The *z*-statistic was calculated to determine differences from zero. The significance level was set at $p<0.05$. Results are reported as mean ± SE.

Results

Blood sampling, hemodynamic variables and Ach injections

There were no differences in arterial blood O_2 saturation (control: 95.3 ± 0.2; SMTC: 94.4 ± 0.7%), pH (control: 7.41 ± 0.01; SMTC: 7.40 ± 0.01), lactate concentration (control: 1.0 ± 0.1; SMTC: 1.1 ± 0.1 mM) and systemic hematocrit (control: 35.6 ± 0.6; SMTC: 34.8 ± 0.6%) between conditions (p>0.05 for all).

The HR and MAP responses during control and SMTC conditions are displayed in Table 3.1. HR and MAP did not change during the control saline infusion whereas MAP increased and HR decreased during the infusion of SMTC. Within each condition, there were no significant differences between rest (post-infusion) and contractions (steady-state).

The hypotensive responses to acetylcholine infusion during control, SMTC and L-NAME conditions are depicted in Fig. 3.1. The relative change in MAP with acetylcholine was not different between control and SMTC but decreased significantly with L-NAME. Similarly, the time to 50% recovery from the drop in MAP with acetylcholine was not different between control and SMTC but speeded significantly with L-NAME. These data are consistent with the notion that SMTC did not impair eNOS function in the present study.

Spinotrapezius PO_2mv

Mean spinotrapezius muscle PO_2mv during control and SMTC infusions are shown in Fig. 3.2. The control infusion did not change PO_2mv (pre-infusion: 36.1 ± 1.2; post-infusion: 37.4 ± 1.3 mmHg; p>0.05) whereas SMTC infusion increased PO_2mv from 35.3 ± 1.6 to 41.9 ± 2.2 mmHg (p<0.05). PO_2mv was not different between control and SMTC at the start or during the first 5 min of infusion (p>0.05) but was increased significantly by the end of SMTC infusion.

Mean spinotrapezius muscle PO_2mv following the onset of contractions during control and SMTC conditions are shown in Fig. 3.3 and average kinetics parameters displayed in Table 3.2. Although the time delay of the PO_2mv fall following the onset of contractions (TD_1; p<0.05) was reduced, SMTC did not change the PO_2mv time constant (τ_1; p>0.05). Furthermore, no differences in the overall dynamics of PO_2mv as represented by the MRT (model dependent), T_{63} (model independent) and $\Delta_1 PO_2mv/\tau_1$ (relative rate of PO_2mv fall) were observed between

conditions (p>0.05 for all). SMTC did, however, increase the amplitude of the PO_2mv fall during contractions ($\Delta_1 PO_2mv$; p<0.05) such that the contracting steady-state PO_2mv ($PO_2mv_{(SS)}$; p>0.05) was not different between conditions. Although SMTC elevated resting PO_2mv, the overall muscle microvascular oxygenation during contractions as represented by the PO_{2AREA} was not significantly different between conditions.

Spinotrapezius blood flow and $\dot{V}O_2$

At rest, blood flow (Fig. 3.4, *top left panel*) and VC (control: 0.09 ± 0.02; SMTC: 0.07 ± 0.01 ml/min/100g/mmHg; p>0.05) were not different between control and SMTC. During contractions, blood flow (Fig. 3.4, *top right panel*) was not different whereas VC (control: 1.01 ± 0.09; SMTC: 0.82 ± 0.08 ml/min/100g/mmHg; p<0.05) was reduced with SMTC compared to control. Accordingly, SMTC did not alter the change in blood flow from rest to contractions (Δblood flow; control: 98.0 ± 9.1; SMTC: 97.1 ± 10.8 ml/min/100g; p>0.05) but attenuated the change in VC during the rest-contraction transient (ΔVC; control: 0.92 ± 0.09; SMTC: 0.75 ± 0.07 ml/min/100g/mmHg; p<0.05).

Relative to the control condition, SMTC reduced significantly resting but not contracting spinotrapezius muscle $\dot{V}O_2$ (Fig. 3.4, *bottom panels*). However, from rest to contractions the change in muscle $\dot{V}O_2$ was not different between conditions ($\Delta\dot{V}O_2$; control: 10.5 ± 1.0; SMTC: 10.2 ± 1.5 ml/min/100g; p>0.05).

Spinotrapezius muscle force production

As illustrated in Fig. 3.5, mean spinotrapezius muscle force production throughout the contraction protocol and the force-time integral were not significantly different between control and SMTC conditions. Similarly, the average steady-state force production-to-$\dot{V}O_2$ ratio was also unaffected by SMTC (force/$\dot{V}O_2$; control: 0.024 ± 0.001; SMTC: 0.023 ± 0.001 N/ml O_2/min; p>0.05).

Abdominal organ blood flow and VC

The effects of SMTC on resting blood flow and VC in the kidneys and organs of the splanchnic region are displayed in Table 3.3. Relative to control, SMTC decreased blood flow in

the kidneys, stomach, adrenals, spleen and large intestine ($p<0.05$ for all). SMTC decreased VC in the kidneys, stomach, adrenals, spleen, pancreas, small intestine and large intestine ($p<0.05$ for all).

Discussion

The present investigation determined the effects of selective nNOS inhibition on skeletal muscle function at rest and during contractions in old rats. The principal novel finding was that the changes in contracting muscle blood flow, $\dot{V}O_2$, PO_2mv kinetics and submaximal force production produced by nNOS-inhibition in healthy young rats (12) were absent in old rats (see Fig. 3.6). Specifically, selective nNOS inhibition in old rats resulted in 1) alterations in resting muscle $\dot{V}O_2$ (↓23%) and PO_2mv (↑18%) but not blood flow; 2) no changes in steady-state blood flow, $\dot{V}O_2$ or PO_2mv during contractions; 3) no changes in the overall dynamics of PO_2mv following the onset of contractions; and 4) no changes in muscle force production. These data suggest that nNOS-mediated control of contracting skeletal muscle microvascular and contractile function is altered in old rats.

Effects of selective nNOS inhibition on skeletal muscle function in old rats

Skeletal muscle PO_2mv is dictated by the dynamic $\dot{Q}O_2/\dot{V}O_2$ matching within the microvascular space (6). We reported recently that selective nNOS inhibition with SMTC in healthy young rats increased resting spinotrapezius PO_2mv via reductions in $\dot{V}O_2$ concomitant with no alterations in muscle blood flow (12). In the present study, similar effects were observed following SMTC infusion in old rats (Figs. 3.2 and 3.4, Table 3.2), thus suggesting that nNOS-mediated function is preserved within aged skeletal muscle at least at rest. The lack of an effect of SMTC on resting skeletal muscle blood flow in both young (12) and old (Fig. 3.4, *top left panel*) anesthetized rats contrasts with that seen previously in the human forearm (53) and awake rat hindlimb (13) circulations. The reasons for this discrepancy are not entirely clear but could relate partially to the effects of anesthesia. However, the reductions in blood flow to the kidneys and organs of the abdominal region following SMTC infusion in old rats at rest (Table 3.3) are consistent with the role of nNOS-derived NO in regulating renal and splanchnic blood flow as reported previously in the awake young rat at rest (13, see also refs. 30, 32). These findings also suggest preserved nNOS-mediated function in the renal and splanchnic circulations with aging at rest.

The SMTC-induced reductions in resting spinotrapezius $\dot{V}O_2$ in both young (12) and old (Fig. 3.4, *bottom left panel*) rats are surprising considering the well-known inhibitory effects of NO on mitochondrial respiration (56) that may actually act to increase resting muscle $\dot{V}O_2$ following non-selective NOS inhibition (e.g., dogs, ref. 20, human, ref. 22). Although our data could be interpreted as reflecting a stimulatory role of NO from nNOS on mitochondrial respiration (66; see also refs. 4, 37) and/or relate to possible differences in NOS isoform compartmentalization across species, evidence from isolated cardiac muscle suggests rather that nNOS-derived NO does not control directly tissue $\dot{V}O_2$ (35, 41). In the latter scenario, reduced resting $\dot{V}O_2$ with SMTC in old rats could result from blockade of uncoupled nNOS which alleviates the inactivation of NO from eNOS and restores partially mitochondrial respiratory inhibition (cf. 35). These intriguing possibilities remain to be tested empirically in aged skeletal muscle.

Despite the apparent preserved contribution of nNOS-derived NO to resting skeletal muscle function with aging (as discussed above), the effects of SMTC on contracting muscle blood flow, $\dot{V}O_2$, PO_2mv kinetics and force production observed presently in old rats differ markedly from those reported previously in young rats (12). Specifically, selective nNOS inhibition in young rats 1) reduced contracting steady-state muscle blood flow and $\dot{V}O_2$; 2) speeded the fall in PO_2mv following the onset of contractions (i.e., shorter MRT, T_{63} and $\Delta_1 PO_2mv/\tau_1$); and 3) increased submaximal force production (12). In old rats, however, SMTC had no significant effects on any of these variables during muscle contractions (Table 3.2, Figs. 3.4 and 3.5). Figure 3.6 summarizes these results and illustrates the contrasting effects of SMTC on skeletal muscle hemodynamic, metabolic and contractile function in young (12) compared with old (present study) rats during contractions. These data thus suggest that nNOS-mediated regulation of skeletal muscle microvascular and contractile function during transitions in metabolic demand is altered with advanced aging.

Alterations in nNOS-mediated regulation of skeletal muscle during contractions, but not at rest, with aging could emanate from age-related disruptions in myocyte redox state. Enhanced reactive oxygen and nitrogen species accumulation during muscle contractions (2, 8) coupled with impaired antioxidant mechanisms in old individuals (65) may exacerbate the underlying oxidative stress characteristic of aging (17) and promote nNOS uncoupling and/or direct NO

inactivation (21, 49, 58). This leads to reduced nNOS-derived NO bioavailability which likely impacts contracting skeletal muscle microvascular and contractile function via multiple mechanisms. Specifically, considerable evidence in young subjects suggests critical regulatory roles for NO derived from nNOS on contracting muscle blood flow (via cGMP formation and/or functional sympatholysis; refs. 15, 39, 60), $\dot{V}O_2$ (contribution to oxidative enzyme inertia at contractions onset; e.g., ref. 34) and, therefore, PO_2mv kinetics (12). In addition, nNOS-derived NO bioavailability likely modulates submaximal force production via inhibitory influences on myofibrillar contractile elements (36).

Clinical implications

Understanding how aging impacts the functional role of nNOS-derived NO on skeletal muscle represents the initial step towards the development of potential therapeutic strategies targeting this isoform. Utilization of isoform selective NOS inhibitors is therefore crucial in such investigations. As discussed in detail elsewhere (12, 13) and demonstrated by previous pharmacological studies (18, 64) and the current hypotensive responses to Ach (Fig. 3.1), SMTC represents a viable tool for this purpose based on its selectivity for nNOS over both eNOS and iNOS inhibition. Acute selective pharmacological inhibition as utilized herein also minimizes the potential for chronic compensation of genetically modified nNOS models by other isoforms (33).

It is noteworthy that alterations in skeletal muscle nNOS expression and/or activity with aging (9, 11, 50, 55) may not predict nNOS-mediated function particularly in conditions associated with significant oxidative stress (e.g., aging, chronic heart failure and diabetes), which promotes nNOS uncoupling and/or direct NO inactivation (21, 49, 58). Our current results therefore suggest that nNOS-mediated regulation of skeletal muscle microvascular and contractile function is altered in old individuals. Important clinical implications arise from these findings when considering that endurance exercise training could improve nNOS-mediated function via upregulation of nNOS expression and/or activity (55) in conjunction with augmented antioxidant capacity (62).

Besides its effects on nNOS-mediated function, it is important to acknowledge that advanced age results in downregulation of eNOS alongside upregulation of iNOS which is consistent with a greater role for NO in inflammatory processes and a reduced participation in contractile function in aged skeletal muscle (55). This shift in the muscle NOS isoform profile

with aging is hallmarked by oxidative stress and endothelial dysfunction (14, 24, 26, 54, 59, 61, 65) which likely contribute to exercise intolerance in this population (47).

Experimental considerations

In view of the greater relative expression and activity of nNOS in fast-twitch compared to slow-twitch muscles (36, 39), potential alterations in skeletal muscle fiber type composition with aging could partly underlie the responses seen herein following SMTC. However, it must be noted that potential age-related shifts in muscle phenotype may not only favor an increased abundance of slow-twitch fibers as traditionally considered, but also promote alterations in the opposite direction (i.e., increased abundance of fast-twitch fibers) in both humans and animals (see ref. 10 for discussion). Despite these possibilities, F344xBN rats do not appear to experience significant changes in fiber type composition within representative skeletal muscles across the age range used herein (42).

In accordance with the latter and the fact that F344xBN rats do not develop many of the age-related pathologies seen in their highly inbred counterparts (which is essential to discern healthy aging from pathological decay; ref. 40), the National Institutes of Health supports currently the use of the F344xBN rat as a model of aging. In the absence of evidence to the contrary, we therefore consider that these key facets outweigh any likely interspecies differences in nNOS-mediated control and thus facilitate comparison with young Sprague-Dawley rats (12) and suggest that differences in strain are unlikely to play a major role in the responses seen herein following selective nNOS inhibition with SMTC (Fig. 3.6).

Conclusions

Pharmacological isoform-specific NOS inhibition revealed that nNOS-mediated control of contracting skeletal muscle function is altered with advanced aging. In marked contrast to the responses seen previously in young rats (12), nNOS inhibition with SMTC evoked no alterations in contracting muscle blood flow, $\dot{V}O_2$, PO_2mv kinetics and submaximal force production in old rats (as illustrated in Fig. 3.6). These novel findings suggest that, in addition to the documented deterioration in eNOS function (e.g., refs. 54, 65), alterations in nNOS-mediated regulation of contracting skeletal muscle microvascular function with aging may contribute to reduced exercise capacity in this population.

Table 3.1 Heart rate (HR) and mean arterial pressure (MAP) before (control) and after selective nNOS inhibition with SMTC

	Control	SMTC
At rest (pre-infusion)		
HR, bpm	297 ± 9	307 ± 4
MAP, mmHg	109 ± 3	112 ± 3
At rest (post-infusion)		
HR, bpm	305 ± 6	294 ± 4*†
MAP, mmHg	111 ± 4	126 ± 3*†
Contractions (steady-state)		
HR, bpm	309 ± 7	292 ± 6*†
MAP, mmHg	107 ± 3	129 ± 3*†

Values are mean ± SE. * $p<0.05$ *vs.* control. † $p<0.05$ *vs.* rest (pre-infusion). Within each condition, there were no significant differences between rest (post-infusion) and contractions (steady-state).

Table 3.2 Muscle PO_2mv at rest and following the onset of contractions before (control) and after selective nNOS inhibition with SMTC

	Control	SMTC
$PO_2mv_{(BL)}$, mmHg	37.7 ± 1.2	44.2 ± 2.1*
$\Delta_1 PO_2mv$, mmHg	12.4 ± 0.9	17.6 ± 2.1*
$\Delta_2 PO_2mv$, mmHg	2.3 ± 0.2	2.6 ± 0.5
$\Delta_{Total} PO_2mv$, mmHg	11.0 ± 0.7	17.2 ± 2.1*
$PO_2mv_{(SS)}$, mmHg	26.9 ± 1.3	27.3 ± 2.4
TD_1, s	10.1 ± 1.5	6.3 ± 0.7*
TD_2, s	73.1 ± 11.7	52.8 ± 14.5
τ_1, s	9.6 ± 0.9	13.7 ± 1.8
τ_2, s	59.5 ± 15.1	55.7 ± 4.7
MRT, s	19.7 ± 1.5	20.0 ± 2.0
T_{63}, s	20.9 ± 1.9	19.6 ± 1.4
$\Delta_1 PO_2mv/\tau_1$, mmHg/s	1.3 ± 0.1	1.4 ± 0.2
PO_{2AREA}, mmHg·s	4920 ± 244	5195 ± 402

Values are mean ± SE. $PO_2mv_{(BL)}$, pre-contracting PO_2mv; $\Delta_1 PO_2mv$, amplitude of the first component; $\Delta_2 PO_2mv$, amplitude of the second component; $\Delta_{Total} PO_2mv$, overall amplitude regardless of one- or two-component model fit; $PO_2mv_{(SS)}$, contracting steady-state PO_2mv; TD_1, time delay for the first component; TD_2, time delay for the second component; τ_1, time constant for the first component; τ_2, time constant for the second component; MRT, mean response time; T_{63}, time to reach 63% of the overall amplitude as determined independent of modeling procedures; $\Delta_1 PO_2mv/\tau_1$, relative rate of PO_2mv fall; PO_{2AREA}, area under the PO_2mv curve over the 3 min contraction period. The two-component exponential model was used to analyze the PO_2mv kinetics in the majority of instances (7 out of 11) in the control condition while the one-component model was required to fit the SMTC response in most rats (9 out of 11). * $p<0.05$ *vs.* control.

Table 3.3 Resting blood flow and vascular conductance in the kidneys and organs of the splanchnic region before (control) and after selective nNOS inhibition with SMTC

	Blood flow, ml/min/100g		Vascular conductance, ml/min/100g/mmHg	
	Control	**SMTC**	**Control**	**SMTC**
Kidneys	515 ± 52	319 ± 25*	4.88 ± 0.57	2.49 ± 0.19*
Stomach	55 ± 7	34 ± 2*	0.52 ± 0.08	0.27 ± 0.02*
Adrenals	798 ± 75	542 ± 55*	7.47 ± 0.72	4.20 ± 0.39*
Spleen	256 ± 28	217 ± 26*	2.43 ± 0.29	1.72 ± 0.21*
Pancreas	105 ± 19	101 ± 26	0.98 ± 0.16	0.76 ± 0.17*
Small intestine	342 ± 37	290 ± 18	3.24 ± 0.40	2.27 ± 0.17*
Large intestine	116 ± 8	95 ± 5*	1.09 ± 0.08	0.75 ± 0.05*
Liver †	23 ± 3	25 ± 5	0.21 ± 0.03	0.19 ± 0.04

Values are mean ± SE. † Designates arterial, not portal blood flow and vascular conductance. * $p<0.05$ *vs.* control.

Figure 3.1 Effects of SMTC and L-NAME on the hypotensive responses to acetylcholine

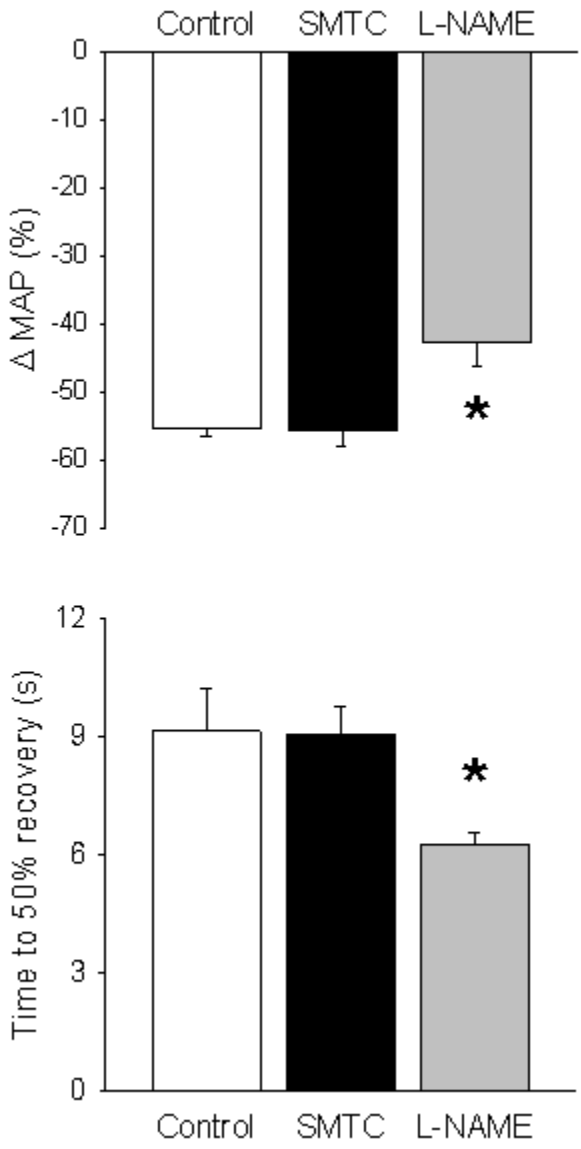

Figure 3.1 Effects of selective nNOS inhibition (SMTC) and non-selective NOS inhibition (L-NAME) on the hypotensive responses to acetylcholine. *Top* and *bottom* panels depict the relative drop in mean arterial pressure (MAP) and time to 50% recovery from the hypotensive response to acetylcholine, respectively. * $p<0.05$ *vs.* control and SMTC.

Figure 3.2 Muscle *PO_2mv* during infusion of saline or SMTC

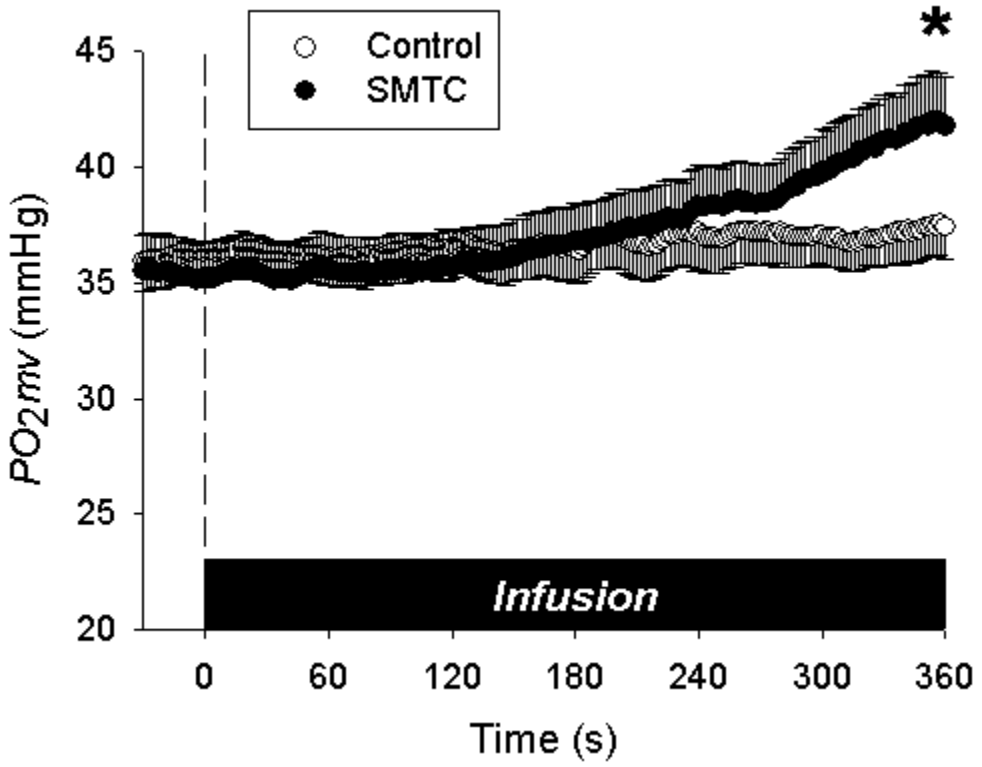

Figure 3.2 Mean resting spinotrapezius muscle *PO_2mv* during infusion of saline (control) or SMTC (selective nNOS inhibition). Time zero denotes start of infusion. * $p<0.05$ *vs.* control for end-infusion *PO_2mv* (last 10 s average).

Figure 3.3 Muscle PO_2mv at rest and following the onset of contractions under control and SMTC conditions

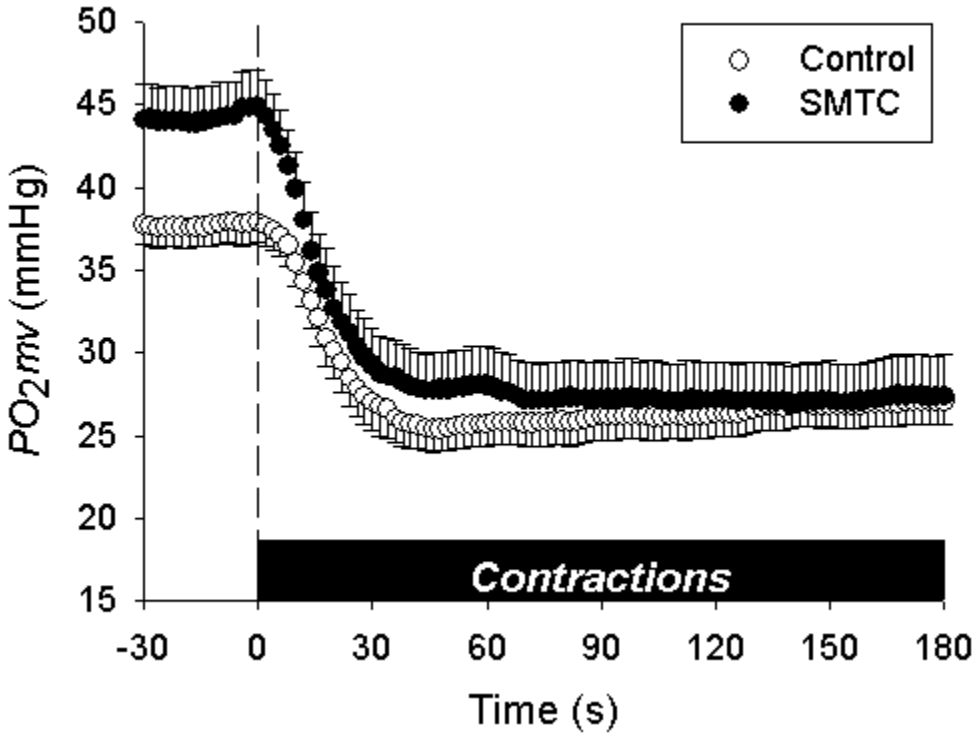

Figure 3.3 Mean spinotrapezius muscle PO_2mv at rest and following the onset of contractions under control and selective nNOS inhibition (SMTC) conditions. Time zero denotes the onset of muscle contractions. Average kinetics parameters are displayed in Table 3.2. See text for further details.

Figure 3.4 Muscle blood flow and O_2 utilization at rest and during contractions under control and SMTC conditions

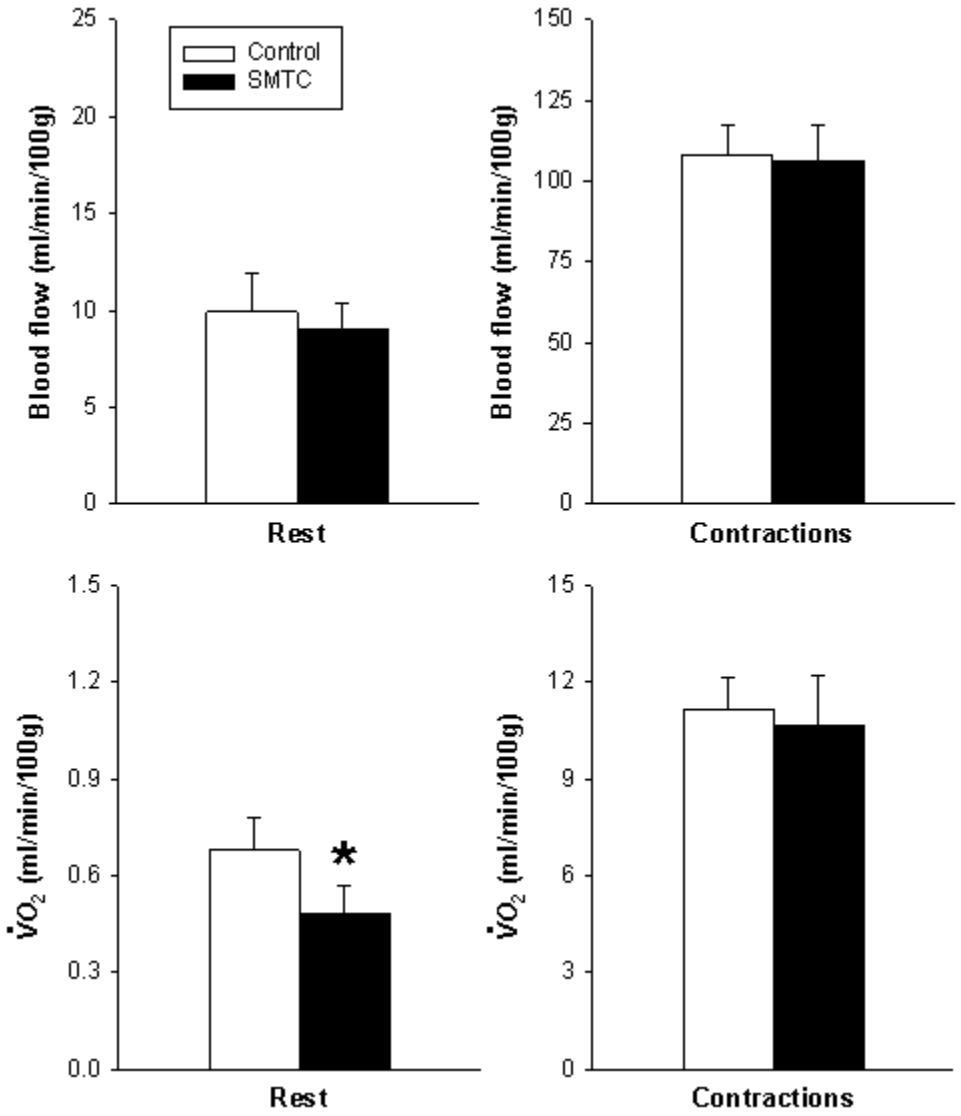

Figure 3.4 Mean spinotrapezius muscle blood flow (*top panels*) and O_2 utilization ($\dot{V}O_2$; *bottom panels*) at rest and during contractions under control and selective nNOS inhibition (SMTC) conditions. Note different scales on vertical axes.* $p<0.05$ *vs.* control.

Figure 3.5 Muscle force production under control and SMTC conditions

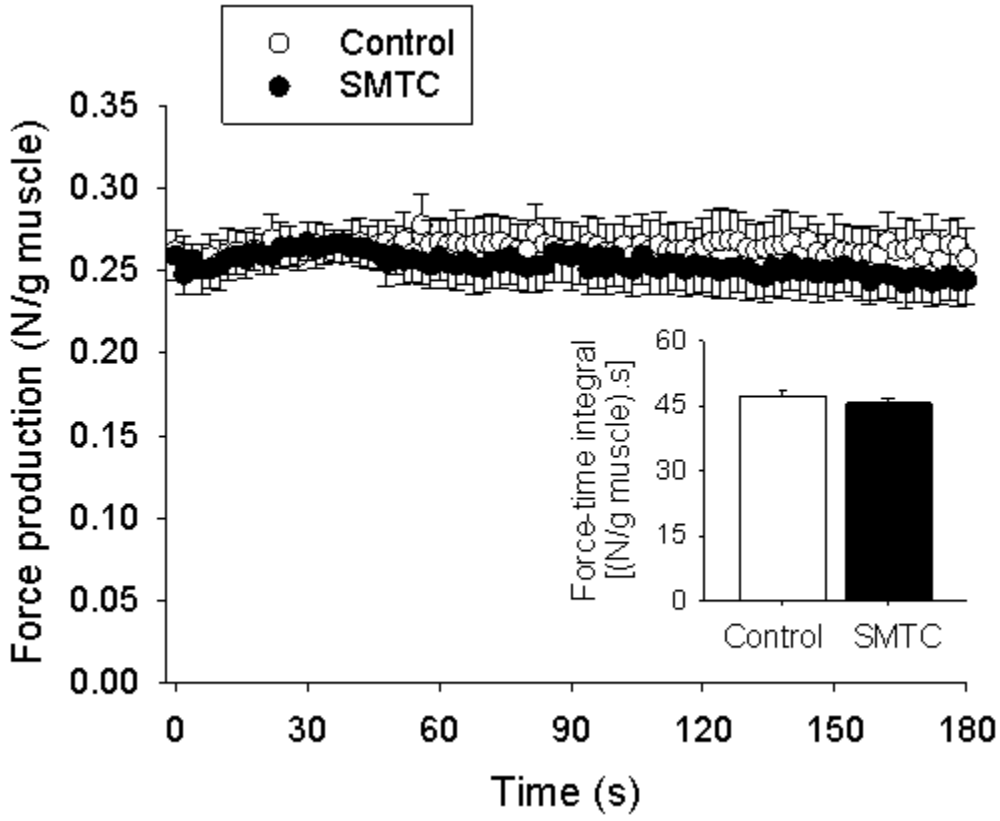

Figure 3.5 Mean spinotrapezius muscle force production under control and selective nNOS inhibition (SMTC) conditions. Note that muscle force production was not significantly different throughout the contraction period between control and SMTC. The *inset* shows that force-time integral values were also not significantly different between conditions.

Figure 3.6 Effects of SMTC on contracting muscle blood flow, $\dot{V}O_2$, *PO₂mv* kinetics and force production in young and old rats

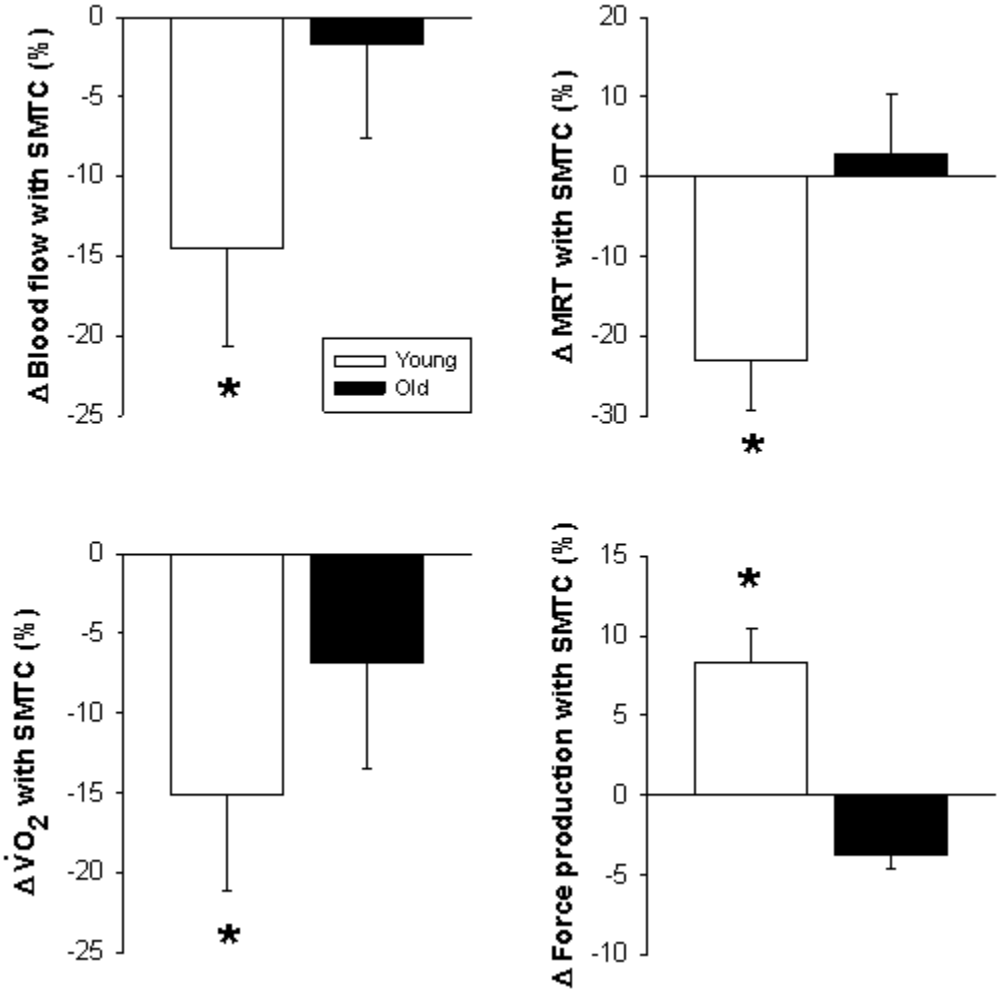

Figure 3.6 Effects of selective nNOS inhibition (SMTC) on contracting spinotrapezius muscle blood flow, O_2 utilization ($\dot{V}O_2$), overall *PO₂mv* kinetics (MRT, mean response time) and submaximal force production in young Sprague-Dawley (data from ref. 12; $n = 10$) and old F344xBN (present study; $n = 11$) rats. Note that SMTC evoked significant changes in these variables in young but not old rats. * $p<0.05$ *vs.* zero. See text for discussion.

References

1. **Altman PL, and Dittmer DS**. *Biology Data Book*. Bethesda, MD: FASEB, 1974.

2. **Bailey DM, McEneny J, Mathieu-Costello O, Henry RR, James PE, McCord JM, Pietri S, Young IS, and Richardson RS**. Sedentary aging increases resting and exercise-induced intramuscular free radical formation. *J Appl Physiol* 109: 449-456, 2010.

3. **Bailey JK, Kindig CA, Behnke BJ, Musch TI, Schmid-Schoenbein GW, and Poole DC**. Spinotrapezius muscle microcirculatory function: effects of surgical exteriorization. *Am J Physiol Heart Circ Physiol* 279: H3131-3137, 2000.

4. **Baker DJ, Krause DJ, Howlett RA, and Hepple RT**. Nitric oxide synthase inhibition reduces O_2 cost of force development and spares high-energy phosphates following contractions in pump-perfused rat hindlimb muscles. *Exp Physiol* 91: 581-589, 2006.

5. **Behnke BJ, Delp MD, Dougherty PJ, Musch TI, and Poole DC**. Effects of aging on microvascular oxygen pressures in rat skeletal muscle. *Respir Physiol Neurobiol* 146: 259-268, 2005.

6. **Behnke BJ, Kindig CA, Musch TI, Koga S, and Poole DC**. Dynamics of microvascular oxygen pressure across the rest-exercise transition in rat skeletal muscle. *Respir Physiol* 126: 53-63, 2001.

7. **Behnke BJ, Kindig CA, Musch TI, Sexton WL, and Poole DC**. Effects of prior contractions on muscle microvascular oxygen pressure at onset of subsequent contractions. *J Physiol* 539: 927-934, 2002.

8. **Bejma J, and Ji LL**. Aging and acute exercise enhance free radical generation in rat skeletal muscle. *J Appl Physiol* 87: 465-470, 1999.

9. **Capanni C, Squarzoni S, Petrini S, Villanova M, Muscari C, Maraldi NM, Guarnieri C, and Caldarera CM**. Increase of neuronal nitric oxide synthase in rat skeletal muscle during ageing. *Biochem Biophys Res Commun* 245: 216-219, 1998.

10. **Carter EE, Thomas MM, Murynka T, Rowan SL, Wright KJ, Huba E, and Hepple RT**. Slow twitch soleus muscle is not protected from sarcopenia in senescent rats. *Exp Gerontol* 45: 662-670, 2010.

11. **Chang WJ, Iannaccone ST, Lau KS, Masters BS, McCabe TJ, McMillan K, Padre RC, Spencer MJ, Tidball JG, and Stull JT**. Neuronal nitric oxide synthase and dystrophin-deficient muscular dystrophy. *Proc Natl Acad Sci U S A* 93: 9142-9147, 1996.

12. **Copp SW, Hirai DM, Ferguson SK, Musch TI, and Poole DC**. Role of neuronal nitric oxide synthase in modulating microvascular and contractile function in rat skeletal muscle. *Microcirculation* 18: 501-511, 2011.

13. **Copp SW, Hirai DM, Schwagerl PJ, Musch TI, and Poole DC**. Effects of neuronal nitric oxide synthase inhibition on resting and exercising hindlimb muscle blood flow in the rat. *J Physiol* 588: 1321-1331, 2010.

14. **Eskurza I, Monahan KD, Robinson JA, and Seals DR**. Effect of acute and chronic ascorbic acid on flow-mediated dilatation with sedentary and physically active human ageing. *J Physiol* 556: 315-324, 2004.

15. **Fadel PJ, Zhao W, and Thomas GD**. Impaired vasomodulation is associated with reduced neuronal nitric oxide synthase in skeletal muscle of ovariectomized rats. *J Physiol* 549: 243-253, 2003.

16. **Ferreira LF, Padilla DJ, Williams J, Hageman KS, Musch TI, and Poole DC**. Effects of altered nitric oxide availability on rat muscle microvascular oxygenation during contractions. *Acta Physiol (Oxf)* 186: 223-232, 2006.

17. **Finkel T, and Holbrook NJ**. Oxidants, oxidative stress and the biology of ageing. *Nature* 408: 239-247, 2000.

18. **Furfine ES, Harmon MF, Paith JE, Knowles RG, Salter M, Kiff RJ, Duffy C, Hazelwood R, Oplinger JA, and Garvey EP**. Potent and selective inhibition of human nitric oxide synthases. Selective inhibition of neuronal nitric oxide synthase by S-methyl-L-thiocitrulline and S-ethyl-L-thiocitrulline. *J Biol Chem* 269: 26677-26683, 1994.

19. **Grange RW, Isotani E, Lau KS, Kamm KE, Huang PL, and Stull JT**. Nitric oxide contributes to vascular smooth muscle relaxation in contracting fast-twitch muscles. *Physiol Genomics* 5: 35-44, 2001.

20. **Grassi B, Hogan MC, Kelley KM, Howlett RA, and Gladden LB**. Effects of nitric oxide synthase inhibition by L-NAME on oxygen uptake kinetics in isolated canine muscle in situ. *J Physiol* 568: 1021-1033, 2005.

21. **Gryglewski RJ, Palmer RM, and Moncada S**. Superoxide anion is involved in the breakdown of endothelium-derived vascular relaxing factor. *Nature* 320: 454-456, 1986.

22. **Heinonen I, Saltin B, Kemppainen J, Sipila HT, Oikonen V, Nuutila P, Knuuti J, Kalliokoski K, and Hellsten Y**. Skeletal muscle blood flow and oxygen uptake at rest and during exercise in humans: a pet study with nitric oxide and cyclooxygenase inhibition. *Am J Physiol Heart Circ Physiol* 300: H1510-1517, 2011.

23. **Hirai DM, Copp SW, Ferreira LF, Musch TI, and Poole DC**. Nitric oxide bioavailability modulates the dynamics of microvascular oxygen exchange during recovery from contractions. *Acta Physiol (Oxf)* 200: 159-169, 2010.

24. **Hirai DM, Copp SW, Hageman KS, Poole DC, and Musch TI**. Aging alters the contribution of nitric oxide to regional muscle hemodynamic control at rest and during exercise in rats. *J Appl Physiol* 111: 989-98, 2011.

25. **Hirai DM, Copp SW, Herspring KF, Ferreira LF, Poole DC, and Musch TI**. Aging impacts microvascular oxygen pressures during recovery from contractions in rat skeletal muscle. *Respir Physiol Neurobiol* 169: 315-322, 2009.

26. **Hirai DM, Copp SW, Schwagerl PJ, Haub MD, Poole DC, and Musch TI**. Acute antioxidant supplementation and skeletal muscle vascular conductance in aged rats: role of exercise and fiber type. *Am J Physiol Heart Circ Physiol* 300: H1536-1544, 2011.

27. **Hirai DM, Copp SW, Schwagerl PJ, Musch TI, and Poole DC**. Acute effects of hydrogen peroxide on skeletal muscle microvascular oxygenation from rest to contractions. *J Appl Physiol* 110: 1290-1298, 2011.

28. **Hirschfield W, Moody MR, O'Brien WE, Gregg AR, Bryan RM, Jr., and Reid MB**. Nitric oxide release and contractile properties of skeletal muscles from mice deficient in type III NOS. *Am J Physiol Regul Integr Comp Physiol* 278: R95-R100, 2000.

29. **Hogan MC, Arthur PG, Bebout DE, Hochachka PW, and Wagner PD**. Role of O_2 in regulating tissue respiration in dog muscle working in situ. *J Appl Physiol* 73: 728-736, 1992.

30. **Ichihara A, Inscho EW, Imig JD, and Navar LG**. Neuronal nitric oxide synthase modulates rat renal microvascular function. *Am J Physiol* 274: F516-524, 1998.

31. **Ishise S, Pegram BL, Yamamoto J, Kitamura Y, and Frohlich ED**. Reference sample microsphere method: cardiac output and blood flows in conscious rat. *Am J Physiol* 239: H443-H449, 1980.

32. **Jansson L, Carlsson PO, Bodin B, Andersson A, and Kallskog O**. Neuronal nitric oxide synthase and splanchnic blood flow in anaesthetized rats. *Acta Physiol Scand* 183: 257-262, 2005.

33. **Kavdia M, and Popel AS**. Contribution of nNOS- and eNOS-derived NO to microvascular smooth muscle NO exposure. *J Appl Physiol* 97: 293-301, 2004.

34. **Kindig CA, McDonough P, Erickson HH, and Poole DC**. Effect of L-NAME on oxygen uptake kinetics during heavy-intensity exercise in the horse. *J Appl Physiol* 91: 891-896, 2001.

35. **Kinugawa S, Huang H, Wang Z, Kaminski PM, Wolin MS, and Hintze TH**. A defect of neuronal nitric oxide synthase increases xanthine oxidase-derived superoxide anion and attenuates the control of myocardial oxygen consumption by nitric oxide derived from endothelial nitric oxide synthase. *Circ Res* 96: 355-362, 2005.

36. **Kobzik L, Reid MB, Bredt DS, and Stamler JS**. Nitric oxide in skeletal muscle. *Nature* 372: 546-548, 1994.

37. **Krause DJ, Hagen JL, Kindig CA, and Hepple RT**. Nitric oxide synthase inhibition reduces the O_2 cost of force development in rat hindlimb muscles pump perfused at matched convective O_2 delivery. *Exp Physiol* 90: 889-900, 2005.

38. **Larkin LM, Halter JB, and Supiano MA**. Effect of aging on rat skeletal muscle beta-AR function in male Fischer 344 x brown Norway rats. *Am J Physiol* 270: R462-468, 1996.

39. **Lau KS, Grange RW, Isotani E, Sarelius IH, Kamm KE, Huang PL, and Stull JT**. nNOS and eNOS modulate cGMP formation and vascular response in contracting fast-twitch skeletal muscle. *Physiol Genomics* 2: 21-27, 2000.

40. **Lipman RD, Chrisp CE, Hazzard DG, and Bronson RT**. Pathologic characterization of brown Norway, brown Norway x Fischer 344, and Fischer 344 x brown Norway rats with relation to age. *J Gerontol A Biol Sci Med Sci* 51: B54-59, 1996.

41. **Loke KE, McConnell PI, Tuzman JM, Shesely EG, Smith CJ, Stackpole CJ, Thompson CI, Kaley G, Wolin MS, and Hintze TH**. Endogenous endothelial nitric oxide synthase-derived nitric oxide is a physiological regulator of myocardial oxygen consumption. *Circ Res* 84: 840-845, 1999.

42. **Lushaj EB, Johnson JK, McKenzie D, and Aiken JM**. Sarcopenia accelerates at advanced ages in Fisher 344xBrown Norway rats. *J Gerontol A Biol Sci Med Sci* 63: 921-927, 2008.

43. **Macdonald M, Pedersen PK, and Hughson RL**. Acceleration of VO_2 kinetics in heavy submaximal exercise by hyperoxia and prior high-intensity exercise. *J Appl Physiol* 83: 1318-1325, 1997.

44. **Musch TI, and Terrell JA**. Skeletal muscle blood flow abnormalities in rats with a chronic myocardial infarction: rest and exercise. *Am J Physiol* 262: H411-419, 1992.

45. **Percival JM, Anderson KN, Huang P, Adams ME, and Froehner SC**. Golgi and sarcolemmal neuronal NOS differentially regulate contraction-induced fatigue and vasoconstriction in exercising mouse skeletal muscle. *J Clin Invest* 120: 816-826, 2010.

46. **Poole DC, Behnke BJ, McDonough P, McAllister RM, and Wilson DF**. Measurement of muscle microvascular oxygen pressures: compartmentalization of phosphorescent probe. *Microcirculation* 11: 317-326, 2004.

47. **Poole DC, and Ferreira LF**. Oxygen exchange in muscle of young and old rats: muscle-vascular-pulmonary coupling. *Exp Physiol* 92: 341-346, 2007.

48. **Poole DC, Wagner PD, and Wilson DF**. Diaphragm microvascular plasma PO_2 measured in vivo. *J Appl Physiol* 79: 2050-2057, 1995.

49. **Pou S, Pou WS, Bredt DS, Snyder SH, and Rosen GM**. Generation of superoxide by purified brain nitric oxide synthase. *J Biol Chem* 267: 24173-24176, 1992.

50. **Richmonds CR, Boonyapisit K, Kusner LL, and Kaminski HJ**. Nitric oxide synthase in aging rat skeletal muscle. *Mech Ageing Dev* 109: 177-189, 1999.

51. **Rumsey WL, Vanderkooi JM, and Wilson DF**. Imaging of phosphorescence: a novel method for measuring oxygen distribution in perfused tissue. *Science* 241: 1649-1651, 1988.

52. **Schild L, Jaroscakova I, Lendeckel U, Wolf G, and Keilhoff G**. Neuronal nitric oxide synthase controls enzyme activity pattern of mitochondria and lipid metabolism. *FASEB J* 20: 145-147, 2006.

53. **Seddon MD, Chowienczyk PJ, Brett SE, Casadei B, and Shah AM**. Neuronal nitric oxide synthase regulates basal microvascular tone in humans in vivo. *Circulation* 117: 1991-1996, 2008.

54. **Sindler AL, Delp MD, Reyes R, Wu G, and Muller-Delp JM**. Effects of ageing and exercise training on eNOS uncoupling in skeletal muscle resistance arterioles. *J Physiol* 587: 3885-3897, 2009.

55. **Song W, Kwak HB, Kim JH, and Lawler JM**. Exercise training modulates the nitric oxide synthase profile in skeletal muscle from old rats. *J Gerontol A Biol Sci Med Sci* 64: 540-549, 2009.

56. **Stamler JS, and Meissner G**. Physiology of nitric oxide in skeletal muscle. *Physiol Rev* 81: 209-237, 2001.

57. **Stary CM, and Hogan MC**. Effect of varied extracellular PO_2 on muscle performance in Xenopus single skeletal muscle fibers. *J Appl Physiol* 86: 1812-1816, 1999.

58. **Sun J, Druhan LJ, and Zweier JL**. Dose dependent effects of reactive oxygen and nitrogen species on the function of neuronal nitric oxide synthase. *Arch Biochem Biophys* 471: 126-133, 2008.

59. **Taddei S, Virdis A, Mattei P, Ghiadoni L, Gennari A, Fasolo CB, Sudano I, and Salvetti A**. Aging and endothelial function in normotensive subjects and patients with essential hypertension. *Circulation* 91: 1981-1987, 1995.

60. **Thomas GD, Sander M, Lau KS, Huang PL, Stull JT, and Victor RG**. Impaired metabolic modulation of alpha-adrenergic vasoconstriction in dystrophin-deficient skeletal muscle. *Proc Natl Acad Sci U S A* 95: 15090-15095, 1998.

61. **Tian J, Yan Z, Wu Y, Zhang SL, Wang K, Ma XR, Guo L, Wang J, Zuo L, Liu JY, Quan L, and Liu HR**. Inhibition of iNOS protects endothelial-dependent vasodilation in aged rats. *Acta Pharmacol Sin* 31: 1324-1328, 2010.

62. **Vincent HK, Powers SK, Stewart DJ, Demirel HA, Shanely RA, and Naito H**. Short-term exercise training improves diaphragm antioxidant capacity and endurance. *Eur J Appl Physiol* 81: 67-74, 2000.

63. **Vinogradov SA, Fernandez-Searra MA, Dugan BW, and Wilson DF**. Frequency domain instrument for measuring phosphorescence lifetime distributions in heterogeneous samples. *Rev Sci Instrum* 72: 3396-3406, 2001.

64. **Wakefield ID, March JE, Kemp PA, Valentin JP, Bennett T, and Gardiner SM**. Comparative regional haemodynamic effects of the nitric oxide synthase inhibitors, S-methyl-L-thiocitrulline and L-NAME, in conscious rats. *Br J Pharmacol* 139: 1235-1243, 2003.

65. **Woodman CR, Price EM, and Laughlin MH**. Aging induces muscle-specific impairment of endothelium-dependent dilation in skeletal muscle feed arteries. *J Appl Physiol* 93: 1685-1690, 2002.

66. **Young ME, and Leighton B**. Fuel oxidation in skeletal muscle is increased by nitric oxide/cGMP--evidence for involvement of cGMP-dependent protein kinase. *FEBS Lett* 424: 79-83, 1998.

Chapter 4 - Acute effects of hydrogen peroxide on skeletal muscle microvascular oxygenation from rest to contractions

Summary

Reactive oxygen species such as hydrogen peroxide (H_2O_2) exert a critical regulatory role on skeletal muscle function. Whether acute increases in H_2O_2 modulate muscle microvascular O_2 delivery-utilization ($\dot{Q}O_2/\dot{V}O_2$) matching (i.e., microvascular partial pressure of O_2; PO_2mv) at rest and following the onset of contractions is unknown. The hypothesis was tested that H_2O_2 treatment (exogenous H_2O_2) would enhance PO_2mv and slow PO_2mv kinetics during contractions compared to control. Anesthetized healthy young Sprague-Dawley rats had their spinotrapezius muscles either exposed for measurement of blood flow (and therefore $\dot{Q}O_2$), $\dot{V}O_2$ and PO_2mv or exteriorized for measurement of force production. Electrically stimulated twitch contractions (1 Hz, ~7 V, 2 ms pulse duration, 3 min) were evoked following acute superfusion with Krebs-Henseleit (control) and H_2O_2 (100 μM). Relative to control, H_2O_2 treatment elicited disproportionate increases in $\dot{Q}O_2$ and $\dot{V}O_2$ that elevated PO_2mv at rest and throughout contractions and slowed overall PO_2mv kinetics (i.e., ~85% slower mean response time; $P<0.05$). Accordingly, H_2O_2 resulted in ~33% greater overall microvascular oxygenation as assessed by the area under the PO_2mv curve ($P<0.05$). Muscle force production was not altered with H_2O_2 treatment ($P>0.05$), evidencing reduced economy during contractions (~40% decrease in the force/$\dot{V}O_2$ relationship; $P<0.05$). These findings indicate that, although increasing the driving force for blood-myocyte O_2 flux (i.e., PO_2mv), transient elevations in H_2O_2 impair skeletal muscle function (i.e., reduced economy during contractions) which mechanistically may underlie, in part, the reduced exercise tolerance in conditions associated with oxidative stress.

Introduction

Reactive oxygen species (ROS) are pivotal elements in signal transduction (8, 20, 21, 46, 56). Hydrogen peroxide (H_2O_2), a small diffusible and ubiquitous molecule with a long half-life relative to other ROS, is regarded as one of the most influential ROS in terms of redox signaling (21). H_2O_2 is generated constantly within skeletal muscle and its vasculature via direct reduction of molecular O_2 (e.g., by NADPH oxidase, xanthine oxidase and uncoupled nitric oxide (NO) synthases) or dismutation of superoxide radicals either spontaneously or enzymatically by superoxide dismutase (SOD) (8, 46, 56). Key scavengers of H_2O_2 include the enzymes catalase, glutathione peroxidase and peroxiredoxin (8, 46, 56).

Alterations in H_2O_2 bioavailability have important implications for skeletal muscle function at rest and during metabolic transients. Transient elevations in H_2O_2 levels could mediate an initial compensatory response to acute oxidative stress (traditionally defined as a disturbance in the oxidant-antioxidant balance in favor of the former) by acting as an endothelium-derived hyperpolarizing factor (EDHF; refs. 34, 51) and/or increasing endothelial NO synthase (eNOS) activity (12, 27, 63, 64), therefore minimizing potential deleterious effects on vasomotor control (15, 35, 43). Consistent with this notion, Csekő et al. (16) reported that exogenously applied H_2O_2 promotes concentration- and time-dependent effects on skeletal muscle arteriolar tone (and by implication O_2 delivery; $\dot{Q}O_2$). At 100 μM concentration, there is a biphasic effect composed of a brief constriction followed by a vasodilation that reaches steady-state within approximately 3 min. In addition to its effects on the vasculature, acute increases in H_2O_2 also modulate skeletal muscle O_2 utilization ($\dot{V}O_2$; ref. 57) and contractile function (4, 37, 49, 55). Exposure of isolated skeletal muscle mitochondria to H_2O_2 (100 μM) uncouples oxidative phosphorylation and reduces energy transfer efficiency (expected to result in relatively greater muscle $\dot{V}O_2$) (57). Brief application of exogenous H_2O_2 (~100 μM) increases force production in isolated unfatigued skeletal muscle fibers (49). However, whether acute redox state modulation via increased H_2O_2 improves the dynamic matching between skeletal muscle $\dot{Q}O_2$ and $\dot{V}O_2$ (i.e., enhanced muscle microvascular oxygenation; PO_2mv) at rest and during contractions is unknown. Resolution of this issue is important given that, as dictated by Fick's

law of diffusion, low PO_2mv impairs blood-myocyte O_2 flux and consequently dysregulates skeletal muscle metabolism (26), an effect that could impact negatively upon contractile performance in oxidative stress conditions such as aging, chronic heart failure, hypertension and diabetes.

The present study examined the effects of acutely increased H_2O_2 on muscle microvascular oxygenation (PO_2mv) and force production following the onset of contractions in healthy rat skeletal muscle *in situ*. Aiming to gain insights into how brief H_2O_2 exposure modulates the $\dot{Q}O_2/\dot{V}O_2$ ratio and therefore PO_2mv, we also determined resting and contracting steady-state $\dot{Q}O_2$ and $\dot{V}O_2$ responses. Based on the evidence summarized above, the hypotheses were tested that acute oxidant treatment (exogenous 100 μM H_2O_2) would increase (i) blood flow (and thus $\dot{Q}O_2$) and $\dot{V}O_2$; (ii) PO_2mv and slow PO_2mv kinetics during contractions and (iii) muscle force production.

Methods

Animals

A total of 43 young male Sprague-Dawley rats (3-4 months old; body mass 354 ± 13 g) were used in the present study for measurements of PO_2mv (phosphorescence quenching; n = 20), muscle blood flow (radiolabelled microspheres; n = 13) and force production (n = 10). Rats were obtained from Charles River Laboratories and maintained on a 12:12-h light-dark cycle with food and water provided *ad libitum*. Upon completion of the study, all rats were euthanized with pentobarbital sodium overdose. All experimental procedures were conducted under the guidelines established by the National Institutes of Health and approved by the Institutional Animal Care and Use Committee of Kansas State University.

Surgical preparation

Animals were anesthetized initially with 5% isoflurane gas. Subsequently, while being maintained on a 2-3% isoflurane-O_2 mixture, the caudal (tail) artery was isolated surgically and cannulated (PE-10 connected to PE-50; Intra-Medic Tubing, Clay Adams Brand) for continuous monitoring of mean arterial pressure (MAP; Digi-Med BPA model 200) and infusion of the phosphorescent probe palladium *meso*-tetra (4-carboxyphenyl) porphyrin dendrimer (R2; 15 mg/kg; Oxygen Enterprises). Blood from the tail catheter was sampled at the end of each experimental protocol within a subset of ten animals for the determination of arterial blood gases, pH, systemic hematocrit and plasma lactate. For blood flow measurements, an additional catheter (PE-10 connected to PE-50) was placed in the ascending aorta via the right carotid artery to allow the injection of differently radiolabelled 15 μm diameter microspheres into the aortic arch as described previously (38). Anesthetized rats were kept on a heating pad to maintain core temperature, measured via rectal probe, at ~37-38 °C.

After catheter placement procedures, isoflurane inhalation was progressively discontinued and rats were kept under anesthesia with intra-arterial pentobarbital sodium throughout the experiment. The level of anesthesia was monitored frequently via the toe-pinch and blink reflexes and supplemented as necessary. Overlying skin and fascia from the mid-dorsal region of the rat was removed carefully to expose the spinotrapezius muscle. The muscle was

moistened constantly during the surgical preparation via superfusion of Krebs-Henseleit (K-H) bicarbonate-buffered solution (4.7 mM KCl, 2.0 mM $CaCl_2$, 2.4 mM $MgSO_4$, 131 mM NaCl and 22 mM $NaHCO_3$) equilibrated with 5% CO_2 and 95% N_2 at ~38 °C whereas surrounding tissue was covered with Saran Wrap (Dow Brands). Stainless steel electrodes were sutured to the rostral (cathode) and caudal (anode) regions of the spinotrapezius muscle for electrically-induced contractions. We have previously demonstrated that these surgical procedures do not alter the microvascular integrity and responsiveness of the spinotrapezius muscle (9).

Experimental protocol

Two separate contraction bouts were performed under control (3 mL K-H) and H_2O_2 (100 µM in 3 mL K-H) superfusion conditions. This concentration was selected based on previous studies in which similar exogenous H_2O_2 concentrations impacted significantly rat skeletal muscle arteriolar tone (16), mitochondrial respiration (57) and force production (49). Given that intracellular H_2O_2 reaches a value that is approximately an order of magnitude lower than that of the applied exogenous concentration (6), our experimental protocol was expected to elevate acutely H_2O_2 to those levels measured in the early stages of senescence and cardiovascular diseases (i.e., from ~10 µM in the healthy young rat skeletal muscle interstitial fluid and mesenteric artery *in vivo* to ~20-40 µM in conditions such as hypertension; refs. 59, 63, 64). Also relevant in this regard is that exposure of isolated skeletal muscle fibers to 100 µM H_2O_2 does not produce gross histological damage (41, see also ref. 47). Exogenous H_2O_2 treatment does not produce oxidative damage to hemoglobin in intact red blood cells (12.5-100 µM; refs.33, 39) or myoglobin in isolated skeletal muscle (1 mM; ref. 19). Due to its time-dependent actions on eNOS and NADPH oxidase activity (12, 27), H_2O_2 was the last treatment to prevent residual long-term effects on vascular and skeletal muscle function.

The experimental protocol is illustrated in Fig. 4.1. The spinotrapezius muscle was superfused with each solution (average flow rate ~2 mL/min) for a total time of ~1.5 min, after which a 3 min incubation period followed to allow arteriolar vasodilation (and consequently $\dot{Q}O_2$ and PO_2mv) to reach steady-state under H_2O_2 treatment based on data from Csekő et al. (16) and preliminary studies from our laboratory (Hirai DM, Copp SW, Schwagerl PJ, Musch TI, Poole DC; unpublished data). Subsequently, electrical stimulation (1 Hz, ~7 V, 2 ms pulse duration) of the muscle was evoked via a Grass Stimulator (model s48) for 3 min. The muscle

was then allowed to recover for ~25 min before the next condition was initiated (stimulation parameters were held constant).

The spinotrapezius preparation exhibits reproducible PO_2mv kinetic parameters during transitions in metabolic demand evoked by 1 Hz twitch contractions when a minimum of 20 min of recovery is allowed between contraction bouts (14, 23). Accordingly, highly reproducible overall PO_2mv kinetics (mean response time; MRT) from repeated contraction bouts separated by ~25 min were obtained herein (within-animal coefficient of variation: 3 ± 2 s; n = 6) with no ordering effect (overall within-animal difference: 1 ± 3 s; P>0.05). Moreover, the 25-30 min period between contractions (3 min off-transition, ~20 min recovery, ~1.5 min superfusion, 3 min incubation; see Fig. 4.1) was employed herein to avoid any priming effect that might confound the experimental interpretation of the PO_2mv responses to muscle contractions (11).

Measurement of PO_2mv

PO_2mv was measured by phosphorescence quenching using a Frequency Domain Phosphorometer (PMOD 5000; Oxygen Enterprises). The principles of the phosphorescence quenching method have been discussed in detail previously (10). Briefly, this method applies the Stern-Volmer relationship (50), which describes quantitatively the O_2 dependence of the phosphorescent probe (i.e., R2) via the following equation:

$$PO_2mv = \frac{(\tau^\circ / \tau) - 1}{k_Q \times \tau^\circ}$$

where k_Q is the quenching constant and τ° is the phosphorescence lifetime in an O_2-free environment. The τ of phosphorescence decay was determined using 10 scans (100 ms) in the single frequency mode (50, 61). The phosphor R2 ($\tau^\circ = 601\,\mu s$ and $k_Q = 409$ $mmHg^{-1}{\cdot}s^{-1}$ at pH = 7.4 and temperature ~38 °C) was infused ~15 min prior to initiation of muscle contractions. The R2 probe is bound to albumin and is distributed uniformly in the plasma thus providing a signal corresponding to the volume-weighed O_2 pressure in the microvascular compartment (mainly the PO_2 within the capillaries, which volumetrically constitutes the major intramuscular space; ref. 45). In addition to albumin binding, the negative charge of the R2 probe also

facilitates its restriction to the intravascular space within the muscle (44). Data from Oter and Ribou (42) suggest that it is highly unlikely that our H_2O_2 treatment could affect oxygen measurements with probes such as metalloporphyrin complexes (e.g., R2). In fact, no interference is expected to occur in lifetime-based measurements using H_2O_2 concentrations lower than 0.1 M.

The common end of the bifurcated light guide was placed 2-4 mm superficial to the dorsal surface of the exposed spinotrapezius muscle. The phosphorometer modulates sinusoidal excitation frequencies between 100 Hz and 20 kHz and allows phosphorescence lifetime measurements from 10 μs to approximately 2.5 ms. The excitation light (524 nm) was focused on a randomly selected area of ~2 mm diameter of exposed muscle and has a resulting penetration depth of ~500 μm which is somewhat less than the spinotrapezius muscle thickness in the region sampled. *PO_2mv* was recorded at 2 s intervals throughout the duration of the experimental protocol (superfusion, incubation, electrical stimulation and recovery periods).

Movement of the light guide (or animal) was avoided so as to monitor the same sampling site throughout the entire experimental protocol. However, alteration of the *PO_2mv* measurement plane during muscle contractions precluded kinetic curve fitting in some instances. Therefore, microvascular oxygenation results from the present study are presented from animals under the following conditions: control, $n = 20$; H_2O_2, $n = 12$.

Analysis of PO_2mv kinetics

The kinetics of *PO_2mv* were described by nonlinear regression analysis using the Marquardt-Levenberg algorithm (SigmaPlot 9.01; Systat Software) for the onset of contractions. Transient *PO_2mv* responses were fit with either a one- or two-component model (10):

One-component:

$$PO_2mv_{(t)} = PO_2mv_{(BL)} - \Delta PO_2mv(1 - e^{-(t-TD)/\tau})$$

Two-component:

$$PO_2mv_{(t)} = PO_2mv_{(BL)} - \Delta_1 PO_2mv(1 - e^{-(t-TD1)/\tau_1}) + \Delta_2 PO_2mv(1 - e^{-(t-TD2)/\tau_2})$$

where $PO_2mv_{(t)}$ is the PO_2mv at a given time *t*, $PO_2mv_{(BL)}$ corresponds to the pre-contracting resting PO_2mv, Δ_1 and Δ_2 are the amplitudes for the first and second components, respectively, TD_1 and TD_2 are the independent time delays for each component, and τ_1 and τ_2 are the time constants (i.e., time taken to achieve 63% of the response) for each component. Goodness of fit was determined using three criteria: (i) the coefficient of determination; (ii) the sum of squared residuals; and (iii) visual inspection.

The mean response time (MRT; ref. 31) was used to describe the overall dynamics of the PO_2mv response:

$$MRT = TD + \tau$$

where TD and τ are defined above. The MRT analysis was limited to the first phase of the PO_2mv response since inclusion of the emergent second phase underestimates the actual rate of PO_2mv fall following the onset of contractions (25). The overall time necessary to attain 63% of the final amplitude of the PO_2mv response during the onset of contractions was determined independent of modeling procedures (T_{63}; ref. 29) as an additional means of checking the accuracy of the model fits to the data.

The area under the PO_2mv curve plotted as function of time (PO_{2AREA}; ref. 24) was calculated during 3 min following the onset of contractions to provide an index of the overall muscle microvascular oxygenation throughout the exercise transient for each condition (i.e., incorporating resting and contracting steady-state PO_2mv, time delays, amplitudes and time constants of the response to yield a value expressed in mmHg·s).

Measurement of muscle blood flow

Spinotrapezius blood flow was measured using the radiolabelled microsphere technique as described in detail previously (38). In each condition (control and H_2O_2), the stimulated right and non-stimulated left spinotrapezius muscles represented the contracting and resting blood flow measurements, respectively (14, 23). Briefly, the tail artery catheter was connected to a 1 mL syringe and blood withdrawal was initiated at a constant rate of 0.25 mL/min via a Harvard pump (model 907). Differentially radiolabelled 15 μm diameter microspheres (^{46}Sc or ^{85}Sr; Perkin Elmer Life and Analytical Sciences) were injected in random order into the aortic arch via

the carotid artery catheter during the contracting steady-state (i.e., ~3 min after initiation of muscle contractions). Upon completion of the experiment, the right and left spinotrapezius muscles and right and left kidneys were carefully dissected, removed and weighed immediately after euthanasia. The thorax was opened, and placement of the carotid artery catheter into the aortic arch was confirmed by anatomical dissection.

Tissue radioactivity was determined on a gamma scintillation counter (Packard Auto Gamma Spectrometer, Cobra model 5003) and muscle blood flow was determined by the reference sample method (28) and expressed as mL/min/100 g tissue. Adequate mixing of the microspheres was verified for each injection by demonstrating a <15% difference in blood flow between the right and left kidneys.

Calculation of muscle $\dot{V}O_2$

Muscle $\dot{V}O_2$ was calculated from PO_2mv and blood flow ($\dot{Q}m$) measurements as described previously (14, 23). Briefly, arterial O_2 concentration (CaO_2) was calculated from arterial blood samples, while venous O_2 concentration (CvO_2) was calculated from both the mean resting or contracting steady-state PO_2mv using the rat O_2 dissociation curve (Hill coefficient of 2.6), the measured hemoglobin (Hb) concentration, a PO_2 at which hemoglobin is 50% saturated (P_{50}) of 38 mmHg, and an O_2 carrying capacity of 1.34 mL O_2/g Hb (2). Mean resting and contracting steady-state spinotrapezius $\dot{Q}m$'s were then used to calculate muscle $\dot{V}O_2$'s via the Fick equation (i.e., $\dot{V}O_2 = \dot{Q}m(CaO_2 - CvO_2)$). Muscle $\dot{V}O_2$ standard errors were estimated from $\dot{Q}m$ measurements.

Measurement of muscle force production

The caudal end of the spinotrapezius muscle was exteriorized and sutured to a swivel apparatus and a non-distensible light weight (0.4 g) cable, which linked the muscle to a Grass force transducer (model FTO3). The preload tension of the muscle was set at ~4 g, which evoked the optimal length of the muscle for twitch force production (14, 23). Superfusion and contraction protocols were performed as described above. Force production was expressed as g/g muscle.

Time-control experiments demonstrated excellent reproducibility of force production measurements (within-animal coefficient of variation: 1 ± 1 g/g muscle; i.e., ≤5%; $n = 6$) with no ordering effect (overall within-animal difference: 2 ± 1 g/g muscle; i.e., ≤10%; $P>0.05$) between two consecutive contraction bouts. Therefore, based on these findings and our previous reports demonstrating the stability and reproducibility of the spinotrapezius preparation (9, 14, 23), it is highly unlikely that fatigue and/or deterioration of the preparation *per se* could account for any changes (or lack thereof) in measured variables under different treatments.

Statistical analyses

PO_2mv and MAP data comparison was performed using unpaired Student's *t*-tests. Blood flow, $\dot{V}O_2$ and force production data comparison was performed using ANOVA techniques. *Post hoc* analyses were performed with the Bonferroni test when a significant *F*-ratio was detected. The level of significance was set at $P<0.05$. Results are reported as mean ± standard error (SE).

Results

Arterial PO_2 averaged 91.5 ± 2.3 mmHg, O_2 saturation 89.0 ± 2.1 %, blood pH 7.38 ± 0.01, systemic hematocrit 34.9 ± 0.7 % and plasma lactate 1.5 ± 0.1 mmol/L.

Muscle microvascular oxygenation (PO_2mv)

The control treatment did not change resting PO_2mv (i.e., similar values before and after K-H superfusion and incubation periods, $PO_2mv_{(Pre)}$ and $PO_2mv_{(Post)}$; Table 4.1). Representative PO_2mv profiles during K-H (control) and H_2O_2 superfusion and incubation periods are depicted in Fig. 4.2. A transient fall in PO_2mv following H_2O_2 superfusion, consistent with the brief arteriolar constriction response reported by Csekő et al. (16) in isolated vessels exposed to 100 μM H_2O_2, was observed in only 2 rats. Nonetheless, H_2O_2 treatment increased PO_2mv in all cases beyond ~30 s.

The time course of PO_2mv following the onset of contractions during H_2O_2 treatment presented significant quantitative differences relative to the control condition (Table 4.1 and Fig. 4.3). The post-treatment resting PO_2mv ($PO_2mv_{(Post)}$) was significantly higher for H_2O_2 compared with control. The one-component exponential model provided an excellent fit to the PO_2mv data for the majority of instances (16 out of 20) in the control condition and in all profiles for H_2O_2. Within the different experimental treatments (control and H_2O_2), MRT (model dependent) and T_{63} (model independent) were not significantly different from one another.

The overall dynamics of the PO_2mv response (MRT and T_{63}) were ~80-90% slower with H_2O_2 compared to control. As a result of the similar overall PO_2mv amplitude regardless of the one- or two-component model fit ($\Delta_{Total}PO_2mv$) in the two experimental treatments, the contracting steady-state PO_2mv ($PO_2mv_{(SS)}$) was ~30% greater with H_2O_2 compared with control. The acute effects of H_2O_2 treatment on PO_2mv kinetics were reflected in the overall muscle microvascular oxygenation (PO_{2AREA}) throughout the on-transition, as H_2O_2 increased PO_{2AREA} by ~33% relative to control (Fig. 4.3, bottom panel).

Muscle blood flow ($\dot{Q}m$)

MAP values were not different during $\dot{Q}m$ measurements when comparing distinct conditions (control: 95 ± 3; H_2O_2: 96 ± 5 mmHg; P>0.05). H_2O_2 treatment augmented significantly resting and contracting $\dot{Q}m$ when compared to control (Fig. 4.4). However, no further increases in $\dot{Q}m$ during the rest-contraction transient occurred with H_2O_2 (P>0.05).

Muscle O_2 utilization ($\dot{V}O_2$)

Relative to the control condition, H_2O_2 treatment augmented significantly resting and contracting $\dot{V}O_2$ (Fig. 4.5). A similar magnitude of increase in muscle $\dot{V}O_2$ ($\Delta\dot{V}O_2$) from rest to contractions was observed for both conditions (control: 5.7 ± 0.8; H_2O_2: 6.0 ± 1.1 mL/min/100g; P>0.05).

Muscle force production

As illustrated in Fig. 4.6, muscle force production was not significantly different throughout the contraction period between control and H_2O_2. Thus, as a consequence of the relatively greater contracting steady-state $\dot{V}O_2$ (Fig. 4.5), H_2O_2 treatment decreased the force/$\dot{V}O_2$ relationship by ~40% when compared to control (Fig. 4.6, inset).

Discussion

This study evaluated the effects of acute H_2O_2 exposure on skeletal muscle function at rest and during contractions in healthy young rats. Consistent with our hypothesis, redox modulation via H_2O_2 treatment elevated PO_2mv at rest and during contractions while slowing its kinetics, an effect that reflected significant disproportionate increases in muscle $\dot{Q}O_2$ and $\dot{V}O_2$. However, contrary to our expectation, H_2O_2 treatment did not increase muscle force production. These results demonstrate that, although enhancing the driving force for blood-myocyte O_2 transfer, increased H_2O_2 reduces acutely the economy of contractions (i.e., decreased force/$\dot{V}O_2$ relationship).

H_2O_2 modulates skeletal muscle function

Acute exposure of isolated skeletal muscle arterioles to H_2O_2 modulates myogenic tone in a concentration- and time-dependent manner, such that exogenous 100 μM H_2O_2 produces biphasic changes composed of a brief constriction followed by a substantial vasodilation that reaches steady-state within ~3 min (16). Enhanced arteriolar tone appears to be primarily mediated by the release of endothelium- and smooth muscle-derived constrictor prostaglandins (prostaglandin H_2 and thromboxane A_2), whereas decreased arteriolar tone is caused mainly by the activation of both eNOS and K^+ channels (including Ca^{2+}-activated and ATP-sensitive K^+ channels) in the smooth muscle (16). These effects are consistent with the stimulatory actions of H_2O_2 on eNOS activity (12, 27, 63, 64) and the identification of H_2O_2 as an EDHF (34, 51). Although the relative importance of each vasodilatory pathway in skeletal muscle is currently unknown, augmented accumulation of endogenous H_2O_2 contributes substantially to functional vasodilation given that catalase treatment blunts the increase in skeletal muscle arteriolar diameter during contractions (32). Elevated $\dot{Q}m$ at rest and during contractions under H_2O_2 treatment in the present investigation (Fig. 4.4) corroborates and extends significantly the aforementioned studies by demonstrating that acute increases in H_2O_2 modulate skeletal muscle blood flow and microvascular oxygenation *in situ*.

Although not every PO_2mv profile exhibited a transient fall consistent with the biphasic arteriolar diameter response reported by Csekő et al. (16), exogenous H_2O_2 increased resting

spinotrapezius PO_2mv in all instances within ~30 s (Fig. 4.2). In addition to differences in experimental design (see below), this behavior could also be explained by the fact that PO_2mv is directly proportional to the $\dot{Q}O_2/\dot{V}O_2$ ratio (10) while arteriolar diameter measurements only provide an index of $\dot{Q}O_2$. This is particularly important considering that altered H_2O_2 levels also impact mitochondrial function (and thus muscle $\dot{V}O_2$). Tonkonogi et al. (57) documented a significant impairment in the coupling between respiration and phosphorylation (as assessed by a decrease in the respiratory control index; i.e., the ratio of state 3 to state 4 mitochondrial respiration) and an approximately 19% reduction in phosphorylation efficiency (decreased P/O ratio; i.e., the relationship between ATP resynthesis and O_2 consumption) in isolated skeletal muscle mitochondria exposed to 100 μM H_2O_2. These effects are partially mediated by an increase in proton leakage through the adenine nucleotide translocase protein (an antiporter that exchanges ADP for ATP across the inner mitochondrial membrane) (57). Teleologically, a greater proton leakage promoted by elevated H_2O_2 levels could serve as a compensatory mechanism, since the consequent reduction in mitochondrial proton gradient and membrane potential would attenuate ROS production and thus limit potential oxidative damage (54, 60). It is important to note that participation of other ROS such as the hydroxyl radical (which can be generated via the interaction between ferrous iron and H_2O_2; i.e., the Fenton reaction) is unlikely to occur given that the iron chelator deferoxamine does not attenuate the effects of H_2O_2 treatment on mitochondrial respiration (52). Our data are consistent with those of Tonkonogi et al. (57) and reveal that H_2O_2 treatment markedly increased resting and contracting steady-state $\dot{V}O_2$ in healthy rat skeletal muscle (Fig. 4.5). The observation of similar $\Delta\dot{V}O_2$ from rest to contractions for control and H_2O_2 treatment supports the notion that H_2O_2 impacted mitochondrial control rather than the contractile apparatus. Although increased NO bioavailability (induced by the stimulatory actions of H_2O_2 on eNOS activity; refs. 12, 27, 63, 64) could act to inhibit mitochondrial respiration (13), that the net effect of acute H_2O_2 treatment is increased basal and contracting $\dot{V}O_2$ (Fig. 4.5) suggests that the actions of H_2O_2 on oxidative phosphorylation overcame those of NO.

The temporal profile of PO_2mv during metabolic transitions reflects the dynamic $\dot{Q}O_2/\dot{V}O_2$ ratio within the microvascular space (10, 25). Collectively, our data indicate that the elevated PO_2mv response from rest to submaximal contractions under H_2O_2 treatment (Table 4.1

and Fig. 4.3) resulted from disproportionate increases in $\dot{Q}O_2$ and $\dot{V}O_2$ (Figs. 4.4 and 4.5). These effects can be summarized by analysis of the PO_{2AREA}, which was ~33% greater with H_2O_2 compared to control (Fig. 4.3, bottom panel). However, the greater potential for blood-myocyte O_2 flux under H_2O_2 treatment occurs at the expense of an elevated O_2 cost of contraction as evidenced by an increased muscle $\dot{V}O_2$ (Fig. 4.5) concurrent with unchanged force production (i.e., ~40% decrease in the force/$\dot{V}O_2$ relationship; Fig. 4.6). Such reduced muscle economy could compromise sustained contractile activity by exacerbating perturbations of the intramyocyte physicochemical milieu (e.g., accentuated depletion of phosphocreatine and glycogen stores; ref. 1).

Skeletal muscle contractile function is influenced by ROS bioavailability and its effects on myocyte redox state (20, 46, 48). The conceptual model developed by Reid et al. (4, 48, 49) describes the relationship between muscle redox balance and submaximal force production as a bell-shaped response profile (Fig. 4.7). This model predicts that a certain level of ROS accumulation is necessary to cause a rightward shift along the response curve from the relatively reduced redox state of unfatigued skeletal muscle towards the optimal redox state where force production is maximized. Exogenous H_2O_2 evokes concentration- and time-dependent effects on skeletal muscle force production (4, 49). Specifically, brief exposure of isolated muscle fibers to H_2O_2 (100-300 μM for 3 min) increases submaximal force production without alterations in myoplasmic Ca^{2+} concentration, supporting the notion of a redox modulation of Ca^{2+} sensitivity (4, see also refs. 37, 55). Elevated myofiber Ca^{2+} sensitivity with increased H_2O_2 could alleviate fatigue momentarily until prolonged exposure and/or further ROS accumulation decrease Ca^{2+} sensitivity and force production (4, 55). The mechanisms involved in the modulation of Ca^{2+} sensitivity by H_2O_2 appear to depend on its interaction with myoglobin and glutathione (a non-enzymatic thiol antioxidant in muscle fibers) in a concentration- and time-dependent manner (37).

Contrary to our hypothesis, we observed that H_2O_2 treatment did not change force production compared to control (Fig. 4.6). The reasons for this divergence are unclear, but may relate to: (i) the utilization of distinct experimental protocols (including the influence of temperature on ROS bioavailability and myofiber Ca^{2+} sensitivity since studies conducted in isolated preparations are commonly performed at subphysiological temperatures to promote stability; refs. 7, 36); (ii) muscle fiber type; as the mixed fiber type spinotrapezius muscle (18)

could retain the resistance to ROS-induced increases in Ca^{2+} sensitivity of the contractile apparatus characteristic of predominantly slow-twitch fibers (37); (iii) a rightward shift along the bell-shaped response profile that places the muscle past the optimal redox state and results in similar force production compared to control (see Fig. 4.7); (iv) compartmentalized ROS scavenging that suppresses the potential effects of H_2O_2 treatment on force production (see below); (v) the opposing effects of endogenous NO on contractile function (e.g., reduced myofiber Ca^{2+} sensitivity; refs. 5, 55).

Experimental considerations

Modulation of physiological responses to altered H_2O_2 bioavailability appears to be specific to the tissue under consideration. Within the cardiovascular system, H_2O_2 is capable of evoking vasoconstriction, vasodilation or a biphasic response depending on the vascular bed (i.e., location and branch order), vascular tone (i.e., basal contractile state, method utilized to induce tone in isolated preparations), resting membrane potential, age and/or disease status (8, 16, 22, 32, 34, 35, 43, 51, 53, 58, 63, 64). Distinct localization, activity and/or expression of antioxidant systems as well as differences in individual peroxidase enzyme kinetics result in redox compartmentalization (i.e., specific tissue and cellular concentrations of ROS) (40). These and potentially other factors interact to regulate local redox state and dictate spatial and temporal heterogeneity in the physiological responses to transient changes in H_2O_2 levels. Caution is therefore required when extrapolating findings from different sites within the cardiovascular system (e.g., skeletal muscle, coronary, cerebral and mesenteric circulations). Furthermore, marked skeletal muscle fiber type differences in ROS generation and scavenging (3, 46) suggest that a given stimulus (e.g., contractions, redox modulation via oxidant or antioxidant treatment) might produce dissimilar outcomes. In this regard, it is pertinent that the rat spinotrapezius muscle exhibits a mixed fiber type composition and oxidative capacity that resemble closely the human quadriceps (18, 30), thus representing a useful surrogate of human skeletal muscle. The spinotrapezius preparation also allows superfusion as a method to deliver specific compounds to the muscle, which is expected to modify only local redox state and avoid the potential for systemic influences (e.g., alterations in MAP).

It is unlikely that our acute H_2O_2 treatment (100 μM) produced loss of vascular and/or skeletal muscle function. Accordingly, H_2O_2 washout in preliminary studies from our laboratory

(Hirai DM, Copp SW, Schwagerl PJ, Musch TI, Poole DC; unpublished data) revealed that PO_2mv returned to pre-treatment values (i.e., $PO_2mv_{(Pre)}$) in approximately 20 min. Data from these preliminary studies also indicated no impairment in force production during an additional third contraction bout performed in identical fashion to the control condition. These findings are consistent with previous studies utilizing similar H_2O_2 concentrations. Specifically, Csekő et al. (16) reported that H_2O_2 washout restored baseline arteriolar diameter and Andrade et al. (4) documented reversible effects of H_2O_2 on muscle force production after incubation with the reductant dithiothreitol.

Although increased H_2O_2 is capable of stimulating metabosensitive afferents in skeletal muscle (17, 62), that no changes in MAP were observed for H_2O_2 treatment when compared to control argues against that possibility. It is feasible that the present H_2O_2 concentration and/or relatively small muscle mass of the spinotrapezius limited the triggering of these events.

Limitations

Given the nature of our experimental protocol, muscle tissue analysis for ROS was not feasible due to the two required contraction bouts (control and H_2O_2). Blood samples were not taken for ROS measurements since, as noted above, the superfusion method utilized herein was expected to impact only local redox state. Nevertheless, the exogenous application of H_2O_2 via superfusion of the rat spinotrapezius muscle is similar to that employed by others and has been demonstrated, although indirectly, to impact effectively intracellular H_2O_2 levels (32).

Conclusions

The current study demonstrates for the first time that acute H_2O_2 treatment promoted disproportionate increases in skeletal muscle $\dot{Q}O_2$ and $\dot{V}O_2$ both at rest and during submaximal contractions *in situ*. These alterations modified significantly microvascular O_2 delivery-utilization balance such that PO_2mv was elevated at rest and throughout contractions (along with ~85% slower overall kinetics) compared to the control condition. However, the greater potential for blood-myocyte O_2 flux under H_2O_2 treatment occurred concurrently with reduced economy of contractions as revealed by the significant decrease in the force/$\dot{V}O_2$ relationship. These novel findings indicate that, while potentially improving vascular function, transient increases in H_2O_2 have detrimental effects on skeletal muscle function (i.e., augmented O_2 cost of force production) that may contribute to exercise intolerance in conditions associated with oxidative stress.

Table 4.1 Muscle PO_2mv at rest and following the onset of contractions under control and H_2O_2 treatments

	Control	H_2O_2
$PO_2mv_{(Pre)}$, mmHg	31.6 ± 1.6	33.5 ± 2.3
$PO_2mv_{(Post)}$, mmHg	31.9 ± 1.6	39.0 ± 2.6*
Δ_1PO_2mv, mmHg	11.7 ± 0.7	12.6 ± 1.4
Δ_2PO_2mv, mmHg	2.9 ± 0.2	-
$\Delta_{Total}PO_2mv$, mmHg	12.3 ± 0.9	12.6 ± 1.4
$PO_2mv_{(SS)}$, mmHg	20.8 ± 1.4	27.0 ± 2.6*
TD_1, s	5.5 ± 1.2	0.2 ± 0.2*
TD_2, s	54.5 ± 15.2	-
τ_1, s	18.7 ± 3.2	43.3 ± 6.6*
τ_2, s	19.0 ± 6.4	-
MRT, s	24.2 ± 3.0	43.5 ± 6.6*
T_{63}, s	24.2 ± 3.1	46.5 ± 7.4*

$PO_2mv_{(Pre)}$, pre-treatment resting PO_2mv; $PO_2mv_{(Post)}$, post-treatment resting PO_2mv; Δ_1PO_2mv, amplitude of the first component; Δ_2PO_2mv, amplitude of the second component; $\Delta_{Total}PO_2mv$, overall amplitude regardless of one- or two-component model fit; $PO_2mv_{(SS)}$, contracting steady-state PO_2mv; TD_1, time delay for the first component; TD_2, time delay for the second component; τ_1, time constant for the first component; τ_2, time constant for the second component; MRT, mean response time; T_{63}, time to reach 63% of the overall amplitude as determined independent of modeling procedures. The one-component exponential model was used to analyze the PO_2mv kinetics in the majority of instances (16 out of 20) in the control condition and in all cases for H_2O_2. * Significantly different from control.

Figure 4.1 Experimental protocol

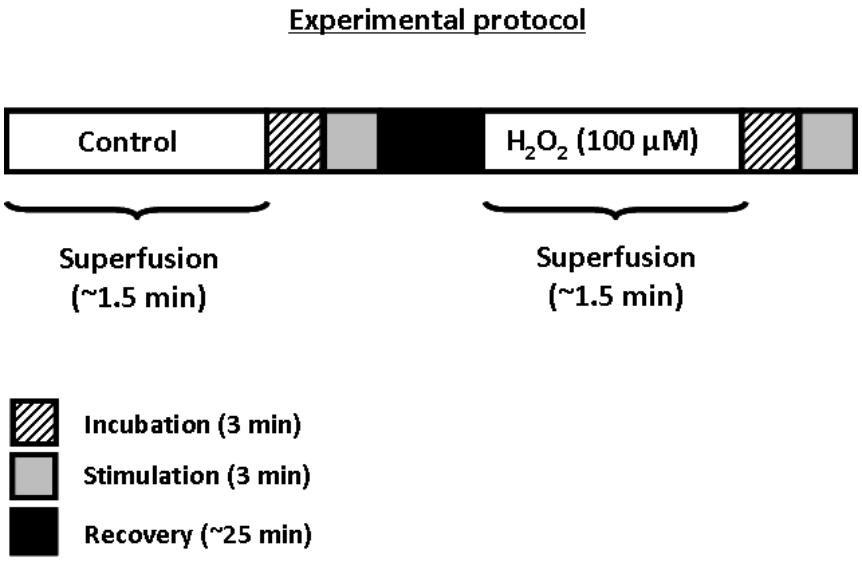

Figure 4.1 Schematic representation of the protocol utilized in the current study (diagram not to scale). Control, Krebs-Henseleit solution; H_2O_2; hydrogen peroxide. See text for details.

Figure 4.2 Muscle *PO_2mv* during control and H_2O_2 superfusion conditions

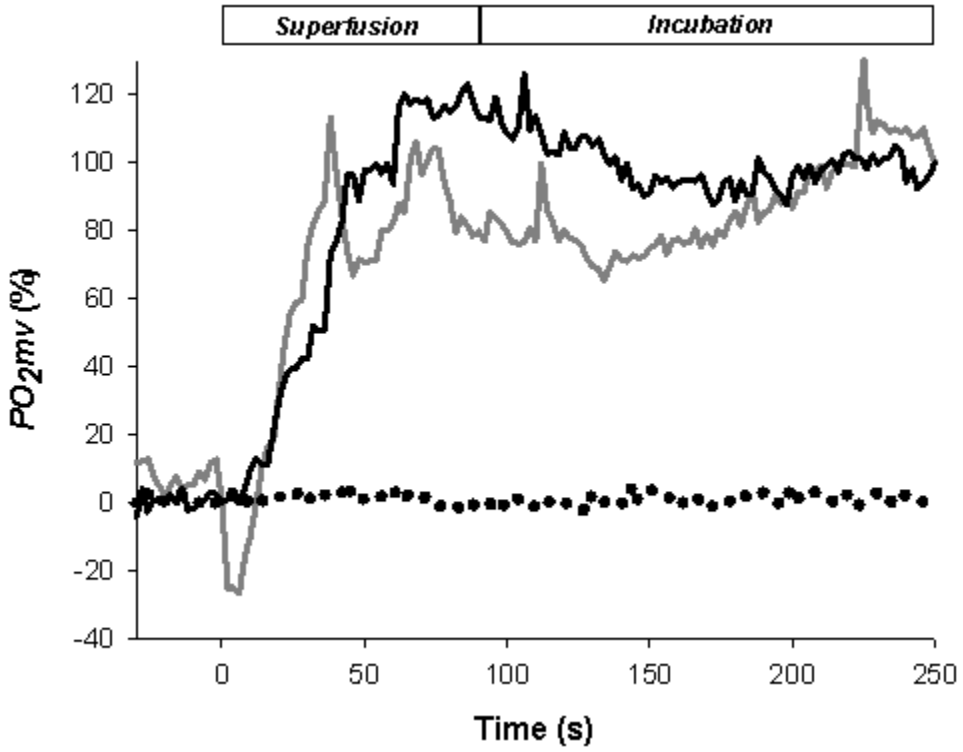

Figure 4.2 Typical relative changes in spinotrapezius muscle microvascular PO_2 (*PO_2mv*) during K-H (control; *dotted line*) and H_2O_2 (100 μM; *continuous lines*) superfusion and incubation periods (approximately 0-90 and 90-250 s, respectively). Note that, although not all *PO_2mv* profiles exhibited an initial transient fall following H_2O_2 superfusion consistent with the brief arteriolar constriction response to exogenous H_2O_2 (100 μM) in isolated vessels reported by Csekő et al. (16), we observed that H_2O_2 treatment increased basal *PO_2mv* in all instances. Steady-state *PO_2mv* values were reached within ~3 min following H_2O_2 superfusion. Time zero denotes start of the H_2O_2 superfusion period. See text for discussion.

Figure 4.3 Muscle *PO_2mv* following the onset of contractions under control and H_2O_2 conditions

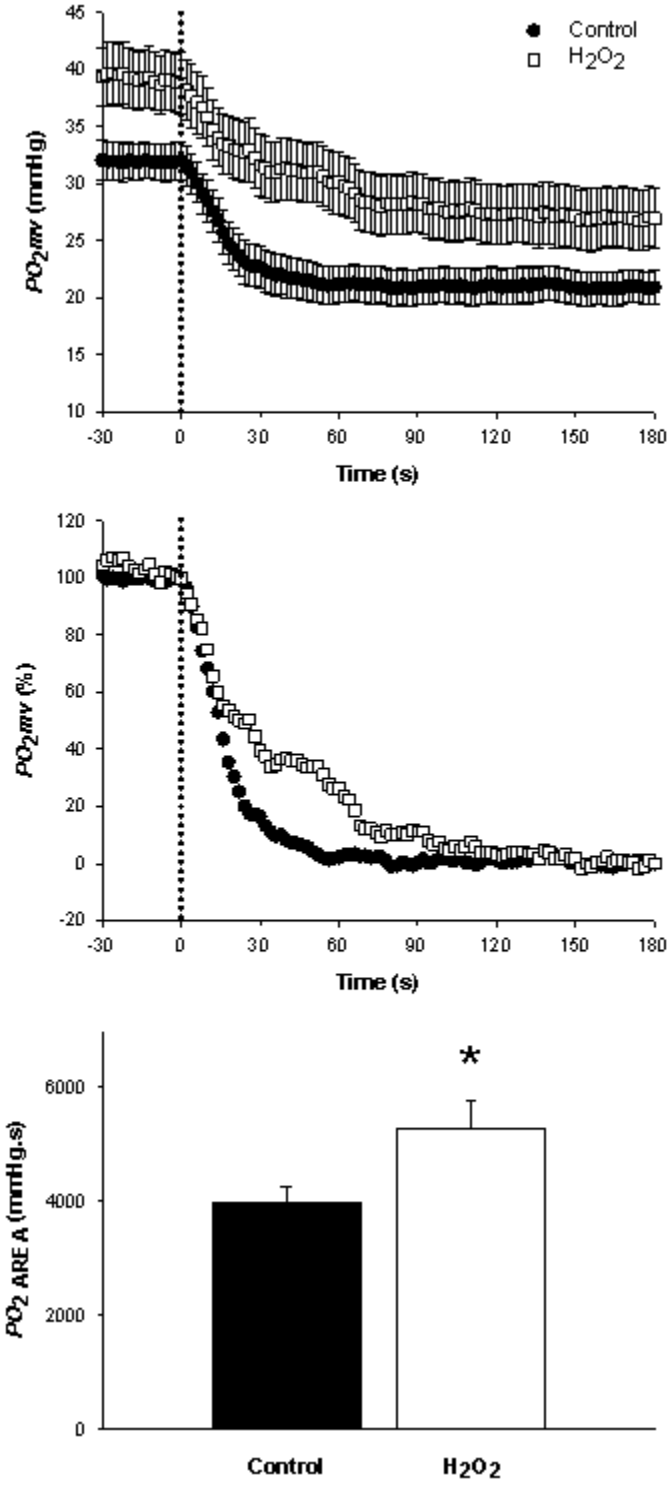

Figure 4.3 Mean spinotrapezius muscle microvascular PO_2 (PO_2mv) following the onset of contractions under control and H_2O_2 treatments. Top and middle panels exhibit absolute and relative PO_2mv, respectively. SE bars omitted from middle panel for clarity. Time zero depicts the onset of muscle contractions. Note that exogenous H_2O_2 affected markedly PO_2mv kinetics during submaximal contractions (see Table 4.1 for details). The bottom panel shows the mean values for the area under the microvascular PO_2 curve (PO_{2AREA}) following the onset of contractions under control and H_2O_2 treatments. PO_{2AREA} was determined through integration of the area under the PO_2mv curve over the 3 min stimulation period for each condition. * Significantly different from control.

Figure 4.4 Muscle blood flow at rest and during contractions under control and H_2O_2 conditions

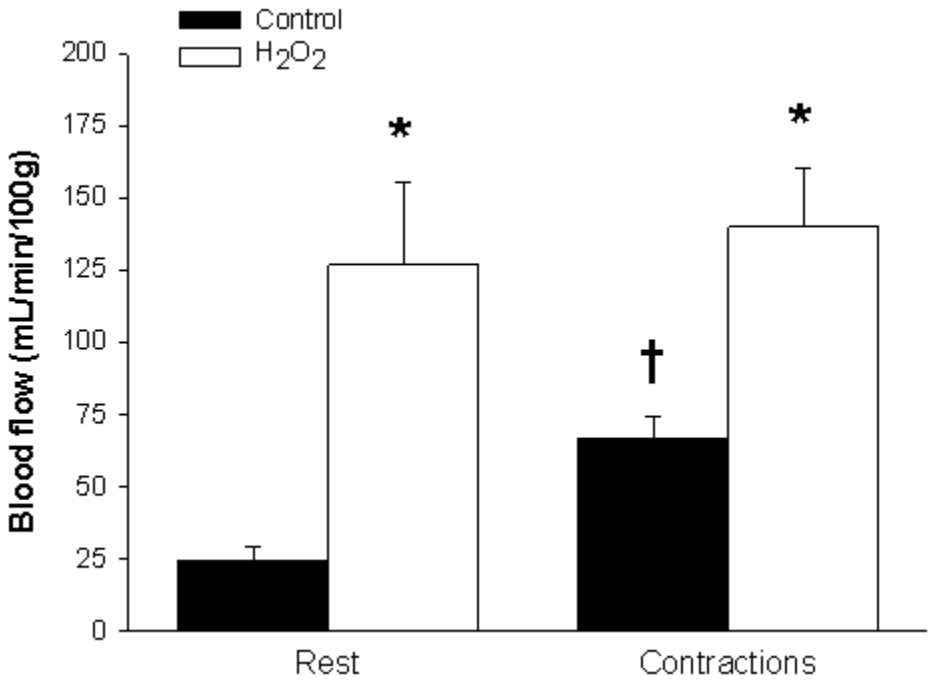

Figure 4.4 Mean spinotrapezius muscle blood flow at rest and during contractions under control and H_2O_2 treatments. * Significantly different from control within the same condition (i.e., rest or contractions). † Significantly different from rest.

Figure 4.5 Muscle $\dot{V}O_2$ at rest and during contractions under control and H_2O_2 conditions

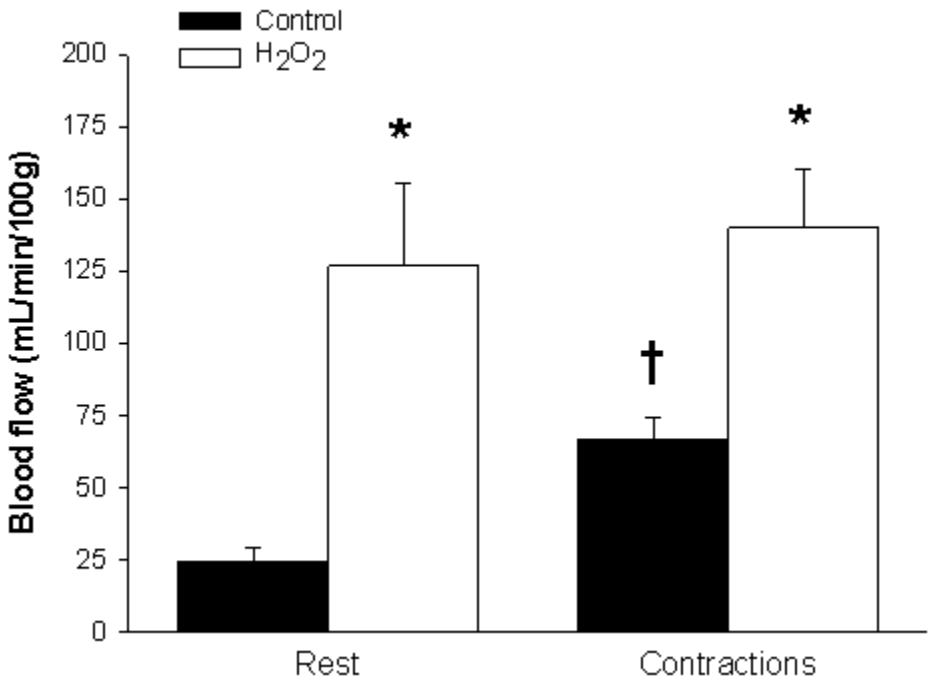

Figure 4.5 Mean spinotrapezius muscle O_2 utilization ($\dot{V}O_2$) at rest and during contractions under control and H_2O_2 treatments. * Significantly different from control within the same condition (i.e., rest or contractions). † Significantly different from rest.

Figure 4.6 Muscle force production under control and H_2O_2 conditions

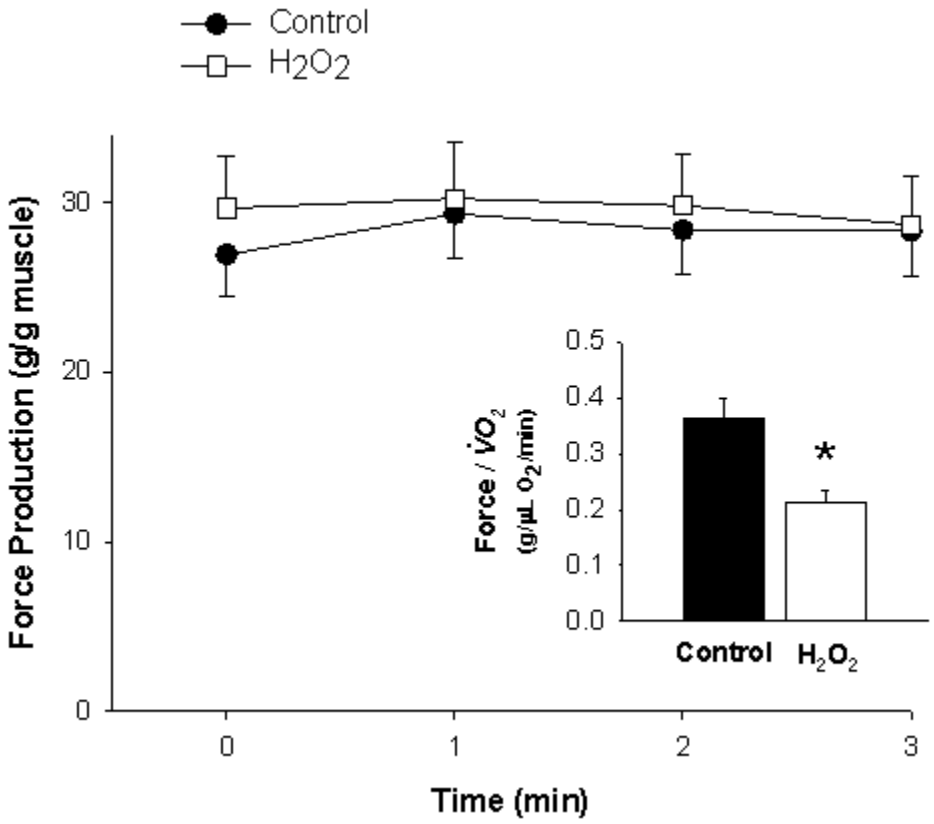

Figure 4.6 Mean spinotrapezius muscle force production under control and H_2O_2 treatments. Note that muscle force production was not significantly different throughout the contraction period between control and H_2O_2. The inset shows the force/$\dot{V}O_2$ relationship for both treatments. As a result of the greater muscle $\dot{V}O_2$ induced by H_2O_2 (Fig. 4.4), a reduction of ~40% in the force/$\dot{V}O_2$ relationship was observed. * Significantly different from control.

Figure 4.7 Redox regulation of submaximal muscle force production

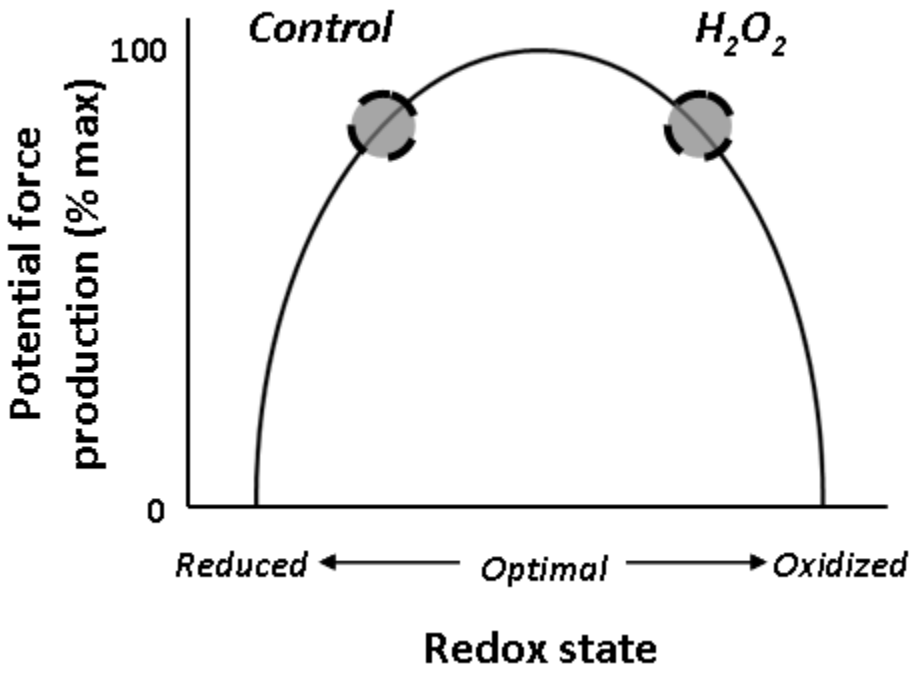

Figure 4.7 Hypothetical model illustrating the redox regulation of submaximal muscle force production as proposed originally by Reid et al. (4, 48, 49). The model predicts that deviations from optimal redox state are associated with reduced muscle force production. For any given condition, the putative location on the biphasic response profile is depicted as a potential range (i.e., circles demarcated by dotted lines) and not as a definite point since it is not possible to precisely and directly determine redox state (46, 48). Unfatigued muscle redox state at rest is located slightly to the left of the optimal for contractile function, whereas muscle contractions under control conditions enhance ROS accumulation thus shifting the muscle to the right towards greater force production. Acute oxidant treatment with H_2O_2 is expected to further push muscle redox state to the right compared to control contractions. Similar force production under H_2O_2 treatment relative to control in the current study may have resulted, in part, from a rightward shift along the bell-shaped response profile placing muscle redox state beyond the optimal point as depicted in the figure. As such, the correspondence between force production in the control and H_2O_2 conditions would be coincidental. See text for discussion.

References

1. **Allen DG, Lamb GD, and Westerblad H**. Skeletal muscle fatigue: cellular mechanisms. *Physiol Rev* 88: 287-332, 2008.

2. **Altman PL, and Dittmer DS**. *Biology Data Book*. Bethesda, MD: FASEB, 1974.

3. **Anderson EJ, and Neufer PD**. Type II skeletal myofibers possess unique properties that potentiate mitochondrial H_2O_2 generation. *Am J Physiol Cell Physiol* 290: C844-851, 2006.

4. **Andrade FH, Reid MB, Allen DG, and Westerblad H**. Effect of hydrogen peroxide and dithiothreitol on contractile function of single skeletal muscle fibres from the mouse. *J Physiol* 509 (Pt 2): 565-575, 1998.

5. **Andrade FH, Reid MB, Allen DG, and Westerblad H**. Effect of nitric oxide on single skeletal muscle fibres from the mouse. *J Physiol* 509 (Pt 2): 577-586, 1998.

6. **Antunes F, and Cadenas E**. Estimation of H_2O_2 gradients across biomembranes. *FEBS Lett* 475: 121-126, 2000.

7. **Arbogast S, and Reid MB**. Oxidant activity in skeletal muscle fibers is influenced by temperature, CO_2 level, and muscle-derived nitric oxide. *Am J Physiol Regul Integr Comp Physiol* 287: R698-705, 2004.

8. **Ardanaz N, and Pagano PJ**. Hydrogen peroxide as a paracrine vascular mediator: regulation and signaling leading to dysfunction. *Exp Biol Med (Maywood)* 231: 237-251, 2006.

9. **Bailey JK, Kindig CA, Behnke BJ, Musch TI, Schmid-Schoenbein GW, and Poole DC**. Spinotrapezius muscle microcirculatory function: effects of surgical exteriorization. *Am J Physiol Heart Circ Physiol* 279: H3131-3137, 2000.

10. **Behnke BJ, Kindig CA, Musch TI, Koga S, and Poole DC**. Dynamics of microvascular oxygen pressure across the rest-exercise transition in rat skeletal muscle. *Respir Physiol* 126: 53-63, 2001.

11. **Behnke BJ, Kindig CA, Musch TI, Sexton WL, and Poole DC**. Effects of prior contractions on muscle microvascular oxygen pressure at onset of subsequent contractions. *J Physiol* 539: 927-934, 2002.

12. **Boulden BM, Widder JD, Allen JC, Smith DA, Al-Baldawi RN, Harrison DG, Dikalov SI, Jo H, and Dudley SC, Jr.** Early determinants of H_2O_2-induced endothelial dysfunction. *Free Radic Biol Med* 41: 810-817, 2006.

13. **Cleeter MW, Cooper JM, Darley-Usmar VM, Moncada S, and Schapira AH**. Reversible inhibition of cytochrome c oxidase, the terminal enzyme of the mitochondrial respiratory chain, by nitric oxide. Implications for neurodegenerative diseases. *FEBS Lett* 345: 50-54, 1994.

14. **Copp SW, Ferreira LF, Herspring KF, Hirai DM, Snyder BS, Poole DC, and Musch TI**. The effects of antioxidants on microvascular oxygenation and blood flow in skeletal muscle of young rats. *Exp Physiol* 94: 961-971, 2009.

15. **Cosentino F, and Katusic ZS**. Tetrahydrobiopterin and dysfunction of endothelial nitric oxide synthase in coronary arteries. *Circulation* 91: 139-144, 1995.

16. **Csekő C, Bagi Z, and Koller A**. Biphasic effect of hydrogen peroxide on skeletal muscle arteriolar tone via activation of endothelial and smooth muscle signaling pathways. *J Appl Physiol* 97: 1130-1137, 2004.

17. **Delliaux S, Brerro-Saby C, Steinberg JG, and Jammes Y**. Reactive oxygen species activate the group IV muscle afferents in resting and exercising muscle in rats. *Pflugers Arch* 459: 143-150, 2009.

18. **Delp MD, and Duan C**. Composition and size of type I, IIA, IID/X, and IIB fibers and citrate synthase activity of rat muscle. *J Appl Physiol* 80: 261-270, 1996.

19. **Eddy L, Arduini A, and Hochstein P**. Reduction of ferrylmyoglobin in rat diaphragm. *Am J Physiol* 259: C995-997, 1990.

20. **Ferreira LF, and Reid MB**. Muscle-derived ROS and thiol regulation in muscle fatigue. *J Appl Physiol* 104: 853-860, 2008.

21. **Forman HJ, Maiorino M, and Ursini F**. Signaling functions of reactive oxygen species. *Biochemistry* 49: 835-842, 2010.

22. **Gao YJ, Zhang Y, Hirota S, Janssen LJ, and Lee RM**. Vascular relaxation response to hydrogen peroxide is impaired in hypertension. *Br J Pharmacol* 142: 143-149, 2004.

23. **Herspring KF, Ferreira LF, Copp SW, Snyder BS, Poole DC, and Musch TI**. Effects of antioxidants on contracting spinotrapezius muscle microvascular oxygenation and blood flow in aged rats. *J Appl Physiol* 105: 1889-1896, 2008.

24. **Hirai DM, Copp SW, Ferreira LF, Musch TI, and Poole DC**. Nitric oxide bioavailability modulates the dynamics of microvascular oxygen exchange during recovery from contractions. *Acta Physiol (Oxf)* 200: 159-169, 2010.

25. **Hirai DM, Copp SW, Herspring KF, Ferreira LF, Poole DC, and Musch TI**. Aging impacts microvascular oxygen pressures during recovery from contractions in rat skeletal muscle. *Respir Physiol Neurobiol* 169: 315-322, 2009.

26. **Hogan MC, Arthur PG, Bebout DE, Hochachka PW, and Wagner PD**. Role of O_2 in regulating tissue respiration in dog muscle working in situ. *J Appl Physiol* 73: 728-736, 1992.

27. **Hu Z, Chen J, Wei Q, and Xia Y**. Bidirectional actions of hydrogen peroxide on endothelial nitric-oxide synthase phosphorylation and function: co-commitment and interplay of Akt and AMPK. *J Biol Chem* 283: 25256-25263, 2008.

28. **Ishise S, Pegram BL, Yamamoto J, Kitamura Y, and Frohlich ED**. Reference sample microsphere method: cardiac output and blood flows in conscious rat. *Am J Physiol* 239: H443-H449, 1980.

29. **Kindig CA, McDonough P, Erickson HH, and Poole DC**. Effect of L-NAME on oxygen uptake kinetics during heavy-intensity exercise in the horse. *J Appl Physiol* 91: 891-896, 2001.

30. **Leek BT, Mudaliar SR, Henry R, Mathieu-Costello O, and Richardson RS**. Effect of acute exercise on citrate synthase activity in untrained and trained human skeletal muscle. *Am J Physiol Regul Integr Comp Physiol* 280: R441-447, 2001.

31. **Macdonald M, Pedersen PK, and Hughson RL**. Acceleration of $\dot{V}O_2$ kinetics in heavy submaximal exercise by hyperoxia and prior high-intensity exercise. *J Appl Physiol* 83: 1318-1325, 1997.

32. **Marvar PJ, Hammer LW, and Boegehold MA**. Hydrogen peroxide-dependent arteriolar dilation in contracting muscle of rats fed normal and high salt diets. *Microcirculation* 14: 779-791, 2007.

33. **Masuoka N, Sugiyama H, Ishibashi N, Wang DH, Masuoka T, Kodama H, and Nakano T**. Characterization of acatalasemic erythrocytes treated with low and high dose hydrogen peroxide. Hemolysis and aggregation. *J Biol Chem* 281: 21728-21734, 2006.

34. **Matoba T, Shimokawa H, Nakashima M, Hirakawa Y, Mukai Y, Hirano K, Kanaide H, and Takeshita A**. Hydrogen peroxide is an endothelium-derived hyperpolarizing factor in mice. *J Clin Invest* 106: 1521-1530, 2000.

35. **Miura H, Bosnjak JJ, Ning G, Saito T, Miura M, and Gutterman DD**. Role for hydrogen peroxide in flow-induced dilation of human coronary arterioles. *Circ Res* 92: e31-40, 2003.

36. **Moopanar TR, and Allen DG**. Reactive oxygen species reduce myofibrillar Ca^{2+} sensitivity in fatiguing mouse skeletal muscle at 37°C. *J Physiol* 564: 189-199, 2005.

37. **Murphy RM, Dutka TL, and Lamb GD**. Hydroxyl radical and glutathione interactions alter calcium sensitivity and maximum force of the contractile apparatus in rat skeletal muscle fibres. *J Physiol* 586: 2203-2216, 2008.

38. **Musch TI, and Terrell JA**. Skeletal muscle blood flow abnormalities in rats with a chronic myocardial infarction: rest and exercise. *Am J Physiol* 262: H411-419, 1992.

39. **Nagababu E, Chrest FJ, and Rifkind JM**. Hydrogen-peroxide-induced heme degradation in red blood cells: the protective roles of catalase and glutathione peroxidase. *Biochim Biophys Acta* 1620: 211-217, 2003.

40. **Neumann CA, Cao J, and Manevich Y**. Peroxiredoxin 1 and its role in cell signaling. *Cell Cycle* 8: 4072-4078, 2009.

41. **Oba T, Kurono C, Nakajima R, Takaishi T, Ishida K, Fuller GA, Klomkleaw W, and Yamaguchi M**. H_2O_2 activates ryanodine receptor but has little effect on recovery of releasable Ca^{2+} content after fatigue. *J Appl Physiol* 93: 1999-2008, 2002.

42. **Oter O, and Ribou AC**. Quenching of long lifetime emitting fluorophores with paramagnetic molecules. *J Fluoresc* 19: 389-397, 2009.

43. **Phillips SA, Hatoum OA, and Gutterman DD**. The mechanism of flow-induced dilation in human adipose arterioles involves hydrogen peroxide during CAD. *Am J Physiol Heart Circ Physiol* 292: H93-100, 2007.

44. **Poole DC, Behnke BJ, McDonough P, McAllister RM, and Wilson DF**. Measurement of muscle microvascular oxygen pressures: compartmentalization of phosphorescent probe. *Microcirculation* 11: 317-326, 2004.

45. **Poole DC, Wagner PD, and Wilson DF**. Diaphragm microvascular plasma PO_2 measured in vivo. *J Appl Physiol* 79: 2050-2057, 1995.

46. **Powers SK, and Jackson MJ**. Exercise-induced oxidative stress: cellular mechanisms and impact on muscle force production. *Physiol Rev* 88: 1243-1276, 2008.

47. **Prochniewicz E, Lowe DA, Spakowicz DJ, Higgins L, O'Conor K, Thompson LV, Ferrington DA, and Thomas DD**. Functional, structural, and chemical changes in myosin associated with hydrogen peroxide treatment of skeletal muscle fibers. *Am J Physiol Cell Physiol* 294: C613-626, 2008.

48. **Reid MB**. Invited Review: redox modulation of skeletal muscle contraction: what we know and what we don't. *J Appl Physiol* 90: 724-731, 2001.

49. **Reid MB, Khawli FA, and Moody MR**. Reactive oxygen in skeletal muscle. III. Contractility of unfatigued muscle. *J Appl Physiol* 75: 1081-1087, 1993.

50. **Rumsey WL, Vanderkooi JM, and Wilson DF**. Imaging of phosphorescence: a novel method for measuring oxygen distribution in perfused tissue. *Science* 241: 1649-1651, 1988.

51. **Shimokawa H**. Hydrogen peroxide as an endothelium-derived hyperpolarizing factor. *Pflugers Arch* 459: 915-922, 2010.

52. **Sims NR, Anderson MF, Hobbs LM, Kong JY, Phillips S, Powell JA, and Zaidan E**. Impairment of brain mitochondrial function by hydrogen peroxide. *Brain Res Mol Brain Res* 77: 176-184, 2000.

53. **Sindler AL, Delp MD, Reyes R, Wu G, and Muller-Delp JM**. Effects of ageing and exercise training on eNOS uncoupling in skeletal muscle resistance arterioles. *J Physiol* 587: 3885-3897, 2009.

54. **Skulachev VP**. Role of uncoupled and non-coupled oxidations in maintenance of safely low levels of oxygen and its one-electron reductants. *Q Rev Biophys* 29: 169-202, 1996.

55. **Spencer T, and Posterino GS**. Sequential effects of GSNO and H_2O_2 on the Ca^{2+} sensitivity of the contractile apparatus of fast- and slow-twitch skeletal muscle fibers from the rat. *Am J Physiol Cell Physiol* 296: C1015-1023, 2009.

56. **Thomas SR, Witting PK, and Drummond GR**. Redox control of endothelial function and dysfunction: molecular mechanisms and therapeutic opportunities. *Antioxid Redox Signal* 10: 1713-1765, 2008.

57. **Tonkonogi M, Walsh B, Svensson M, and Sahlin K**. Mitochondrial function and antioxidative defence in human muscle: effects of endurance training and oxidative stress. *J Physiol* 528 Pt 2: 379-388, 2000.

58. **Trott DW, Seawright JW, Luttrell MJ, and Woodman CR**. NAD(P)H oxidase-derived reactive oxygen species contribute to age-related impairments of endothelium-dependent dilation in rat soleus feed arteries. *J Appl Physiol* (in press), 2011.

59. **Vasilaki A, Mansouri A, Remmen H, van der Meulen JH, Larkin L, Richardson AG, McArdle A, Faulkner JA, and Jackson MJ**. Free radical generation by skeletal muscle of adult and old mice: effect of contractile activity. *Aging Cell* 5: 109-117, 2006.

60. **Vidal-Puig AJ, Grujic D, Zhang CY, Hagen T, Boss O, Ido Y, Szczepanik A, Wade J, Mootha V, Cortright R, Muoio DM, and Lowell BB**. Energy metabolism in uncoupling protein 3 gene knockout mice. *J Biol Chem* 275: 16258-16266, 2000.

61. **Vinogradov SA, Fernandez-Searra MA, Dugan BW, and Wilson DF**. Frequency domain instrument for measuring phosphorescence lifetime distributions in heterogeneous samples. *Rev Sci Instrum* 72: 3396-3406, 2001.

62. **Wang HJ, Pan YX, Wang WZ, Zucker IH, and Wang W**. NADPH oxidase-derived reactive oxygen species in skeletal muscle modulates the exercise pressor reflex. *J Appl Physiol* 107: 450-459, 2009.

63. **Zhou X, Bohlen HG, Miller SJ, and Unthank JL**. NAD(P)H oxidase-derived peroxide mediates elevated basal and impaired flow-induced NO production in SHR mesenteric arteries in vivo. *Am J Physiol Heart Circ Physiol* 295: H1008-H1016, 2008.

64. **Zhou X, Bohlen HG, Unthank JL, and Miller SJ**. Abnormal nitric oxide production in aged rat mesenteric arteries is mediated by NAD(P)H oxidase-derived peroxide. *Am J Physiol Heart Circ Physiol* 297: H2227-2233, 2009.

Chapter 5 - Exercise training and muscle microvascular oxygenation: functional role of nitric oxide

Summary

Exercise training induces multiple adaptations within skeletal muscle that may improve local O_2 delivery-utilization matching (i.e., PO_2mv). We tested the hypothesis that increased nitric oxide (NO) function is intrinsic to improved muscle PO_2mv kinetics from rest to contractions after exercise training. Healthy young Sprague-Dawley rats were assigned to sedentary (n=18) or progressive treadmill exercise training (n=10; 5 d/wk, 6-8 wks, final workload of 60 min/d at 35 m/min, -14% grade) groups. PO_2mv was measured via phosphorescence quenching in the spinotrapezius muscle at rest and during 1 Hz twitch contractions under control (Krebs-Henseleit solution), sodium nitroprusside (SNP, NO donor; 300 μM) and N^G-nitro-L-arginine methyl ester (L-NAME, non-specific NOS blockade; 1.5 mM) superfusion conditions. Exercise trained rats had greater peak oxygen uptake ($\dot{V}O_2\,peak$) than their sedentary counterparts (81 ± 1 *vs*. 72 ± 2 ml/kg/min, respectively; $p<0.05$). Exercise trained rats had significantly slower PO_2mv fall throughout contractions (τ_1; time constant for the first component) during control (sedentary: 8.1 ± 0.6; trained: 15.2 ± 2.8 s). Compared to control, SNP slowed τ_1 to a greater extent in sedentary rats (sedentary: 38.7 ± 5.6; trained: 26.8 ± 4.1 s; $p<0.05$) whereas L-NAME abolished the differences in τ_1 between sedentary and trained rats (sedentary: 12.0 ± 1.7; trained: 11.2 ± 1.4 s; $p<0.05$). Our results indicate that endurance exercise training leads to greater muscle microvascular oxygenation across the metabolic transient following the onset of contractions (i.e., slower PO_2mv kinetics) partly via increased NO-mediated function which likely constitutes an important mechanism for training-induced metabolic adaptations.

Introduction

Endurance exercise training induces multiple structural and functional adaptations that enhance the capacities for skeletal muscle O_2 delivery and utilization ($\dot{Q}O_2$ and $\dot{V}O_2$, respectively; refs. 37, 58, 71). At any given submaximal contractile activity, this cluster of adaptations reduces the level of metabolic perturbations (e.g., changes in ADP, PCr and Cr concentrations) required to drive $\dot{V}O_2$ and improves the coupling between energy utilization and muscle mitochondrial ATP production (70). These properties reduce the rate of glycolysis and reliance on finite energy sources and increase exercise tolerance (37).

Microcirculatory adaptations to training are particularly important considering that the greatest resistance to O_2 flux into skeletal muscle fibers resides primarily in the short distance between the red blood cell and the adjacent subsarcolemmal space (23, 29). As dictated by Fick's law of diffusion, the O_2 pressure within the microvasculature (i.e., muscle PO_2mv) constitutes the exclusive driving force for blood-myocyte O_2 transfer. The time course of skeletal muscle PO_2mv during transitions in metabolic demand is determined by the dynamic matching between $\dot{Q}O_2$ and $\dot{V}O_2$ (i.e., $\dot{Q}O_2/\dot{V}O_2$ ratio) (8). Therefore, because alterations in muscle PO_2mv have a direct impact on oxidative metabolism and contractile performance (36, 68), increased PO_2mv during contractions likely contributes to the beneficial effects of exercise training on muscle function.

Substantial evidence indicates that increased nitric oxide (NO) function is a key factor improving skeletal muscle hemodynamic and metabolic control following exercise training (28, 53). Moreover, previous reports from our laboratory indicate that alterations in NO levels impact profoundly muscle PO_2mv during transitions in metabolic demand in health and disease (24, 25, 31) and suggest that increased NO-mediated function could underlie, at least in part, enhanced muscle microvascular oxygenation in the trained state.

The purpose of the present study was to determine the effects of endurance exercise training on muscle PO_2mv and whether augmented NO-mediated function contributes mechanistically to potential increases in PO_2mv from rest to contractions in rat skeletal muscle *in situ* after training. Based on the potential enhancement of NO-mediated function following endurance exercise training (28, 53), the hypotheses were tested that 1) exercise training would

elevate muscle PO_2mv and slow PO_2mv kinetics (i.e., resulting in higher PO_2mv across the on-contraction transient); 2) increased NO levels (via the NO donor sodium nitroprusside; SNP) would elevate PO_2mv and slow PO_2mv kinetics to a greater extent in sedentary compared to trained rats; and 3) reduced NO levels (non-specific NO synthase blockade with N^G-nitro-L-arginine methyl ester; L-NAME) would lower PO_2mv and speed PO_2mv kinetics to a greater extent in trained compared to sedentary rats during the transition from rest to contractions.

Methods

Animal selection and care

A total of 28 male Sprague-Dawley rats (4-5 months old; Charles Rivers Laboratories, Boston, MA, USA) were used to investigate the effects of exercise training on, and the NO contribution to, skeletal muscle microvascular oxygenation. Additional rats were used in supplementary experiments to 1) evaluate the reproducibility and demonstrate the lack of an ordering effect of the protocol (n=7); and 2) assess potential cyanide-induced impairment of skeletal muscle function with the current SNP superfusion protocol (n=9). All experimental procedures followed guidelines established by the National Institutes of Health and were approved by the Institutional Animal Care and Use Committee of Kansas State University. Rats were maintained on a 12:12-h light-dark cycle with food and water provided *ad libitum*. Before initiation of the experimental protocol, rats were familiarized with downhill running on a custom-built motor-driven treadmill over the course of a 1 wk period (5-10 min/day at a speed of 20 m/min and -14% grade). After the familiarization phase, rats were assigned randomly to either sedentary (n=18) or endurance exercise trained (n=10) groups. Sedentary control rats were confined to cage activities whereas trained rats ran 5 days/wk for 6-8 wks on the declined treadmill (-14% grade). All rats underwent the same training program, in which treadmill running duration and speed were increased progressively from 10 min at 25 m/min to 60 min at 35 m/min. This final workload was kept for at least 3-4 wks. Previous work from our laboratory has demonstrated that downhill treadmill running recruits the rat spinotrapezius muscle (41, 57) and constitutes an effective model for exercise training programs (30).

$\dot{V}O_2$ peak measurements

Upon completion of the training program, peak oxygen uptake ($\dot{V}O_2$ *peak*) was measured in sedentary and trained rats during a downhill (-14% grade) running test performed in a metabolic chamber placed on the treadmill. As described in detail previously (16, 30), the speed was set initially to 25 m/min for 2-3 min and then increased progressively in a ramp-like fashion by ~5-10 m/min until the rat was unable to keep pace with the treadmill belt or no further elevations in $\dot{V}O_2$ were observed despite continued increases in treadmill speed. At this point of

the test $\dot{V}O_2\,peak$ was measured and recorded. Alterations in gait (e.g., lowering of the hindlimbs, dropping of the tail and elevation of the snout) normally occurred immediately prior to termination of the test. Six of the 28 rats tested had to repeat their maximal tests on a separate day (i.e., ≥24 hours of recovery) due to failure to achieve the predetermined criteria. Gas measurements were performed in real time via an inline O_2 analyzer (model S-3A/I; AEI Technologies; Pittsburgh, PA, USA). The analyzer was calibrated before and after each maximal exercise test with precision-mixed gases that spanned the expected range of gas concentrations based on previous studies. We have reported recently highly reproducible $\dot{V}O_2\,peak$ measurements using the aforementioned techniques and protocol (16).

Surgical preparation

On the day of data collection, rats were anesthetized initially with 5% isoflurane-O_2 mixture and subsequently maintained on 2-3% isoflurane-O_2 (Butler Animal Health Supply, Dublin, OH, USA). The left carotid and caudal (tail) arteries were cannulated (PE-10 connected to PE-50; Intra-Medic Tubing, Clay Adams Brand, Sparks, MD, USA) for continuous monitoring of mean arterial pressure (MAP; Digi-Med BPA Model 200, Louisville, KY, USA) and infusion of the phosphorescent probe palladium *meso*-tetra (4-carboxyphenyl) porphyrin dendrimer (R2; 15 mg/kg; Oxygen Enterprises, Philadelphia, PA, USA). Blood from the tail catheter was sampled at the end of each experimental protocol for determination of arterial blood gases, pH and systemic hematocrit (Nova Stat Profile M, Waltham, MA, USA). Anesthetized rats were placed on a heating pad to maintain core temperature, measured via rectal probe, at ~37-38°C.

Following catheter placement procedures, isoflurane inhalation was discontinued progressively and rats were kept under anesthesia with intra-arterial pentobarbital sodium throughout the experiment. The level of anesthesia was monitored frequently via the toe-pinch and blink reflexes and supplemented as necessary. Overlying skin and fascia from the mid-dorsal region of the rat were reflected carefully to expose the right spinotrapezius muscle. The spinotrapezius was moistened constantly during the surgical preparation via superfusion of Krebs-Henseleit (K-H) bicarbonate-buffered solution (4.7 mM KCl, 2.0 mM $CaCl_2$, 2.4 mM $MgSO_4$, 131 mM NaCl and 22 mM $NaHCO_3$; pH = 7.4; equilibrated with 5% CO_2 and 95% N_2 at ~38°C). Surrounding tissue was covered with Saran wrap (Dow Brands, Indianapolis, IN,

USA). Stainless steel electrodes were sutured to the rostral (cathode) and caudal (anode) regions of the spinotrapezius for electrically induced contractions. Previous reports from our laboratory demonstrate that these surgical procedures do not impact the microvascular integrity and responsiveness of the spinotrapezius muscle (3).

Experimental protocol

Three separate contraction bouts were performed under control (5 ml K-H), SNP (NO donor; 5 ml of a 300 μM solution) and L-NAME (non-isoform specific NO synthase inhibitor; 5 ml of a 1.5 mM solution) superfusion conditions. Drugs were purchased from Sigma-Aldrich (St. Louis, MO, USA) and concentrations were chosen based on previous studies in our laboratory (24, 25, 31). All solutions were maintained at ~38°C. The dose of SNP was titrated to elicit consistent alterations in PO_2mv without compromising systemic hemodynamics (i.e., a decrease in MAP below 70 mmHg at any time; refs. 10, 25). Preliminary experiments indicate that significantly greater hypotensive responses and increases in resting PO_2mv are evoked by progressively higher SNP doses (up to 1200 μM; unpublished data). In order to prevent SNP photodecomposition and potential cyanide release (11, 13), SNP solutions were protected from light sources by covering containers and syringes with aluminum foil and, as a mandate for PO_2mv measurements using phosphorescence quenching, performing our experiments in a dark room. While superfusion order was randomized between control and SNP conditions, L-NAME was always the last treatment because of its relatively long half-life. The spinotrapezius was superfused with each solution (average flow rate of ~1.5 ml/min) for a total time of 3 min, followed by a 2-3 min incubation period to allow resting muscle PO_2mv to stabilize. Subsequently, electrical stimulation (1 Hz, 6-7 V, 2 ms pulse duration) of the muscle was evoked via a Grass stimulator (model s48, Quincy, MA, USA) for 3 min. The muscle was then allowed to recover for ~25 min before the next condition was initiated (stimulation parameters were held constant). During the recovery period following the SNP trial, the muscle was superfused at an average flow rate of ~1.5 ml/min with K-H to wash out SNP. At the end of each experiment, rats were euthanized with intra-arterial pentobarbital sodium overdose (~50 mg/kg).

Supplementary experiments

The spinotrapezius preparation exhibits reproducible PO_2mv parameters during transitions in metabolic demand evoked by 1 Hz twitch contractions when a minimum of 20 min of recovery is allowed between contraction bouts (31, 34). A >30 min period between consecutive contractions (i.e., 3 min off-transition, ~25 min recovery, 3 min superfusion, 2-3 min incubation) was employed herein to prevent any priming and drug ordering effects that could confound the experimental interpretation of the PO_2mv responses to muscle contractions (9, 25). Accordingly, supplementary time control experiments (n=7) revealed reproducible PO_2mv profiles from three contraction bouts separated by ~30 min (within-animal coefficient of variation: 13 ± 2% for baseline, steady-state and all primary component kinetics parameters) with no ordering effect (p>0.05 for baseline, steady-state and all kinetics parameters).

Considerable controversy exists surrounding potential cyanide generation from SNP (11, 13, 27) despite widespread usage of this NO donor in both clinical and research arenas (human and animal models). A major source of this controversy may lie within the methods utilized for assaying blood cyanide concentrations and the importance of photodecomposition in generating cyanide from SNP (during both SNP infusion and cyanide measurement; refs. 11, 13). As described above, in the current study SNP solutions were protected from light sources by covering containers and syringes with aluminum foil and performing experiments in a dark room. Nonetheless, supplementary experiments were conducted to examine potential cyanide-induced impairment of skeletal muscle function with the current SNP superfusion protocol. Three contraction bouts were conducted in the following superfusion order: control 1 (K-H), SNP (300 µM), control 2 (K-H). Recovery time and washout procedures were identical to those described above. Spinotrapezius muscle PO_2mv was measured at rest and throughout contractions (n=9). Spinotrapezius muscle blood flow ($\dot{Q}m$) and oxygen utilization ($\dot{V}O_2$) were determined at rest and during the contraction steady-state via radiolabeled microspheres and direct Fick calculation (as described in detail previously, ref. 34), respectively (n=4). In each condition, the stimulated right and non-stimulated left spinotrapezius muscles represented the contracting and resting $\dot{Q}m$ and $\dot{V}O_2$ measurements, respectively.

During $\dot{Q}m$ measurements, the tail artery catheter was connected to a 1 ml syringe and blood withdrawal was initiated at a constant rate of 0.25 ml/min via a Harvard pump (model 907). Differentially radiolabelled microspheres (^{46}Sc and ^{85}Sr, 15 µm diameter; Perkin Elmer Life and Analytical Sciences) were injected in random order into the aortic arch via the carotid

artery catheter during the contracting steady-state (i.e., ~3 min after onset of muscle contractions). Upon completion of the experiment, the right and left spinotrapezius muscles and kidneys were dissected, removed and weighted immediately after euthanasia. The thorax was opened and placement of the artery catheter into the aortic arch was confirmed. Tissue radioactivity was determined on a gamma scintillation counter (Packard Auto Gamma Spectrometer, Cobra model 5003) and $\dot{Q}m$ was determined by the reference method (39) and expressed as ml/min/100 g of tissue. Adequate mixing of the microspheres was verified for each injection by demonstrating a <15% difference in $\dot{Q}m$ between the right and left kidneys.

Spinotrapezius muscle $\dot{V}O_2$ was estimated from PO_2mv and $\dot{Q}m$ measurements as described in detail previously (34). Briefly, arterial O_2 concentration (CaO_2) was calculated from arterial blood samples whereas venous O_2 concentration (CvO_2) was calculated from the resting or contracting steady-state PO_2mv using the rat O_2 dissociation curve (Hill coefficient of 2.6), the measured hemoglobin (Hb) concentration, a P_{50} of 38 mmHg, and an O_2 carrying capacity of 1.34 ml O_2/g Hb (1). Resting and contracting steady-state spinotrapezius $\dot{Q}m$ values were then used to calculate $\dot{V}O_2$ using the Fick equation (i.e., $\dot{V}O_2 = \dot{Q}m(CaO_2 - CvO_2)$). As illustrated in Fig. 5.1, results from these experiments suggest that mitochondrial and vascular control were not impaired following the SNP condition.

Muscle PO_2mv measurement

PO_2mv was measured by phosphorescence quenching using a Frequency Domain Phosphorometer (PMOD 5000; Oxygen Enterprises, Philadelphia, PA, USA). The principles of the phosphorescence quenching method have been described in detail previously (8). Briefly, this method applies the Stern-Volmer relationship (63), which describes quantitatively the O_2 dependence of the phosphorescent probe (R2) via the following equation:

$$PO_2mv = [(\tau^\circ / \tau) - 1]/(k_Q \times \tau^\circ)$$

where k_Q is the quenching constant and τ and τ° are the phosphorescence lifetimes in the absence of O_2 and the ambient O_2 concentration, respectively. The phosphor R2 (τ° = 601 µs

and k_Q = 409 $mmHg^{-1} \cdot s^{-1}$ at pH = 7.4 and temperature ~38°C) (50) was infused ~15 min before initiation of muscle contractions. The R2 probe binds to albumin and is distributed uniformly in the plasma, therefore providing a signal corresponding to the volume-weighted O_2 pressure in the microvascular compartment (mainly the PO_2 within the capillaries, which volumetrically represents the major intramuscular space; ref. 59). The negative charge of the R2 probe also facilitates its restriction to the muscle intravascular space (60). The common end of the bifurcated light guide was positioned 2-4 mm superficial to the dorsal surface of the exposed spinotrapezius muscle. The phosphorometer modulates sinusoidal excitation frequencies between 100 Hz and 20 kHz and allows phosphorescence lifetime measurements from 10 μs to ~2.5 ms. The excitation light (524 nm) was focused on a randomly selected area of ~2 mm diameter of exposed muscle and has a penetration depth of ~500 μm. *PO_2mv* was recorded at 2 s intervals throughout the duration of the experimental protocol (i.e., superfusion, incubation, electrical stimulation and recovery periods).

Movement of the light guide and/or animal was avoided so as to monitor the same sampling site during experiments. However, alteration of the *PO_2mv* measurement plane (e.g., deep sighs, accidental splash of the light guide during superfusion) during muscle contractions precluded kinetic curve fitting in some instances. Thus, *PO_2mv* results from the present study are presented from animals under the following conditions: sedentary control (n=18); sedentary SNP (n=14); sedentary L-NAME (n=14); trained control (n=10); trained SNP (n=9); trained L-NAME (n=10).

PO_2mv kinetics analysis

The kinetics of *PO_2mv* were described by nonlinear regression analysis using the Marquardt-Levenberg algorithm (SigmaPlot 11.2; Systat software, San Jose, CA, USA) for the onset of contractions. Transient *PO_2mv* responses were fit with either a one- or two-component model (7, 8):

One-component:

$$PO_2mv_{(t)} = PO_2mv_{(BL)} - \Delta PO_2mv(1 - e^{-(t-TD)/\tau})$$

Two-component:

$$PO_2mv_{(t)} = PO_2mv_{(BL)} - \Delta_1 PO_2mv(1 - e^{-(t-TD1)/\tau_1}) + \Delta_2 PO_2mv(1 - e^{-(t-TD2)/\tau_2})$$

where $PO_2mv_{(t)}$ is the PO_2mv at a given time *t*, $PO_2mv_{(BL)}$ corresponds to the pre-contracting resting PO_2mv, Δ_1 and Δ_2 are the amplitudes for the first and second components, respectively, TD_1 and TD_2 are the independent time delays for each component, and τ_1 and τ_2 are the time constants (i.e., time to achieve 63% of the response) for each component. Goodness of fit was determined using three criteria: 1) the coefficient of determination; 2) the sum of squared residuals; and 3) visual inspection.

The mean response time (MRT; ref. 51) was used to describe the overall dynamics of the PO_2mv response:

$$MRT = TD + \tau$$

where TD and τ are defined above. The MRT analysis was limited to the first component of the PO_2mv response given that inclusion of an emergent second component underestimates the actual speed of PO_2mv fall following the onset of contractions (33, 34).

Citrate synthase activity measurement

The activity of the mitochondrial enzyme citrate synthase (a marker of oxidative capacity) from the spinotrapezius and select individual hindlimb muscles or muscle parts (soleus, red gastrocnemius, mixed gastrocnemius and plantaris) was measured in duplicate from muscle homogenates by a modification of the method described by Srere (66). Upon termination of the experimental protocol and euthanasia, the muscles were removed, dissected free of connective tissue and weighed. Citrate synthase activity was measured spectrophotometrically (Spectramax M5 microplate, Molecular Devices, Sunnyvale, CA, USA) in 300 µL aliquots at 30°C.

Statistical analyses

Data comparison was performed using unpaired Student's *t*-test, Mann-Whitney rank-sum test or two-way repeated measures ANOVA where appropriate. *F*-statistics were calculated using Type III (adjusted) sums of squares due to the unbalanced nature of the data. Student-

Newman-Keuls *post hoc* test was utilized to determine where the differences were located. A one-tail test was performed when *a priori* directional hypotheses were tested (24, 25). The level of significance was set at $p<0.05$. Results are presented as mean ± SE.

Results

Body mass and spinotrapezius muscle mass were not different between sedentary (462 ± 12 and 0.43 ± 0.1 g; respectively) and exercise trained (480 ± 9 and 0.44 ± 0.1 g; respectively) rats after the training program was completed (p>0.05 for both). There were no differences in arterial O_2 saturation (sedentary: 91.0 ± 1.7; trained: 93.6 ± 1.7%), PO_2 (sedentary: 91.9 ± 3.3; trained: 94.2 ± 3.6 mmHg), PCO_2 (sedentary: 37.3 ± 1.7; trained: 35.5 ± 0.5 mmHg), pH (sedentary: 7.40 ± 0.01; trained: 7.42 ± 0.01) and systemic hematocrit (sedentary: 34.9 ± 0.8; trained: 37.2 ± 0.7%) when comparing sedentary and trained rats (p>0.05 for all).

Exercise trained rats evidenced higher $\dot{V}O_2\,peak$ (sedentary: 72 ± 2; trained: 81 ± 1 ml/kg/min; p<0.05) than sedentary rats. Citrate synthase activity was higher in the soleus (sedentary: 17.5 ± 0.5; trained: 20.9 ± 1.5 µmol/g/min) and red gastrocnemius (sedentary: 24.2 ± 0.5; trained: 30.2 ± 1.1 µmol/g/min) muscles from trained rats (p<0.05 for both). There was a tendency for greater citrate synthase activity in the mixed gastrocnemius (sedentary: 15.9 ± 1.1; trained: 18.7 ± 1.9; µmol/g/min; p=0.064) and plantaris (sedentary: 13.5 ± 0.8; trained: 16.3 ± 1.8 µmol/g/min; p=0.058) muscles from trained rats. Unexpectedly, citrate synthase activity from the spinotrapezius was not different between sedentary and trained rats (13.4 ± 0.7 and 12.9 ± 0.7 µmol/g/min, respectively; p>0.05).

Effects of exercise training on muscle PO_2mv

MAP was not different in sedentary compared to exercise trained rats either before or after K-H superfusion (Table 5.1; p>0.05). Although PO_2mv values at rest ($PO_2mv_{(BL)}$) and during the contracting steady-state ($PO_2mv_{(SS)}$) were not different between groups (p>0.05 for both), exercise training induced significant differences in the time course of PO_2mv at the onset of contractions under the control condition (Figs. 5.2 and 5.3, Table 5.2). Specifically, the speed of PO_2mv fall during contractions (as assessed by the time constant for the first component and relative rate of PO_2mv fall; τ_1 and $\Delta_1 PO2mv/\tau_1$, respectively) was markedly slowed in trained compared to sedentary rats (Fig. 5.3). No significant differences in the time delay for the first component (TD_1, p>0.05) were observed whereas the mean response time (MRT) tended to be longer in trained rats (p = 0.13; Table 5.2).

Effects of altered NO on muscle PO_2mv in sedentary and exercise trained rats

SNP superfusion decreased MAP to a greater degree in trained compared to sedentary rats (Table 5.1; $p<0.05$). Relative to the control condition, SNP increased $PO_2mv_{(BL)}$ in both sedentary and trained rats (Table 5.2; $p<0.05$). Although SNP increased the overall amplitude of PO_2mv fall during contractions ($\Delta_{Total}PO_2mv$) only in trained rats, there were no differences in $PO_2mv_{(SS)}$ between sedentary and trained rats (Table 5.2). Both groups exhibited greater $PO_2mv_{(SS)}$ with SNP when compared to the control condition ($p<0.05$; Table 5.2). As illustrated in Fig. 5.2, SNP had strikingly distinct effects on the PO_2mv time course following the onset of contractions in sedentary and trained rats. Albeit no differences between groups were found in TD_1 with SNP ($p>0.05$), τ_1 and MRT were increased to a greater extent in sedentary compared to trained rats ($p<0.05$; Table 5.2 and Fig. 5.3). Analysis of Δ_1PO_2mv/τ_1 indicates that SNP slowed the relative rate of PO_2mv fall during contractions in sedentary but not trained rats (Fig. 5.3; $p<0.05$). Additionally, there was a tendency for Δ_1PO_2mv/τ_1 to be slower in sedentary compared to trained rats during the SNP condition (Fig. 5.3; $p = 0.12$).

L-NAME superfusion did not change MAP in either sedentary or exercise trained rats (Table 5.1; $p>0.05$). Although L-NAME did not significantly modify $PO_2mv_{(BL)}$ and $\Delta_{Total}PO_2mv$, both sedentary and trained rats had lower $PO_2mv_{(SS)}$ compared to their control conditions (Table 5.2; $p<0.05$). The effects of NO synthase inhibition with L-NAME were such that the spinotrapezius muscle PO_2mv profile from rest to contractions in trained rats was similar to that of sedentary rats (Figs. 5.2 and 5.3, Table 5.2). Relative to the control condition, L-NAME significantly speeded TD_1 in both sedentary and trained rats (Table 5.2). Notably, L-NAME abolished the differences in τ_1, Δ_1PO_2mv/τ_1 and MRT between sedentary and trained rats evident during the control condition ($p>0.05$ for all; Table 5.2 and Fig. 5.3). Moreover, L-NAME speeded Δ_1PO_2mv/τ_1 in trained rats to similar values found in sedentary rats (Fig. 5.3).

Discussion

The present study demonstrates that endurance exercise training improves significantly the microvascular oxygenation profile (i.e., slowed PO_2mv kinetics and therefore enhanced PO_2mv) across the metabolic transient following the onset of contractions in the spinotrapezius muscle of healthy young rats. Compared to the control condition, increased NO with SNP slowed the PO_2mv fall throughout contractions (τ_1) to a greater extent in sedentary rats whereas decreased NO with L-NAME abolished the differences in τ_1 between sedentary and trained rats. These results suggest that the enhanced driving force for blood-myocyte O_2 flux during contractions with exercise training is mediated, at least in part, via increased NO-mediated function.

Exercise training and muscle microvascular oxygenation

As stated above, muscle PO_2mv kinetics is dictated by the dynamic $\dot{Q}O_2/\dot{V}O_2$ matching within the microvascular space (8). Slowed PO_2mv kinetics in trained rats (Figs. 5.2 and 5.3, Table 5.2) therefore suggest that the rate of adjustment in $\dot{Q}O_2$ during contractions was relatively faster than that of $\dot{V}O_2$ compared to sedentary rats (5, 21, 26), such that fractional O_2 extraction was reduced up until the steady-state is achieved. The unexpected lack of change in citrate synthase activity found herein with training further supports this notion (see discussion below). Enhanced $\dot{Q}O_2$ across the rest-contractions transient with training is important to support potential augmented mitochondrial function (37, 70) and/or attenuate regional $\dot{Q}O_2/\dot{V}O_2$ mismatch (45), both of which might be linked mechanistically to faster muscle $\dot{V}O_2$ kinetics and improved exercise tolerance. With respect to the capacity to extract O_2 it is important to note that there is an interdependence between the diffusive and conductive O_2 transport components (62):

$$\%O_2 extraction = 1 - e^{-DO_2/\beta\dot{Q}m}$$

where DO_2 is the effective muscle O_2 diffusing capacity, β corresponds to the slope of the O_2 dissociation curve in the physiologically relevant range and $\dot{Q}m$ is muscle blood flow. Although DO_2 represents a lumped parameter that includes the impediments to blood-myocyte O_2 transfer and is determined by a complex interaction between structural and functional factors, it appears that DO_2 is dictated largely by capillary hematocrit and the volume density of red blood cell flowing capillaries (23, 29, 58, 62). As β is unlikely to be affected appreciably by exercise training, alterations in O_2 extraction will depend on the $DO_2/\dot{Q}m$ ratio (62). The significance of the abovementioned relationship is that it provides information regarding alterations in diffusive and conductive components of O_2 transport. Given that exercise training is known to improve both DO_2 (4, 54, 62) and $\dot{Q}m$ kinetics (65), it can be surmised that trained rats had a relatively greater increase in microvascular $\dot{Q}m$ than in DO_2 (i.e., lower $DO_2/\dot{Q}m$ ratio, which dictates reduced fractional O_2 extraction) across the rest-contractions transient. This analysis suggests that adaptations in conductive (mainly red blood cell flux; f_{RBC}) rather than diffusive capillary mechanisms with exercise training are of relatively greater importance in setting enhanced muscle microvascular oxygenation during metabolic transients as measured herein (Fig. 5.2 and Table 5.2). Importantly, the resultant slowed PO_2mv kinetics and reduced fractional O_2 extraction act to increase the pressure head for O_2 diffusion at a time when $\dot{V}O_2$ is rising at its fastest rate and would therefore be expected to improve muscle O_2 supply and oxidative function (5, 8, 36, 44, 68).

Effects of altered NO on PO_2mv kinetics

NO and its derivatives modulate multiple physiological processes including muscle hemodynamic and metabolic control (12, 67). More specifically, NO contributes to the increase in muscle $\dot{Q}O_2$ during contractions mainly via endothelium-dependent vasodilation (28, 32, 35, 53) and to the inertia of oxidative metabolism (i.e., finite $\dot{V}O_2$ kinetics) via inhibition of mitochondrial respiration (40, 43). Accordingly, alterations in NO levels modulate the dynamic $\dot{Q}O_2/\dot{V}O_2$ matching during metabolic transitions in health and disease (24, 25, 31). The lack of change in citrate synthase activity with training in the current investigation support that SNP and L-NAME treatments had similar effects on $\dot{V}O_2$ dynamics of sedentary and trained rats.

Consequently, this implies that differences in the PO_2mv profiles between sedentary and trained rats with SNP and L-NAME resulted primarily from alterations in $\dot{Q}O_2$.

The main effects of altered NO with either SNP or L-NAME were seen during the contraction transient (Figs. 5.2 and 5.3, Table 5.2). Specifically, SNP slowed τ_1 to a greater extent in sedentary rats whereas L-NAME abolished the differences in τ_1 between sedentary and trained rats that were evident in the control condition (Fig. 5.3). These results suggest that exercise training increases the contribution of NO to the dynamic $\dot{Q}O_2/\dot{V}O_2$ matching and enhances the capacity for O_2 flux across metabolic transients in healthy skeletal muscle.

Primary mechanisms for slowed PO_2mv kinetics with training

From the above it becomes apparent that the principal mechanisms improving microvascular oxygenation with exercise training likely involve enhanced NO-mediated regulation of f_{RBC}. Potential candidates include 1) enhanced endothelial-mediated vasodilation (28, 53); and/or 2) enhanced attenuation of sympathetic vasoconstriction (i.e., functional sympatholysis; ref. 69); and/or 3) training-induced alterations in $\dot{Q}m$ distribution (2, 35) that could attenuate spatial heterogeneities in contracting muscle microvascular oxygenation (45).

Although it must be acknowledged that aging and disease states also present impairments in muscle DO_2, it is interesting to note that these conditions are characterized by reduced NO-mediated function (20, 32, 56) and demonstrate opposite effects on capillary hemodynamics (i.e., impaired f_{RBC}; refs. 17, 61) and $\dot{Q}O_2/\dot{V}O_2$ matching (i.e., faster PO_2mv kinetics; refs. 6, 21) during contractions when compared to healthy young individuals. In this context, endurance exercise training has profound clinical implications especially for aged and diseased populations as it constitutes a non-pharmacological therapeutic intervention capable of mitigating microcirculatory deficits.

Vascular control mechanisms (35, 48) and vascular adaptations to exercise training (2, 52) are known to vary according to muscle fiber type composition and oxidative capacity. Consequently, differences might exist in the relative contribution of NO to alterations in gas exchange properties of the microcirculation with training in muscles comprised of distinct fiber types. In this regard, it is noteworthy that the spinotrapezius possesses a mixed fiber type

composition and oxidative capacity that resembles the human quadriceps (19, 49), therefore representing a useful analogue of human locomotor muscle.

Experimental considerations

Downhill treadmill running was used herein as a model of endurance exercise training given that this protocol recruits the rat spinotrapezius muscle (41, 57) and may promote training adaptations that include increased $\dot{V}O_2 peak$, muscle citrate synthase activity and resistance to fatigue (30). Accordingly, exercise training protocols that do not recruit the spinotrapezius (e.g., inclined treadmill running) do not induce changes in PO_2mv kinetics in healthy young rats (55, cf. refs. 46, 47). It is important to note that, in the current investigation, trained rats had ~12% greater $\dot{V}O_2 peak$ as well as distinct MAP and PO_2mv responses following SNP and L-NAME superfusion (Tables 5.1 and 5.2, Figs. 5.2 and 5.3) when compared to sedentary rats, thus providing compelling evidence of a training effect. Furthermore, the markedly slowed PO_2mv kinetics (Figs. 5.2 and 5.3, Table 5.2) is consistent with expected adaptations to training. While the lack of change in citrate synthase activity of the spinotrapezius muscle in trained rats is surprising, it suggests that adaptations in vascular control (i.e., improved f_{RBC} as discussed above) likely facilitated the enhanced microvascular oxygenation seen herein during contractions in the trained state. In this sense, potential structural and/or functional vascular adaptations (i.e., ↑ flow capacity; the potential for conductive delivery of blood to and from exchange vessels) that occurred independent of alterations in mitochondrial oxidative capacity in trained rats could enhance the dynamic $\dot{Q}O_2 / \dot{V}O_2$ matching and improve the ability of the microcirculation to support skeletal muscle metabolism.

Eccentric exercise such as downhill running promotes muscle damage that impairs capillary hemodynamics and microvascular O_2 transfer during subsequent contractile activity (42, see also ref. 18). Interestingly, evidence from both human and animal studies indicates that muscle damage from a single bout of eccentric exercise is considerably reduced following repeated bouts as performed herein and any damage from the first bout(s) would be expected to have ameliorated during the ~2 month training period (14, 64). Although unlikely, any potential deleterious effects of eccentric exercise on muscle function would therefore only underestimate the improvements in PO_2mv kinetics with training.

Reduced driving pressure with SNP (Table 5.1) could constrain blood flow dynamics and influence PO_2mv kinetics during metabolic transitions. However, previous studies from our laboratory (10) indicate that this effect is negligible when MAP is above ~70 mmHg as herein.

Conclusions

Resolution of muscle PO_2mv kinetics and their mechanistic bases in the exercise trained state are essential to understand how muscle microcirculatory plasticity evokes improvements in contractile performance. The current novel findings in healthy skeletal muscle suggest that endurance exercise training enhances microvascular oxygenation during contractions (i.e., slowed PO_2mv kinetics) partly via increased NO-mediated function. As mentioned above, enhanced PO_2mv during metabolic transitions facilitates blood-myocyte O_2 flux to support oxidative phosphorylation and consequently reduces the rate of anaerobic glycolysis and reliance on finite energy sources, all of which likely contribute to improved muscle contractile performance following exercise training (36, 37, 58, 68, 70). Important clinical implications arise from our results considering that aged and patient (e.g., chronic heart failure; CHF) populations are characterized by reduced NO signaling (20, 32, 56), impaired microvascular oxygenation (6, 21) and poor exercise capacity (15, 38). It is noteworthy that CHF patients, for instance, retain considerable plasticity within their skeletal muscle O_2 transport system (both convective and diffusive components) in response to exercise training programs (22). Taken together, these observations suggest that exercise training is a powerful non-pharmacological strategy to improve NO-mediated function, thereby likely ameliorating muscle microvascular oxygenation deficits and exercise intolerance in aging and disease states.

Table 5.1 Mean arterial pressure (MAP; expressed in mmHg) pre- and post-superfusion of Krebs-Henseleit (Control), SNP and L-NAME in sedentary and exercise trained rats

	Control		SNP		L-NAME	
	Pre	**Post**	**Pre**	**Post**	**Pre**	**Post**
Sedentary	123 ± 4	124 ± 4	125 ± 5	111 ± 4*	128 ± 4	132 ± 5
Trained	132 ± 3	133 ± 4	134 ± 5	95 ± 6*†	134 ± 4	137 ± 4

Values are mean ± SE. Results are presented from animals under the following conditions: sedentary control (n=18); sedentary SNP (n=14); sedentary L-NAME (n=14); trained control (n=10); trained SNP (n=9); trained L-NAME (n=10). Significantly different from: * all other conditions within group; † sedentary post-SNP superfusion.

Table 5.2 Muscle PO_2mv kinetics following the onset of contractions under control, SNP and L-NAME conditions in sedentary and exercise trained rats

	Control		SNP		L-NAME	
	Sedentary	**Trained**	**Sedentary**	**Trained**	**Sedentary**	**Trained**
$PO_2mv_{(BL)}$, mmHg	29.2 ± 1.3	27.8 ± 1.2	38.7 ± 2.3*	42.9 ± 3.5*	25.5 ± 1.7†	26.4 ± 1.5†
Δ_1PO_2mv, mmHg	11.4 ± 1.2	10.6 ± 0.8	9.3 ± 2.3	15.6 ± 3.3‡	13.0 ± 1.0	13.0 ± 1.2
Δ_2PO_2mv, mmHg	2.3 ± 0.3	2.5 ± 0.3	-	-	2.3 ± 0.4	2.8 ± 1.3
$\Delta_{Total}PO_2mv$, mmHg	9.8 ± 1.2	8.6 ± 0.8	9.3 ± 1.5	15.6 ± 3.3*‡	11.2 ± 0.9	12.1 ± 1.1
$PO_2mv_{(SS)}$, mmHg	19.4 ± 1.0	19.2 ± 1.5	29.4 ± 1.5*	27.3 ± 1.4*	14.3 ± 0.8*†	14.2 ± 0.9*†
TD_1, s	10.2 ± 0.7	10.3 ± 1.6	8.3 ± 1.6	11.8 ± 3.6	6.2 ± 0.5*	6.5 ± 0.9*†
TD_2, s	55.1 ± 9.5	53.4 ± 12.4	-	-	55.0 ± 6.8	41.3 ± 7.2
τ_2, s	39.5 ± 7.8	32.3 ± 10.1	-	-	55.5 ± 8.9	51.9 ± 18.9
MRT, s	18.3 ± 0.9	25.5 ± 3.3#	47.0 ± 5.8*	38.6 ± 5.2*‡	18.1 ± 1.7†	17.7 ± 1.6†

Values are mean ± SE. $PO_2mv_{(BL)}$, resting PO_2mv; Δ_1PO_2mv, amplitude of the first component; Δ_2PO_2mv, amplitude of the second component; $\Delta_{Total}PO_2mv$, overall amplitude regardless of one- or two-component model fit; $PO_2mv_{(SS)}$, contracting steady-state PO_2mv; TD_1, time delay for the first component; TD_2, time delay for the second component; τ_2, time constant for the second component, MRT, mean response time. The time constant for the first component (τ_1) and relative rate of PO_2mv fall (Δ_1PO_2mv/τ_1) are shown in Fig. 5.3. The one-component exponential model was used to analyze the PO_2mv kinetics in the following conditions: sedentary control (6/18), sedentary SNP (14/14), sedentary L-NAME (3/14), trained control (2/10), trained SNP (9/9), trained L-NAME (7/10). Significantly different from: * control within group; † SNP within group; ‡ sedentary within superfusion condition. # p=0.13 vs. sedentary control.

Figure 5.1 Investigation of potential cyanide-induced impairment of skeletal muscle function

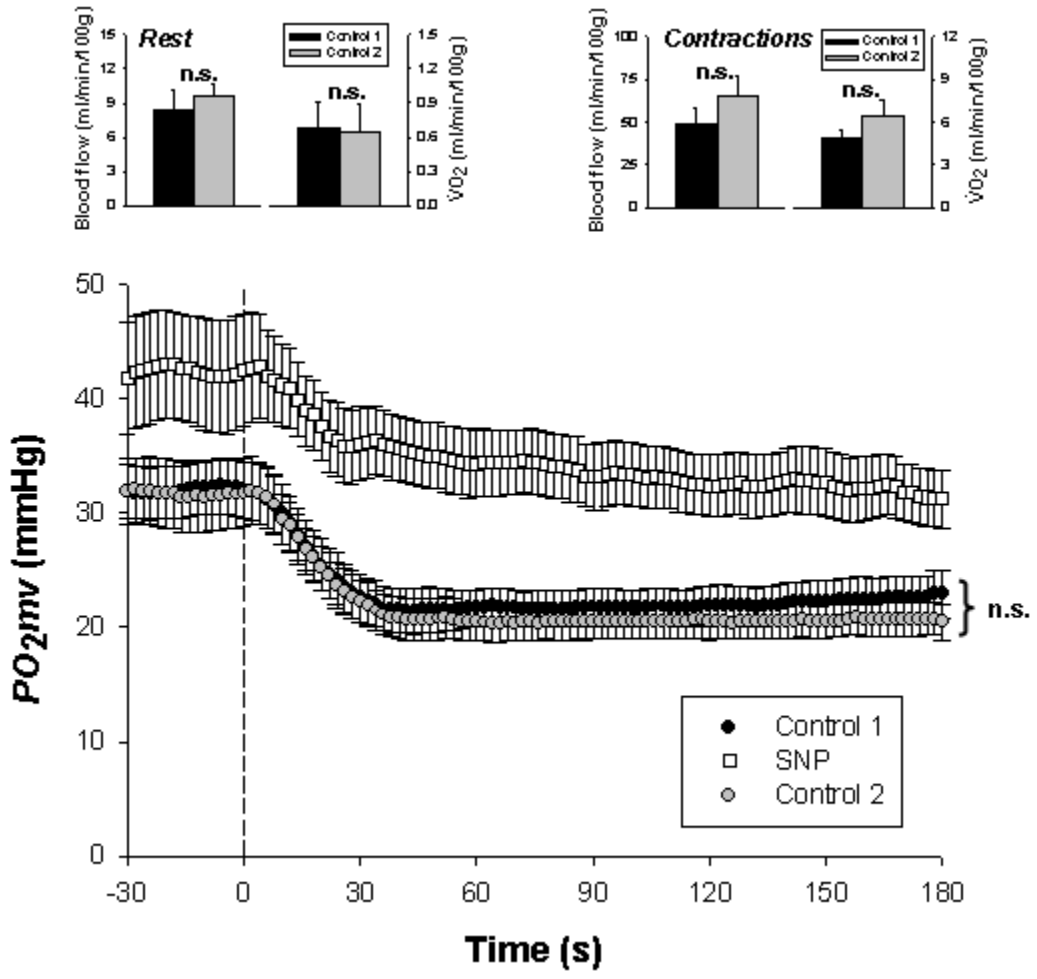

Figure 5.1 Results from experiments performed to examine potential cyanide-induced impairment of skeletal muscle function with the current SNP superfusion protocol. Three contraction bouts were conducted in the following superfusion order: control 1 (K-H), SNP (300 μM), control 2 (K-H). Spinotrapezius muscle PO_2mv was measured at rest and throughout contractions (n=9). Spinotrapezius muscle blood flow ($\dot{Q}m$) and oxygen utilization ($\dot{V}O_2$) were determined at rest and during the contraction steady-state via radiolabeled microspheres and direct Fick calculation, respectively (n=4). *Top panels*: Spinotrapezius $\dot{Q}m$ and $\dot{V}O_2$ at rest and during the contraction steady-state during the first and third bouts (i.e., control 1 and 2, respectively). *Bottom panel*: Spinotrapezius PO_2mv at rest and following the onset of contractions under all three conditions (control 1, SNP and control 2). Time zero denotes the

onset of contractions. That resting and contracting spinotrapezius muscle $\dot{V}O_2$ did not differ between the first and third bouts (i.e., control 1 vs. control 2; $p>0.05$) suggests preserved mitochondrial function post-SNP condition. The possibility of prolonged and/or irreversible vasodilation following the SNP condition is not supported based on similar resting and contraction steady-state $\dot{Q}m$ between the first and third bouts (i.e., control 1 vs. control 2; $p>0.05$). Similar PO_2mv profiles during the first and third bouts (i.e., control 1 vs. control 2; $p>0.05$ for all kinetics parameters) are also consistent with the notion that mitochondrial and vascular control were not impaired following the SNP condition (i.e., second bout). n.s., not significantly different.

Figure 5.2 Muscle *PO_2mv* from sedentary and exercise trained rats under control, SNP and L-NAME conditions

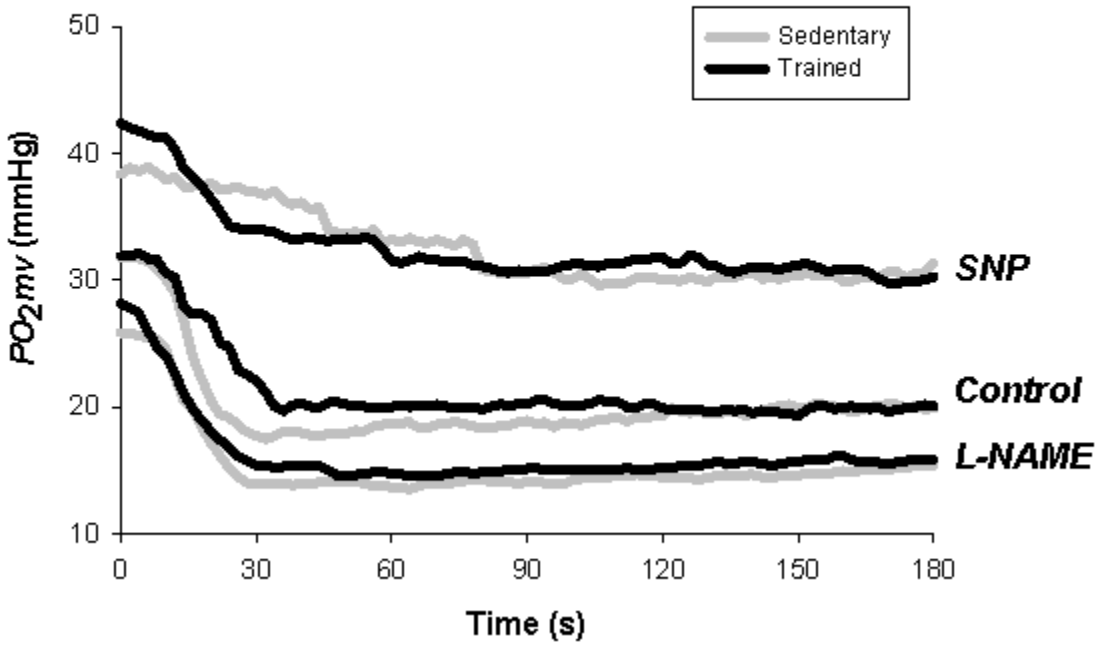

Figure 5.2 Spinotrapezius muscle *PO_2mv* response from representative sedentary and exercise trained rats under control, SNP and L-NAME conditions. Time zero denotes the onset of contractions. Note that exercise training slowed the *PO_2mv* fall during contractions (τ_1, time constant for the first component) under control. SNP slowed τ_1 to a greater extent in sedentary rats whereas L-NAME abolished the differences in τ_1 between sedentary and trained rats (see text for details).

Figure 5.3 Muscle *PO_2mv* kinetics in sedentary and exercise trained rats under control, SNP and L-NAME conditions

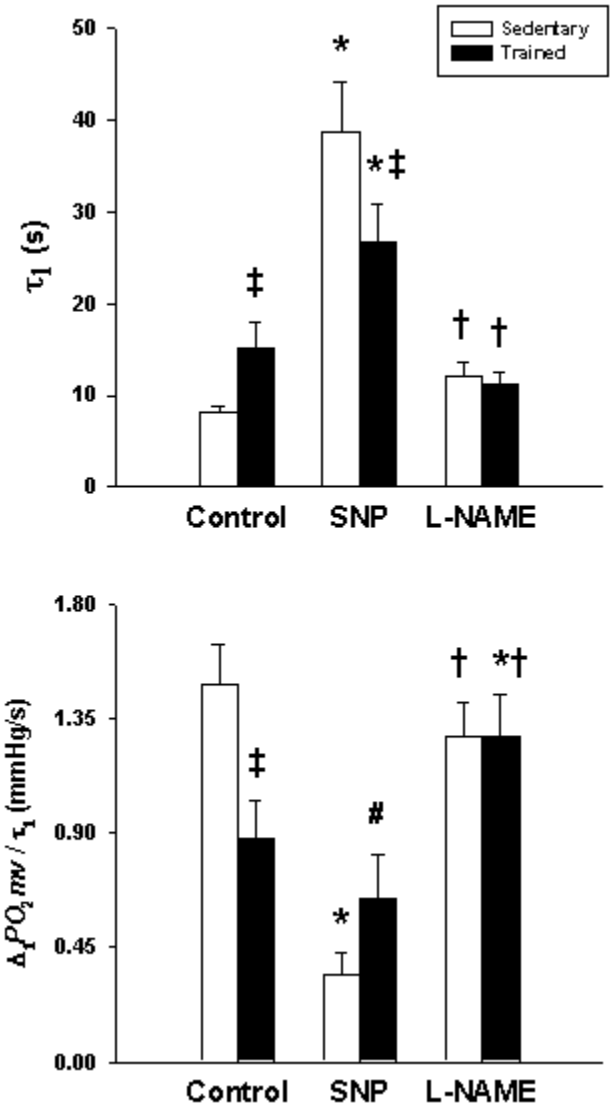

Figure 5.3 Spinotrapezius muscle *PO_2mv* kinetics (*top panel*: τ_1, time constant for the first component; *bottom panel*: $\Delta_1 PO_2 mv/\tau_1$, relative rate of *PO_2mv* fall) in sedentary and exercise trained rats under control, SNP and L-NAME conditions. Significantly different from: * control within group; † SNP within group; ‡ sedentary within superfusion condition. # p=0.12 vs. sedentary SNP.

References

1. **Altman PL, and Dittmer DS**. *Biology Data Book*. Bethesda, MD: FASEB, 1974.

2. **Armstrong RB, and Laughlin MH**. Exercise blood flow patterns within and among rat muscles after training. *Am J Physiol* 246: H59-68, 1984.

3. **Bailey JK, Kindig CA, Behnke BJ, Musch TI, Schmid-Schoenbein GW, and Poole DC**. Spinotrapezius muscle microcirculatory function: effects of surgical exteriorization. *Am J Physiol Heart Circ Physiol* 279: H3131-3137, 2000.

4. **Bebout DE, Hogan MC, Hempleman SC, and Wagner PD**. Effects of training and immobilization on $\dot{V}O_2$ and DO_2 in dog gastrocnemius muscle in situ. *J Appl Physiol* 74: 1697-1703, 1993.

5. **Behnke BJ, Barstow TJ, Kindig CA, McDonough P, Musch TI, and Poole DC**. Dynamics of oxygen uptake following exercise onset in rat skeletal muscle. *Respir Physiol Neurobiol* 133: 229-239, 2002.

6. **Behnke BJ, Delp MD, Dougherty PJ, Musch TI, and Poole DC**. Effects of aging on microvascular oxygen pressures in rat skeletal muscle. *Respir Physiol Neurobiol* 146: 259-268, 2005.

7. **Behnke BJ, Kindig CA, McDonough P, Poole DC, and Sexton WL**. Dynamics of microvascular oxygen pressure during rest-contraction transition in skeletal muscle of diabetic rats. *Am J Physiol Heart Circ Physiol* 283: H926-932, 2002.

8. **Behnke BJ, Kindig CA, Musch TI, Koga S, and Poole DC**. Dynamics of microvascular oxygen pressure across the rest-exercise transition in rat skeletal muscle. *Respir Physiol* 126: 53-63, 2001.

9. **Behnke BJ, Kindig CA, Musch TI, Sexton WL, and Poole DC**. Effects of prior contractions on muscle microvascular oxygen pressure at onset of subsequent contractions. *J Physiol* 539: 927-934, 2002.

10. **Behnke BJ, Padilla DJ, Ferreira LF, Delp MD, Musch TI, and Poole DC**. Effects of arterial hypotension on microvascular oxygen exchange in contracting skeletal muscle. *J Appl Physiol* 100: 1019-1026, 2006.

11. **Bisset WI, Butler AR, Glidewell C, and Reglinski J**. Sodium nitroprusside and cyanide release: reasons for re-appraisal. *Br J Anaesth* 53: 1015-1018, 1981.

12. **Brown GC**. Nitric oxide and mitochondrial respiration. *Biochim Biophys Acta* 1411: 351-369, 1999.

13. **Butler AR, Glidewell C, McGinnis J, and Bisset WI**. Further investigations regarding the toxicity of sodium nitroprusside. *Clin Chem* 33: 490-492, 1987.

14. **Byrnes WC, Clarkson PM, White JS, Hsieh SS, Frykman PN, and Maughan RJ**. Delayed onset muscle soreness following repeated bouts of downhill running. *J Appl Physiol* 59: 710-715, 1985.

15. **Clark AL, Poole-Wilson PA, and Coats AJ**. Exercise limitation in chronic heart failure: central role of the periphery. *J Am Coll Cardiol* 28: 1092-1102, 1996.

16. **Copp SW, Davis RT, Poole DC, and Musch TI**. Reproducibility of endurance capacity and $\dot{V}O_2 peak$ in male Sprague-Dawley rats. *J Appl Physiol* 106: 1072-1078, 2009.

17. **Copp SW, Ferreira LF, Herspring KF, Musch TI, and Poole DC**. The effects of aging on capillary hemodynamics in contracting rat spinotrapezius muscle. *Microvasc Res* 77: 113-119, 2009.

18. **Davies RC, Eston RG, Poole DC, Rowlands AV, DiMenna F, Wilkerson DP, Twist C, and Jones AM**. Effect of eccentric exercise-induced muscle damage on the dynamics of muscle oxygenation and pulmonary oxygen uptake. *J Appl Physiol* 105: 1413-1421, 2008.

19. **Delp MD, and Duan C**. Composition and size of type I, IIA, IID/X, and IIB fibers and citrate synthase activity of rat muscle. *J Appl Physiol* 80: 261-270, 1996.

20. **Didion SP, and Mayhan WG**. Effect of chronic myocardial infarction on in vivo reactivity of skeletal muscle arterioles. *Am J Physiol* 272: H2403-2408, 1997.

21. **Diederich ER, Behnke BJ, McDonough P, Kindig CA, Barstow TJ, Poole DC, and Musch TI**. Dynamics of microvascular oxygen partial pressure in contracting skeletal muscle of rats with chronic heart failure. *Cardiovasc Res* 56: 479-486, 2002.

22. **Esposito F, Reese V, Shabetai R, Wagner PD, and Richardson RS**. Isolated quadriceps training increases maximal exercise capacity in chronic heart failure: the role of skeletal muscle convective and diffusive oxygen transport. *J Am Coll Cardiol* 58: 1353-1362, 2011.

23. **Federspiel WJ, and Popel AS**. A theoretical analysis of the effect of the particulate nature of blood on oxygen release in capillaries. *Microvasc Res* 32: 164-189, 1986.

24. **Ferreira LF, Hageman KS, Hahn SA, Williams J, Padilla DJ, Poole DC, and Musch TI**. Muscle microvascular oxygenation in chronic heart failure: role of nitric oxide availability. *Acta Physiol (Oxf)* 188: 3-13, 2006.

25. **Ferreira LF, Padilla DJ, Williams J, Hageman KS, Musch TI, and Poole DC**. Effects of altered nitric oxide availability on rat muscle microvascular oxygenation during contractions. *Acta Physiol (Oxf)* 186: 223-232, 2006.

26. **Ferreira LF, Poole DC, and Barstow TJ**. Muscle blood flow-O_2 uptake interaction and their relation to on-exercise dynamics of O_2 exchange. *Respir Physiol Neurobiol* 147: 91-103, 2005.

27. **Friederich JA, and Butterworth JFt**. Sodium nitroprusside: twenty years and counting. *Anesth Analg* 81: 152-162, 1995.

28. **Green DJ, Maiorana A, O'Driscoll G, and Taylor R**. Effect of exercise training on endothelium-derived nitric oxide function in humans. *J Physiol* 561: 1-25, 2004.

29. **Groebe K, and Thews G**. Calculated intra- and extracellular PO_2 gradients in heavily working red muscle. *Am J Physiol* 259: H84-92, 1990.

30. **Hahn SA, Ferreira LF, Williams JB, Jansson KP, Behnke BJ, Musch TI, and Poole DC**. Downhill treadmill running trains the rat spinotrapezius muscle. *J Appl Physiol* 102: 412-416, 2007.

31. **Hirai DM, Copp SW, Ferreira LF, Musch TI, and Poole DC**. Nitric oxide bioavailability modulates the dynamics of microvascular oxygen exchange during recovery from contractions. *Acta Physiol (Oxf)* 200: 159-169, 2010.

32. **Hirai DM, Copp SW, Hageman KS, Poole DC, and Musch TI**. Aging alters the contribution of nitric oxide to regional muscle hemodynamic control at rest and during exercise in rats. *J Appl Physiol* 111: 989-998, 2011.

33. **Hirai DM, Copp SW, Herspring KF, Ferreira LF, Poole DC, and Musch TI**. Aging impacts microvascular oxygen pressures during recovery from contractions in rat skeletal muscle. *Respir Physiol Neurobiol* 169: 315-322, 2009.

34. **Hirai DM, Copp SW, Schwagerl PJ, Musch TI, and Poole DC**. Acute effects of hydrogen peroxide on skeletal muscle microvascular oxygenation from rest to contractions. *J Appl Physiol* 110: 1290-1298, 2011.

35. **Hirai T, Visneski MD, Kearns KJ, Zelis R, and Musch TI**. Effects of NO synthase inhibition on the muscular blood flow response to treadmill exercise in rats. *J Appl Physiol* 77: 1288-1293, 1994.

36. **Hogan MC, Arthur PG, Bebout DE, Hochachka PW, and Wagner PD**. Role of O_2 in regulating tissue respiration in dog muscle working in situ. *J Appl Physiol* 73: 728-736, 1992.

37. **Holloszy JO, and Coyle EF**. Adaptations of skeletal muscle to endurance exercise and their metabolic consequences. *J Appl Physiol* 56: 831-838, 1984.

38. **Inbar O, Oren A, Scheinowitz M, Rotstein A, Dlin R, and Casaburi R**. Normal cardiopulmonary responses during incremental exercise in 20- to 70-yr-old men. *Med Sci Sports Exerc* 26: 538-546, 1994.

39. **Ishise S, Pegram BL, Yamamoto J, Kitamura Y, and Frohlich ED**. Reference sample microsphere method: cardiac output and blood flows in conscious rat. *Am J Physiol* 239: H443-H449, 1980.

40. **Jones AM, Wilkerson DP, Koppo K, Wilmshurst S, and Campbell IT**. Inhibition of nitric oxide synthase by L-NAME speeds phase II pulmonary $\dot{V}O_2$ kinetics in the transition to moderate-intensity exercise in man. *J Physiol* 552: 265-272, 2003.

41. **Kano Y, Padilla D, Hageman KS, Poole DC, and Musch TI**. Downhill running: a model of exercise hyperemia in the rat spinotrapezius muscle. *J Appl Physiol* 97: 1138-1142, 2004.

42. **Kano Y, Padilla DJ, Behnke BJ, Hageman KS, Musch TI, and Poole DC**. Effects of eccentric exercise on microcirculation and microvascular oxygen pressures in rat spinotrapezius muscle. *J Appl Physiol* 99: 1516-1522, 2005.

43. **Kindig CA, McDonough P, Erickson HH, and Poole DC**. Nitric oxide synthase inhibition speeds oxygen uptake kinetics in horses during moderate domain running. *Respir Physiol Neurobiol* 132: 169-178, 2002.

44. **Kindig CA, Richardson TE, and Poole DC**. Skeletal muscle capillary hemodynamics from rest to contractions: implications for oxygen transfer. *J Appl Physiol* 92: 2513-2520, 2002.

45. **Koga S, Poole DC, Ferreira LF, Whipp BJ, Kondo N, Saitoh T, Ohmae E, and Barstow TJ**. Spatial heterogeneity of quadriceps muscle deoxygenation kinetics during cycle exercise. *J Appl Physiol* 103: 2049-2056, 2007.

46. **Lash JM**. Exercise training enhances adrenergic constriction and dilation in the rat spinotrapezius muscle. *J Appl Physiol* 85: 168-174, 1998.

47. **Lash JM, and Bohlen HG**. Functional adaptations of rat skeletal muscle arterioles to aerobic exercise training. *J Appl Physiol* 72: 2052-2062, 1992.

48. **Laughlin MH, and Armstrong RB**. Adrenoreceptor effects on rat muscle blood flow during treadmill exercise. *J Appl Physiol* 62: 1465-1472, 1987.

49. **Leek BT, Mudaliar SR, Henry R, Mathieu-Costello O, and Richardson RS**. Effect of acute exercise on citrate synthase activity in untrained and trained human skeletal muscle. *Am J Physiol Regul Integr Comp Physiol* 280: R441-447, 2001.

50. **Lo LW, Vinogradov SA, Koch CJ, and Wilson DF**. A new, water soluble, phosphor for oxygen measurements in vivo. *Adv Exp Med Biol* 428: 651-656, 1997.

51. **Macdonald M, Pedersen PK, and Hughson RL**. Acceleration of $\dot{V}O_2$ kinetics in heavy submaximal exercise by hyperoxia and prior high-intensity exercise. *J Appl Physiol* 83: 1318-1325, 1997.

52. **McAllister RM, Jasperse JL, and Laughlin MH**. Nonuniform effects of endurance exercise training on vasodilation in rat skeletal muscle. *J Appl Physiol* 98: 753-761, 2005.

53. **McAllister RM, Newcomer SC, and Laughlin MH**. Vascular nitric oxide: effects of exercise training in animals. *Appl Physiol Nutr Metab* 33: 173-178, 2008.

54. **McAllister RM, and Terjung RL**. Training-induced muscle adaptations: increased performance and oxygen consumption. *J Appl Physiol* 70: 1569-1574, 1991.

55. **McCullough DJ, Davis RT, 3rd, Dominguez JM, 2nd, Stabley JN, Bruells CS, and Behnke BJ**. Effects of aging and exercise training on spinotrapezius muscle microvascular PO_2 dynamics and vasomotor control. *J Appl Physiol* 110: 695-704, 2011.

56. **Muller-Delp JM, Spier SA, Ramsey MW, and Delp MD**. Aging impairs endothelium-dependent vasodilation in rat skeletal muscle arterioles. *Am J Physiol Heart Circ Physiol* 283: H1662-1672, 2002.

57. **Musch TI, and Poole DC**. Blood flow response to treadmill running in the rat spinotrapezius muscle. *Am J Physiol* 271: H2730-2734, 1996.

58. **Poole DC**. Influence of exercise training on skeletal muscle oxygen delivery and utilization. In: *The Lung: Scientific Foundations*, edited by Crystal RG, West JB, Weibel ER, and Barnes PJ. New York: Raven Press, 1997, p. 1957-1967.

59. **Poole DC, Behnke BJ, McDonough P, McAllister RM, and Wilson DF**. Measurement of muscle microvascular oxygen pressures: compartmentalization of phosphorescent probe. *Microcirculation* 11: 317-326, 2004.

60. **Poole DC, Wagner PD, and Wilson DF**. Diaphragm microvascular plasma PO_2 measured in vivo. *J Appl Physiol* 79: 2050-2057, 1995.

61. **Richardson TE, Kindig CA, Musch TI, and Poole DC**. Effects of chronic heart failure on skeletal muscle capillary hemodynamics at rest and during contractions. *J Appl Physiol* 95: 1055-1062, 2003.

62. **Roca J, Agusti AG, Alonso A, Poole DC, Viegas C, Barbera JA, Rodriguez-Roisin R, Ferrer A, and Wagner PD**. Effects of training on muscle O_2 transport at $\dot{V}O_2$ max . *J Appl Physiol* 73: 1067-1076, 1992.

63. **Rumsey WL, Vanderkooi JM, and Wilson DF**. Imaging of phosphorescence: a novel method for measuring oxygen distribution in perfused tissue. *Science* 241: 1649-1651, 1988.

64. **Schwane JA, and Armstrong RB**. Effect of training on skeletal muscle injury from downhill running in rats. *J Appl Physiol* 55: 969-975, 1983.

65. **Shoemaker JK, Phillips SM, Green HJ, and Hughson RL**. Faster femoral artery blood velocity kinetics at the onset of exercise following short-term training. *Cardiovasc Res* 31: 278-286, 1996.

66. **Srere PA**. Citrate synthase. *Methods in Enzymology* 13: 3-11, 1969.

67. **Stamler JS, and Meissner G**. Physiology of nitric oxide in skeletal muscle. *Physiol Rev* 81: 209-237, 2001.

68. **Stary CM, and Hogan MC**. Effect of varied extracellular PO_2 on muscle performance in Xenopus single skeletal muscle fibers. *J Appl Physiol* 86: 1812-1816, 1999.

69. **Thomas GD, and Victor RG**. Nitric oxide mediates contraction-induced attenuation of sympathetic vasoconstriction in rat skeletal muscle. *J Physiol* 506 (Pt 3): 817-826, 1998.

70. **Tonkonogi M, and Sahlin K**. Physical exercise and mitochondrial function in human skeletal muscle. *Exerc Sport Sci Rev* 30: 129-137, 2002.

71. **Whyte JJ, and Laughlin MH**. The effects of acute and chronic exercise on the vasculature. *Acta Physiol (Oxf)* 199: 441-450, 2010.

Chapter 6 - Conclusions

Integrating the investigations described in this dissertation, we conclude that alterations in NO bioavailability have a substantial impact on skeletal muscle $\dot{Q}O_2/\dot{V}O_2$ matching following both the onset and cessation of contractions. Disparate muscle PO_2mv kinetics in health and disease can be ascribed partially to alterations in NO levels. Specifically, our data demonstrate that increased NO levels (via the NO donor sodium nitroprusside; SNP) elevates muscle PO_2mv whereas reduced NO levels (non-specific NOS inhibition with N^G-nitro-L-arginine methyl ester; L-NAME) diminishes muscle PO_2mv across the metabolic transient following the onset and cessation of contractions in the spinotrapezius muscle of healthy young rats. Moreover, utilization of selective nNOS inhibition (*S*-methyl-L-thiocitrulline; SMTC) reveals that alterations in nNOS-mediated regulation of contracting skeletal muscle microvascular function with advanced age likely contribute to reduced exercise capacity in this population. Pronounced oxidative stress is implicated in these pathological responses observed in aged and diseased states. Accordingly, transient elevations in the oxidant H_2O_2 to levels found in the early stages of senescence and cardiovascular diseases have detrimental effects on skeletal muscle function (i.e., augmented oxygen cost of force production). On the other hand, endurance exercise training improves muscle microvascular oxygenation (i.e., greater PO_2mv across the metabolic transient and slower PO_2mv kinetics) partly via enhanced NO-mediated function in healthy young individuals. Important clinical applications arise from these investigations when considering that exercise training could ameliorate NO-mediated function, muscle microvascular oxygenation deficits and exercise intolerance in aged and diseased populations.

Appendix A - Curriculum Vitae

Daniel Muller Hirai

Date of Birth: September 29, 1981

Place of Birth: Santo André, SP, Brazil

Current Address: 122 Coles Hall
1600 Denison Avenue
Manhattan, KS, 66506
E-mail: dhirai@vet.ksu.edu
Office: 785 532-4476

Education

2008-	Ph.D. in Physiology (*in progress*; Dept. of Anatomy and Physiology, Kansas State University)
Feb 2008	M.S. (Kinesiology, Londrina State University - Brazil)
Dec 2004	B.S. (Physical Therapy, Londrina State University - Brazil)

Academic Appointments

2010-present	Graduate Research Assistant – *Cardiorespiratory Exercise Physiology Laboratory, Department of Anatomy and Physiology, Kansas State University.*

2009-present Laboratory Teaching Assistant - *Department of Anatomy and Physiology, Kansas State University* (Veterinary Physiology II, AP747). Assist in instructing a laboratory experience for 1st year veterinary students focused on lung structure and function in health and disease. Demonstrations performed include maximal exercise tests and various pulmonary function tests.

Professional Memberships

The Microcirculatory Society
The American College of Sports Medicine

Grant Funding

2010-2011 American College of Sports Medicine, Doctoral Student Research Grant. "Exercise training and muscle microvascular oxygenation." *Role*: PI, *Total costs*: $5,000. *Effective dates*: 07/01/10 – 06/30/11.

2008-2012 Fulbright Foreign Student Program – Brazilian Ministry of Education (CAPES) scholarship.

Awards and Honors

Kansas State University, Graduate Student Council Award, Travel Grant, 2012

Kansas State University, College of Veterinary Medicine Travel Award, 2012

Kansas State University, College of Veterinary Medicine, Dr. Leo and Gloria Whitehair Research Award, 2011

Kansas State University, Graduate Student Council Award, Travel Grant, 2011

The Microcirculatory Society, Benjamin Zweifach Graduate Student Travel Award, 2011

American College of Sports Medicine, Steven M. Horvath Travel Award, 2011

Kansas State University, Notable Scholarly Graduate Student Achievements, 2011

Golden Key International Honour Society, 2010

Kansas State University, Notable Scholarly Graduate Student Achievements, 2010

Peer-reviewed Manuscripts

1. Brunetto AF, Roseguini BT, Silva BM, **Hirai DM**, Guedes DP. Cardiac autonomic responses to head-up tilt in obese adolescents. *Rev Assoc Med Bras* 2005, 51(5):256-60.

2. Brunetto AF, Roseguini BT, Silva BM, **Hirai DM**, Guedes DP. Effects of gender and aerobic fitness on cardiac autonomic responses to head-up tilt in healthy adolescents. *Pediatr Cardiol* 2005, 26(4):418-24.

3. Copp SW, Ferreira LF, Herspring KF, **Hirai DM**, Snyder BS, Poole DC, Musch TI. The effects of antioxidants on microvascular oxygenation and blood flow in skeletal muscle of young rats. *Exp Physiol* 2009, 94(9):961-71.

4. **Hirai DM**, Copp SW, Herspring KF, Ferreira LF, Poole DC, Musch TI. Aging impacts microvascular oxygen pressures during recovery from contractions in rat skeletal muscle. *Respir Physiol Neurobiol* 2009, 169(3):315-22.

5. Copp SW, **Hirai DM**, Hageman KS, Poole DC, Musch TI. Nitric oxide synthase inhibition during treadmill exercise reveals fiber-type specific vascular control in the rat hindlimb. *Am J Physiol Regul Integr Comp Physiol* 2010, 298(2):R478-85.

6. Copp SW, **Hirai DM**, Schwagerl PJ, Musch TI, Poole DC. Effects of neuronal nitric oxide synthase inhibition on resting and exercising hindlimb muscle blood flow in the rat. *J Physiol* 2010, 588(Pt 8):1321-31.

7. **Hirai DM**, Copp SW, Ferreira LF, Musch TI, Poole DC. Nitric oxide bioavailability modulates the dynamics of microvascular oxygen exchange during recovery from contractions. *Acta Physiol (Oxf)* 2010, 200(2):159-69.

8. **Hirai DM**, Roseguini BT, Diefenthaeler F, Carpes FP, Vaz MA, Ferlin EL, Ribeiro JP, Nakamura FY. Effects of altering pedal frequency on the slow component of pulmonary $\dot{V}O_2$ kinetics and EMG activity. *Int J Sports Med* 2010, 31(8):529-36.

9. Copp SW, **Hirai DM**, Ferreira LF, Poole DC, Musch TI. Progressive chronic heart failure slows the recovery of microvascular O_2 pressures after contractions in the rat spinotrapezius muscle. *Am J Physiol Heart Circ Physiol* 2010, 299(6):H1755-61.

10. Margiocco ML, Borgarelli M, Musch TI, **Hirai DM**, Hageman KS, Fels RJ, Garcia AA, Kenney MJ. Effects of combined aging and heart failure on visceral sympathetic nerve and cardiovascular responses to progressive hyperthermia in F344 rats. *Am J Physiol Regul Integr Comp Physiol* 2010, 299(6):R1555-63.

11. Copp SW, **Hirai DM**, Musch TI, Poole DC. Critical speed in the rat: implications for hindlimb muscle blood flow distribution and fibre recruitment. *J Physiol* 2010, 588(Pt 24):5077-87.

12. **Hirai DM**, Copp SW, Schwagerl PJ, Haub MD, Poole DC, Musch TI. Acute antioxidant supplementation and skeletal muscle vascular conductance in aged rats: role of exercise and fiber type. *Am J Physiol Heart Circ Physiol* 2011, 300(4): H1536-44.

13. **Hirai DM**, Copp SW, Schwagerl PJ, Musch TI, Poole DC. Acute effects of hydrogen peroxide on skeletal muscle microvascular oxygenation from rest to contractions. *J Appl Physiol* 2011, 110(5): 1290-8.

14. Copp SW, **Hirai DM**, Ferguson SK, Musch TI, Poole DC. Role of neuronal nitric oxide synthase in modulating microvascular and contractile function in rat skeletal muscle. *Microcirculation* 2011, 18(6): 501-11.

15. **Hirai DM**, Copp SW, Hageman KS, Poole DC, Musch TI. Ageing alters the contribution of nitric oxide to regional muscle hemodynamic control at rest and during exercise in rats. *J Appl Physiol* 2011, 111(4): 989-998.

16. Copp SW, Schwagerl PJ, **Hirai DM**, Poole DC, Musch TI. Acute ascorbic acid and hindlimb skeletal muscle blood flow distribution in old rats: rest and exercise. *Can J Physiol Pharmacol* 2012, (accepted).

17. **Hirai DM**, Copp SW, Ferguson SK, Holdsworth CT, McCullough DJ, Behnke BJ, Musch TI, Poole DC. Exercise training and muscle microvascular oxygenation: functional role of nitric oxide. *J Appl Physiol* 2012, 113(4): 557-565.

18. Copp SW, **Hirai DM**, Ferguson SK, Holdsworth CT, Musch TI, Poole DC. Effects of chronic heart failure on neuronal nitric oxide synthase-mediated control of microvascular O_2 pressure in contracting rat skeletal muscle. *J Physiol* 2012, 590(15): 3585-3596.

19. **Hirai DM**, Copp SW, Holdsworth CT, Ferguson SK, Musch TI, Poole DC. Effects of neuronal nitric oxide synthase inhibition on microvascular and contractile function in skeletal muscle of aged rats. *Am J Physiol Heart Circ Physiol* 2012, 303(8): H1076–H1084, 2012.

20. Ferguson SK, **Hirai DM**, Copp SW, Holdsworth CT, Allen JD, Jones AM, Musch TI, Poole DC. Impact of dietary nitrate supplementation via beetroot juice on exercising muscle vascular control in rats. *J Physiol* 2012, (in press).

21. **Hirai DM**, Copp SW, Ferguson SK, Holdsworth CT, Musch TI, Poole DC. The NO donor sodium nitroprusside: evaluation of skeletal muscle vascular and metabolic dysfunction. *Microvascular Research* 2012, (in press).

22. Copp SW, Inagaki T, White MJ, **Hirai DM**, Ferguson SK, Holdsworth CT, Sims GE, Poole DC, Musch TI. (-)-Epicatechin administration and exercising skeletal muscle vascular control and microvascular oxygenation in healthy rats. *Am J Physiol Heart Circ Physiol* 2012, (in press).

23. Copp SW, **Hirai DM**, Sims GE, Musch TI, Poole DC, Kenney MJ. Neuronal nitric oxide synthase inhibition and regional sympathetic nerve discharge: implications for peripheral vascular control. *Respir Physiol Neurobiol* 2012 (submitted).

24. **Hirai DM**, Copp SW, Holdsworth CT, Ferguson SK, McCullough DJ, Behnke BJ, Musch TI, Poole DC. Skeletal muscle microvascular oxygenation in heart failure: effects of exercise training. (in preparation).

Abstracts

1. **Hirai DM**, SW Copp, LF Ferreira, TI Musch, DC Poole. Nitric Oxide (NO) bioavailability underlies muscle microvascular O_2 delivery/utilization imbalance in chronic heart failure (CHF) rats. *The FASEB Journal* 2009; 23: 948.12.

2. Copp SW, **Hirai DM**, Schwagerl PJ, Herspring KF, Musch TI, Poole DC. Acute antioxidant (AOX) treatment increases muscle microvascular O_2 extraction in young rats. *The FASEB Journal* 2009; 23: 948.3.

3. Copp SW, **Hirai DM**, Musch TI, Poole DC. Microvascular oxygenation during the on-transient and recovery from contractions in aged muscle: implications for fatigue. *Med Sci Sports Exerc* 2009, 41(5):8

3. **Hirai DM**, Copp SW, Schwagerl PJ, Musch TI, Poole DC. Hydrogen peroxide controls microvascular oxygenation in contracting skeletal muscle of healthy young rats. *Med Sci Sports Exerc* 2010, 45(5): S90.

4. Copp SW, **Hirai DM**, Schwagerl PJ, Musch TI, Poole DC. Neuronal NOS inhibition modulates resting but not exercising blood flow in rat hindlimb muscles. *Med Sci Sports Exerc* 2010, 45(5): S91.

5. Schwagerl PJ, Copp SW, **Hirai DM**, Davis RT, Synder BS, Poole DC, Musch TI. The effects of ascorbic acid supplementation on muscle blood flow in aged rats. *Med Sci Sports Exerc* 2010, 45(5): S91.

6. **Hirai DM**, Copp SW, Musch TI, Poole DC. Effects of nNOS inhibition on resting and contracting skeletal muscle microvascular oxygenation in aged rats. *Med Sci Sports Exerc* 2011, 43: S82.

7. Copp SW, **Hirai DM**, Ferguson SK, Poole DC, Musch TI. Skeletal muscle vascular and contractile function: role of nNOS inhibition. *Med Sci Sports Exerc* 2011, 43: S63.

8. **Hirai DM**, Copp SW, Poole DC, Musch TI. Novel skeletal muscle microvascular oxygenation indices as a function of chronic heart failure severity in rats. *The FASEB Journal* 2011; 25: 814.5.

9. Copp SW, **Hirai DM**, Ferguson SK, Poole DC, Musch TI. Effects of neuronal nitric oxide synthase (nNOS) inhibition on microvascular O_2 pressures during contractions in rat skeletal muscle. *The FASEB Journal* 2011; 25: 814.6.

10. **Hirai DM**, Copp SW, Ferguson SK, Holdsworth CT, Musch TI, Poole DC. Exercise training and muscle microvascular oxygenation: role of nitric oxide bioavailability. *The FASEB Journal* 2012; 26: 860.18.

11. Copp SW, **Hirai DM**, Ferguson SK, Holdsworth CT, Poole DC, Musch TI. Chronic heart failure (CHF) alters nNOS-mediated control of skeletal muscle contractile function. *The FASEB Journal* 2012: 26: 860.19.

12. Ferguson SK, **Hirai DM**, Copp SW, Holdsworth CT, Hageman KS, Jones AM, Musch TI, Poole DC. Acute dietary nitrate supplementation on resting and exercising hemodynamic control in the rat. *Med Sci Sports Exerc* 44: S879.

13. Holdsworth CT, Copp SW, **Hirai DM**, Ferguson SK, Hageman KS, Stebbins CL, Poole DC, Musch TI. Effects of dietary fish oil on exercising muscle blood flow in chronic heart failure rats. *Med Sci Sports Exerc* 44: S388.

14. **Hirai DM**, Copp SW, Ferguson SK, Holdsworth CT, Poole DC, Musch TI. Exercise training and skeletal muscle blood flow: functional role of neuronal nitric oxide synthase (nNOS). *Med Sci Sports Exerc* 44: S583.

15. **Hirai DM**, Copp SW, Ferguson SK, Holdsworth CT, Jones AM, Musch TI, Poole DC. Diet impacts blood flow control and matching muscle O_2-delivery-to-utilization. *Med Sci Sports Exerc* 44.

16. Copp SW, **Hirai DM**, Ferguson SK, Holdsworth CT, Musch TI, Poole DC. Chronic heart failure alters nNOS-mediated control of skeletal muscle microvascular O_2 delivery and utilization. *Med Sci Sports Exerc* 44: S734.

17. Copp SW, **Hirai DM**, Ferguson SK, Holdsworth CT, Musch TI, Poole DC. Efficacy of nitric oxide treatments to improve peripheral vascular function: implications for chronic heart failure. *Kansas State University Research Forum 2012*.

18. **Hirai DM**, Copp SW, Ferguson SK, Holdsworth CT, Sims GE, Musch TI, Poole DC. Chronic heart failure and muscle microvascular oxygenation: effects of exercise training. *2012 APS Intersociety Meeting: Integrative Biology of Exercise*

19. Copp SW, **Hirai DM**, Inagaki T, White MJ, Sims GE, Holdsworth CT, Ferguson SK, Poole DC, Musch TI. Chronic oral (-)-epicatechin does not affect rat hindlimb skeletal muscle vascular function during exercise. *2012 APS Intersociety Meeting: Integrative Biology of Exercise*

20. Holdsworth CT, Copp SW, Inagaki T, **Hirai DM**, Ferguson SK, Sims GE, White MJ, Poole DC, Musch TI. Chronic (-)-epicatechin administration does not affect contracting skeletal muscle microvascular oxygenation. *2012 APS Intersociety Meeting: Integrative Biology of Exercise*

21. Ferguson SK, **Hirai DM**, Copp SW, Holdsworth CT, Musch TI, Poole DC. The effects of acute dietary nitrate supplementation on muscle microvascular oxygenation in contracting rat skeletal muscle. *2012 APS Intersociety Meeting: Integrative Biology of Exercise*

22. Holdsworth CT, Sims GE, Ferguson SK, Copp SW, **Hirai DM**, White MJ, Hageman SK, Poole DC, Musch Ti. Effects of pentoxifylline on contracting skeletal muscle microvascular oxygenation in chronic heart failure rats. *ACSM 2013*

23. Sims GE, Hageman SK, Copp SW, **Hirai DM**, Ferguson SK, Holdsworth CT, Poole DC, Musch TI. Effects of pentoxifylline on skeletal muscle vascular control in rats with chronic heart failure. ACSM 2013. *ACSM 2013*

24. Ferguson SK, **Hirai DM**, Copp SW, Holdsworth CT, Sims GE, Musch TI, Poole DC. Effects of low dose nitrate supplementation on contracting rat skeletal muscle microvascular oxygen pressure. *ACSM 2013*

25. Copp SW, **Hirai DM**, Sims GE, Musch TI, Kenney MJ, Poole DC. Neuronal nitric oxide synthase (nNOS) and regional sympathetic nerve discharge: implications for peripheral vascular control. *FASEB Journal 2013*

Review Articles

1. Poole DC, Copp SW, **Hirai DM**, Musch TI. Dynamics of muscle microcirculatory and blood-myocyte O_2 flux during contractions. *Acta Physiol (Oxf)* 2011, 202(3):293-310.

2. Poole DC, **Hirai DM**, Copp SW, Musch TI. Muscle oxygen transport and utilization in heart failure: implications for exercise (in)tolerance. *Am J Physiol Heart Circ Physiol* 2012, 302:H1050-H1063.

Letters

1. Poole DC, Copp SW, **Hirai DM**. Comments on point: counterpoint: The kinetics of oxygen uptake during muscular exercise do/do not manifest time-delayed phase. Experimental evidence does support a model of oxygen uptake kinetics with time-delayed phases. *J Appl Physiol* 2009, 107(5):1670-1.

Book Chapters

1. Poole DC, Copp SW, **Hirai DM**, Musch TI. Oxygen Partial Pressure (PO_2) in Heavy Exercise. Encyclopedia of Exercise Medicine in Health and Disease (in press).

Journals reviewed

European Journal of Applied Physiology

Journal of Applied Physiology

National Presentations

ACSM National Meeting 2010. Baltimore, MD.
"Hydrogen peroxide controls microvascular oxygenation in contracting skeletal muscle of healthy young rats"

ACSM National Meeting 2011. Denver, CO.
"Effects of nNOS inhibition on resting and contracting skeletal muscle microvascular oxygenation in aged rats"

ACSM National Meeting, 2012. San Francisco, CA.
Cardiovascular, Renal and Respiratory Physiology (Featured Science Session)
Changing the oxygen cost of exercise: new discoveries, novel implications
"Diet impacts blood flow control and matching of muscle O_2 delivery-to-utilization."

Departmental Seminars

Kansas State University College of Veterinary Medicine, 2008.
Department of Anatomy and Physiology Seminar Series
"Control of muscle oxygen dynamics: effects of aging"

Kansas State University College of Veterinary Medicine, 2009.
Department of Anatomy and Physiology Seminar Series
"Muscle microvascular oxygenation in health and disease: hanging in the balance"

Kansas State University College of Veterinary Medicine, 2012.
Department of Anatomy and Physiology Seminar Series
"Oxygen delivery-utilization matching in skeletal muscle"